Supplementary Information

Unprecedented sesterterpenoids orientanoids A–C: Discovery, bioinspired total synthesis and antitumor immunity

Cheng-Yu Zheng,‡[ac] Jin-Xin Zhao,‡[a] Chang-Hao Yuan,‡[ad] Xia Peng,[a] Meiyu Geng,[ad] Jing Ai,*[a] Yao-Yue Fan*[a] and Jian-Min Yue*[abc]

[a]State Key Laboratory of Drug Research, Shanghai Institute of Materia Medica, Chinese Academy of Sciences, Shanghai 201203, China. [b]Research Units of Discovery of New Drug Lead Molecules, Chinese Academy of Medical Sciences, Shanghai 201203, China. [c]University of Chinese Academy of Science, No.19A Yuquan Road, Beijing 100049, China. [d]School of Pharmaceutical Science and Technology, Hangzhou Institute for Advanced Study, University of Chinese Academy of Sciences, Hangzhou 310024, China.

*E-mail: jai@simm.ac.cn; s040500290@126.com; jmyue@simm.ac.cn

‡ These authors contributed equally.

Table of Contents

1. General Information

General Experimental Procedures. Melting points were carried out on a SGW X-4 melting point apparatus. Optical rotations were obtained on a Perkin-Elmer 341 polarimeter at room temperature. UV spectra were measured on a Shimadzu UV-2550 UV-visible spectrophotometer. IR spectra were recorded on a Perkin-Elmer 577 IR spectrometer with KBr disks. ESIMS were measured on a Bruker Daltonics esquire 3000 plus instrument, a Finnigan LCQ-DECA instrument, or a Finnigan LTQ instrument. HRESIMS were measured with a LCT Premier XE mass spectrometer. NMR spectra were acquired on Bruker Avance III 400 or 500 spectrometers with TMS as the internal reference. X-ray crystallographic analyses were performed on a Bruker APE-II CCD detector (Bruker Biospo Rheinstetten, Germany) employing graphite-monochromated Cu Kα radiation (λ = 1.54178 Å). Silica gel (300–400 mesh), MCI gel (CHP20P, 75–150 μm), C_{18} reverse-phased silica gel (150–200 mesh), and Sephadex LH-20 were used for column chromatography. Semi-preparative HPLC was performed on a Waters 1525 pump with a Waters 2489 detector (254 nm and 210 nm) and an YMC-Pack ODS-A column (250 × 10 mm, S-5 μm, 12 nm). All solvents were of analytical grade (Shanghai Chemical Reagents Co. Ltd., China), and solvents used for HPLC were of HPLC grade (J & K Scientific Ltd., China). High power LED light sources were purchased from Beijing Perfectlight Technology Co., Ltd. (PLS-LED100C). Unless otherwise stated, all reactions were carried out under anhydrous conditions. Solvents were dried by standard method and all other commercial reagents were used without further purification.

Plant Material. The twigs and leaves of *Hedyosmum orientale* were collected from Hainan Province, People's Republic of China.

Extraction and Isolation. The dried sample powder (2.5 kg) was extracted at r.t. with 95% EtOH (3 × 10 L) to obtain the crude extract (210 g). The crude was dissolved in 1.5 L water to give a suspension, and then partitioned with EtOAc. The EtOAc-soluble part (90 g) was fractionated using a column of MCI gel (MeOH-H_2O,

30 to 100%) to give five fractions F1–F5. Fraction F4 (1.7 g) was separated on a silica gel column eluted with petroleum ether/acetone gradient (20:1 to 1:1) to yield fractions F1a–F1i. Fraction F1e (0.47 g) was chromatographed on an RP-18 silica gel column (MeOH/H_2O, 30 to 100%) to give subfractions F1e1-F1e7. Fraction F1e6 (30mg) was purified by semi-preparative HPLC (mobile phase: 50% MeCN in H_2O) to give compounds **1** (2.8 mg, t_R = 15 min) and **2** (1.9 mg, t_R = 16 min). Fraction F1f (0.18 g) was separated over a Sephadex LH-20 column eluted with MeOH to afford subfractions F1f1-F1f3. Fraction F1f2 (25 mg) was purified by semi-preparative HPLC (mobile phase: 40% MeCN in H_2O) to yield compound **3** (3.5 mg, t_R = 15 min).

ECD Calculations. The ChemDraw_Pro_14.1 software with MM2 force field was used to establish the initial conformations of target molecules. Conformational searches were conducted with the torsional sampling (Monte Carlo Multiple Minimum, MCMM) method under OPLS3[1] force field by Macromodel 10.2 program (Schrödinger Release 2015-2: MacroModel, Schrödinger, LLC, New York, NY). The value of the 'Energy window for saving structures' was set as 3.01 kcal/mol. All conformations found at least ten times in the result table of conformational searches were examined for geometry and energy to ensure that there were no redundant conformers and that all logically anticipated conformers had been located. Suitable conformations showing appropriate dihedral angle in agreement with the experiment *J* coupling constant and NOE signals were selected as candidate conformers. All the candidate conformers were subjected to geometry optimization at the b3lyp/6-311g(d,p) level of theory in the corresponding solvents applied in the ECD experiments with IEFPCM solvent model, followed by frequency calculations to compute the Gibbs free energies and ensure that all geometries to be at local minima. All quantum chemical calculations were executed in Gaussian 09 program package.[2] All TDDFT calculations were computed at the b3lyp/6-311g(d,p) level of theory in methanol. The Boltzmann-averaged ECD spectra were obtained with *SpecDis* 1.71.[3–5]

2. Physical Constants and Spectral Data for Orientanoids A–C and Synthetic Isomers

*Orientanoid A (**1**)*: Colorless crystals; m.p. 189–190 °C; $[\alpha]_D^{20.3}$: +58.1 (*c* = 0.27 in Methanol); UV/Vis (MeOH): λ_{max} (log ε) 204 (4.00), 241 (4.09) nm; CD (MeOH): λ ($\Delta\varepsilon$) 199 (20.10), 237 (–4.78), 314 (3.00) nm; IR (KBr) ν_{max} 3470, 2970, 1768, 1702, 1655 cm^{-1}; ^1H NMR and ^{13}C NMR (methanol-d_4) see Table S1; (+)-ESIMS *m*/*z* 435.3 $[M + Na]^+$; (+)-HRESIMS *m/z* 435.2145 $[M + Na]^+$ (calcd for $C_{25}H_{32}O_5Na$, 435.2147).

*Orientanoid B (**2**)*: White amorphous solid; $[\alpha]_D^{20.4}$: –84.0 (*c* = 0.15 in MeOH); UV/Vis (MeOH): λ_{max} (log ε) 204 (4.07), 241 (4.00) nm; CD (MeOH): λ ($\Delta\varepsilon$) 198 (–26.30), 237 (–4.25), 314 (1.94) nm; IR (KBr) ν_{max} 3446, 2928, 1767, 1704, 1657 cm^{-1}; ^1H NMR and ^{13}C NMR (methanol-d_4) see Table S1; (+)-ESIMS *m*/*z* 435.3 $[M + Na]^+$; (–)-ESIMS *m*/*z* 411.0 $[M - H]^-$; (+)-HRESIMS *m/z* 435.2157 $[M + Na]^+$ (calcd for $C_{25}H_{32}O_5Na$, 435.2147).

*Orientanoid C (**3**)*: Colorless crystals; m.p. 249–250 °C; $[\alpha]_D^{20.3}$: +174.1 (*c* = 0.09 in MeOH); UV/Vis (MeOH): λ_{max} (log ε) 270 (3.76), 204 (4.05), 241 (4.01) nm ; CD (MeOH): λ ($\Delta\varepsilon$) 198 (–7.25), 225 (4.90), 253 (4.50), 321 (2.95) nm; IR (KBr) ν_{max} 3437, 2923, 1769, 1701, 1655 cm^{-1}; ^1H NMR and ^{13}C NMR (methanol-d_4) see Table S1; (–)-ESIMS *m*/*z* 470.9 $[M + HCO_2]^-$; (–)-HRESIMS *m*/*z* 471.2018 $[M + HCO_2]^-$ (calcd for $C_{26}H_{31}O_8$, 471.2019).

Table S1. ^{1}H (500 Hz) and ^{13}C (125 Hz) NMR data for 1–3.

	1[a]		**2**[a]		**3**[a]	
no.	δ_H (mult, *J*, Hz)	δ_C	δ_H (mult, *J*, Hz)	δ_C	δ_H (mult, *J*, Hz)	δ_C
1	2.88 m	50.4	2.87 m	50.4	2.93 m	50.2
2	*α* 2.46 dd (19.1, 7.2)	37.0	*α* 2.46 dd (19.1, 6.7)	37.0	*α* 2.48 dd (19.1, 6.7)	37.0
	β 1.92 m		*β* 1.92 dd (19.1, 2.6)		*β* 1.95 dd (19.1, 2.4)	
3		210.0		210.1		209.8
4		137.8		138.1		138.5
5		170.2		170.3		168.9
6	*β* 2.97 d (14.9)	35.0	*β* 2.76 d (14.8)	33.0	*β* 2.75 d (14.9)	34.2
	α 2.85 d (14.9)		*α* 2.69 d (14.8)		*α* 2.59 d (14.9)	
7		91.3		92.0		90.8
8	4.40 dd (7.0, 1.6)	86.0	4.70 dd (6.8, 1.4)	85.6	4.45 dd (7.2, 1.9)	86.7
9	*β* 2.02 (m)	39.7	*β* 2.02 m	39.5	*β* 2.11 dd (14.6, 7.2)	39.5
	α 1.63 ddd (14.6, 1.6, 1.6)		*α* 1.62 ddd (14.7, 1.4, 1.4)		*α* 1.72 ddd (14.6, 1.9, 1.9)	
10		86.7		87.4		87.9
11		56.1		54.0		57.5
12		181.9		179.9		178.9
13	2.31 dd (13.2, 5.8)	27.5	1.98-2.05 m (2H)	21.1	2.59 m	27.6
	1.94 m				2.39 m	
14	1.74 t (1.6)	7.9	1.72 t (1.5)	7.8	1.67 t (1.6)	8.1
15	1.42 s	24.9	1.41 s	24.9	1.47 s	24.8
1′	2.42 m	23.6	2.24-2.31 m (2H)	23.1	2.76 m	34.5
	2.22 m				2.63 m	
2′	5.62 brs	124.0	5.63 brs	124.4		199.5
3′		134.0		133.8		136.7
4′	3.20 brd (10.3)	50.4	2.67 d (9.1)	45.8		148.2
5′	5.79 dd (15.1, 10.3)	123.5	5.45 dd (15.4, 9.1)	126.3	6.06 dd (16.1, 1.0)	122.2
6′	5.71 d (15.1)	146.1	5.67 d (15.4)	142.4	6.17 d (16.1)	150.7
7′		71.1		71.1		71.5
8′	1.23 s	29.6	1.249 s	29.6	1.34 s	29.60
9′	1.26 s	30.2	1.253 s	29.8	1.32 s	29.64
10′	1.72 brs	22.3	1.74 dd (3.1, 1.7)	22.6	1.97 d (0.9)	13.6

[a]Measured in methanol-d_4.

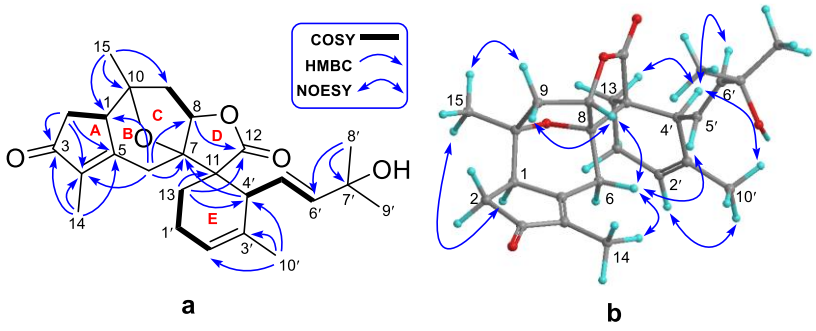

Fig. S1. The key 2D NMR correlations of **1**.

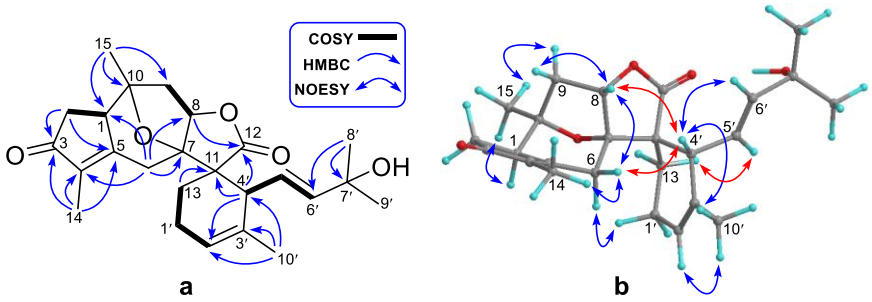

Fig. S2. The key 2D NMR correlations of **2**.

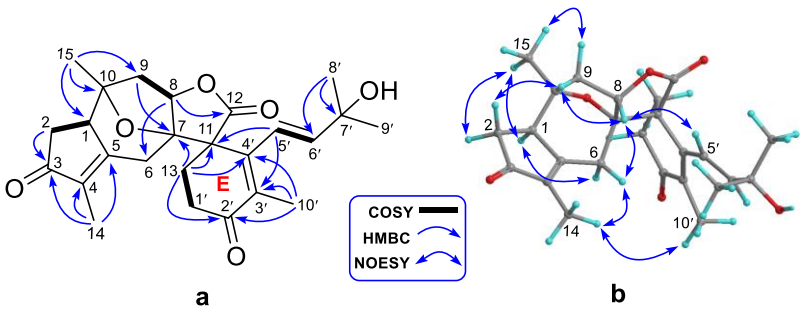

Fig. S3. The key 2D NMR correlations of **3**.

Table S2. X-ray crystallographic data for natural orientanoid A (1) [a]

Identification code	cu_dm16184_0m
Empirical formula	$C_{25}H_{32}O_5$
Formula weight	412.50
Temperature/K	296.15
Crystal system	orthorhombic
Space group	$P2_12_12_1$
a/Å	9.1977(11)
b/Å	9.2073(11)
c/Å	26.829(3)
α/°	90
β/°	90
γ/°	90
Volume/Å^3	2272.1(5)
Z	4
ρ_{calc}g/cm^3	1.206
μ/mm^{-1}	0.667
F(000)	888.0
Crystal size/mm^3	0.12 × 0.1 × 0.08
Radiation	CuKα (λ = 1.54178)
2Θ range for data collection/°	6.588 to 140.134
Index ranges	$-10 \leq h \leq 10$, $-11 \leq k \leq 10$, $-30 \leq l \leq 31$
Reflections collected	15484
Independent reflections	4104 [R_{int} = 0.0311, R_{sigma} = 0.0290]
Data/restraints/parameters	4104/0/278
Goodness-of-fit on F^2	1.037
Final R indexes [I>=2σ (I)]	R_1 = 0.0340, wR_2 = 0.0925
Final R indexes [all data]	R_1 = 0.0362, wR_2 = 0.0939
Largest diff. peak/hole / e Å^{-3}	0.16/-0.15
Flack parameter	0.10(7)

[a]Crystals of **1** were obtained from MeOH.

Table S3. X-ray crystallographic data for natural orientanoid C (3)[a]

Identification code	dm16180
Empirical formula	$C_{25}H_{31}O_{6.5}$
Formula weight	435.50
Temperature/K	296.15
Crystal system	orthorhombic
Space group	$P2_12_12$
a/Å	12.4675(9)
b/Å	21.6679(15)
c/Å	9.6367(6)
α/°	90
β/°	90
γ/°	90
Volume/Å^3	2603.3(3)
Z	4
ρ_{calc}g/cm^3	1.111
μ/mm^{-1}	0.652
F(000)	932.0
Crystal size/mm^3	0.2 × 0.18 × 0.1
Radiation	CuKα (λ = 1.54178)
2Θ range for data collection/°	8.16 to 138.9
Index ranges	$-15 \leq h \leq 13$, $-25 \leq k \leq 24$, $-11 \leq l \leq 11$
Reflections collected	16866
Independent reflections	4730 [R_{int} = 0.0511, R_{sigma} = 0.0413]
Data/restraints/parameters	4730/0/294
Goodness-of-fit on F^2	1.045
Final R indexes [I>=2σ (I)]	R_1 = 0.0369, wR_2 = 0.1008
Final R indexes [all data]	R_1 = 0.0393, wR_2 = 0.1031
Largest diff. peak/hole / e Å^{-3}	0.12/-0.17
Flack parameter	-0.08(9)

[a]Crystals of **3** were obtained from petroleum ether/acetone = 10:1.

Structure elucidation of compound 14. Compound **14**, amorphous white powder, shared the same molecular formula of $C_{25}H_{32}O_5$ with **2** based on its HRESIMS ion at *m/z* 435.2137 $[M + Na]^+$ (calcd for $C_{25}H_{32}O_5Na$, 435.2147) and its ^{13}C NMR data (Table S4), indicative of their isomeric nature. The 1D NMR data of compounds **2** and **14** (Table S1 and Table S4) showed high similarity, and detailed analysis of ^1H-^1H COSY and HMBC spectra of **14** (Fig. S4a) indicated that its 2D structure was identical to that of **2**. Examination of NOESY spectrum (Fig. S4b) and the key coupling constants revealed that the stereochemistry of A–D rings, the *R*-configuration of C-4′, and the *E*-geometry of $\triangle^{5'}$ double bond ($J_{5',6'}$ = 15.7 Hz) in **14** were retained as those of **2**, and the major difference was evident in the spiro C-11 configuration. The relative configuration of C-11 in **14** was assigned as *R** by the key NOESY correlations of H-13 with H-6*β* and H-8, H-5′ with H-6*α* and H-13, as well as H-4′ with H-6′. The absolute configuration of **14** was then determined as 1*R*, 7*S*, 8*S*, 10*R*, 11*R*, 4′*R*, 5′*E* by the roughly matched experimental and calculated ECD curves (Fig. S6). The absolute configuration of **14** was finally determined as 1*R*, 7*S*, 8*S*, 10*R*, 11*R*, 4′*R*, 5′*E* [absolute structure parameter: 0.08 (7); CCDC 2181591] by X-ray crystallography study with Cu K*α* radiation (Table S20).

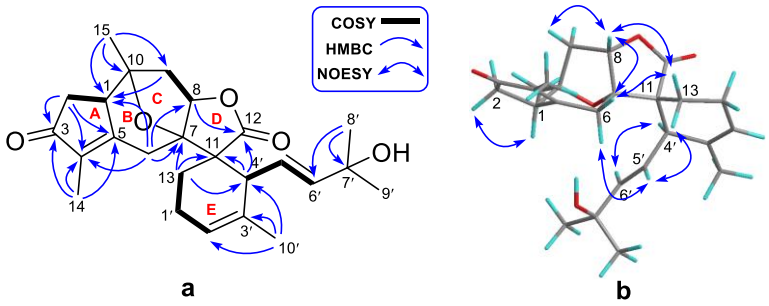

Fig. S4. The key 2D NMR correlations of **14**.

Structure elucidation of compound 15. Compound **15** was also obtained as amorphous white powder and was assigned the same molecular formula of $C_{25}H_{32}O_5$ as **14** according to its HRESIMS ion and ^{13}C NMR data (Table S4). The planar structure of **15** was elucidated to be identical to that of **14** as deduced from its 1D and 2D NMR spectra (Fig. S5). As in the case of compounds **1** and **2**, the 1D NMR data of compounds **14** and **15** showed high similarity with the major differences occurring in

the chemical shifts of C-13, C-4′, C-5′, and C-6′, which suggested that **15** was the C-4′ epimer of **14**. This assignment was validated by the key NOESY correlations of H-4′ with H-13 and H-6α. The absolute configuration of **15** was determined as 1*R*, 7*S*, 8*S*, 10*R*, 11*S*, 4′*S*, 5′*E* by comparison of its experimental ECD spectrum with the computed one (Fig. S6).

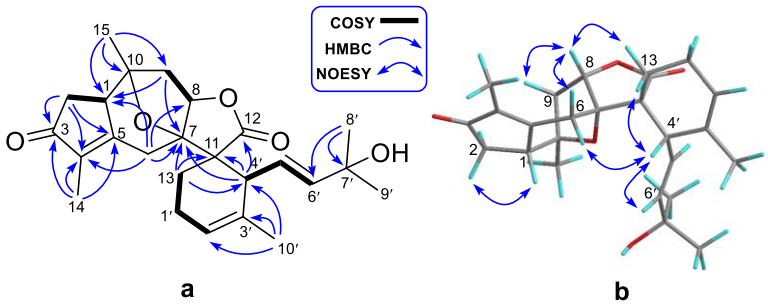

Fig. S5. The key 2D NMR correlations of **15**.

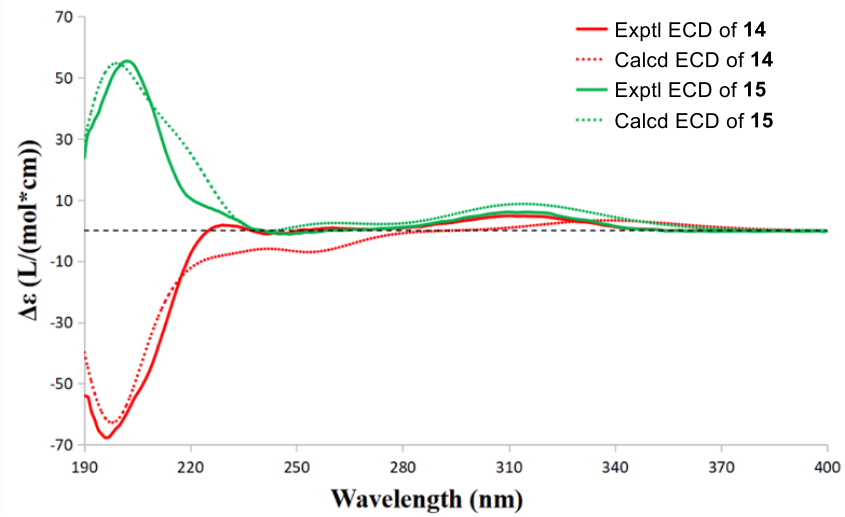

Fig. S6. Experimental and calculated ECD spectra of compounds **14** and **15**.

Table S4. ^{1}H (500 Hz) and ^{13}C (125 Hz) NMR data for 14 and 15

	14[a]		**15**[a]	
no.	δ_H [ppm, mult, *J* (Hz)]	δ_C (ppm)	δ_H [ppm, mult, *J* (Hz)]	δ_C (ppm)
1	2.86 m	50.9	2.84 m	50.7
2	*α* 2.46 dd (19.1, 6.6)	37.1	*α* 2.46 dd (19.1, 6.3)	37.1
	β 1.91 m		*β* 1.91 m	
3		210.0		210.1
4		138.3		138.5
5		170.2		170.4
6	*α* 2.92 d (14.8)	32.1	*β* 2.98 d (14.4)	32.3
	β 2.82 d (14.8)		*α* 2.76 d (14.4)	
7		92.6		93.2
8	4.59 dd (6.7, 1.3)	85.4	4.60 dd (6.9, 1.6)	85.4
9	*β* 1.99 m	39.5	*β* 2.01 dd (14.7, 6.9)	39.6
	α 1.62 m		*α* 1.63 dt (14.7, 1.4)	
10		87.4		87.4
11		52.9		53.8
12		179.2		179.4
13	1.98 m (2H)	22.5	1.85 m (2H)	26.3
			1.94 m	
14	1.71 t (1.7)	7.8	1.72 t (1.7)	7.8
15	1.44 s	25.0	1.42 s	25.3
1′	2.01 m	23.7	2.21 m (2H)	22.8
	2.20 m			
2′	5.51 brs	122.3	5.58 brs	122.9
3′		133.9		135.1
4′	2.95 d (8.2)	45.2	3.23 d (8.8)	44.5
5′	5.80 dd (15.7, 8.2)	125.5	5.68 dd (15.6, 8.8)	127.0
6′	5.71 d (15.7)	143.6	5.60 d (15.6)	140.8
7′		71.4		71.4
8′	1.28 s	29.9	1.28 s	30.0
9′	1.29 s	30.1	1.29 s	30.1
10′	1.66 brs	22.7	1.68 brs	22.9

[a]Measured in methanol-d_4.

Comparison of the NMR data of natural and synthetic compounds.

Table S5. Comparison of the ^{1}H NMR spectroscopic data (methanol-d_4) of natural and synthetic orientanoid A (1)

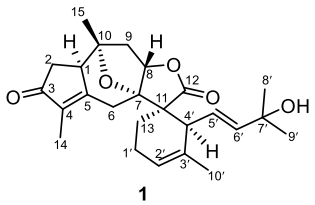

1

position	Natural δ_H [ppm, mult, *J* (Hz)] 500 MHz	Synthetic δ_H [ppm, mult, *J* (Hz)] 600 MHz	Err (Natural–Synthetic) $\Delta\delta_H$ (ppm)
1	2.88 m (1H)	2.90–2.88 m (1H)	-
2α	2.46 dd (19.1, 7.2, 1H)	2.47 dd (19.1, 6.7, 1H)	–0.01
2β	1.92 m (1H)	1.94–1.91 m (1H)	-
6α	2.85 d (14.9, 1H)	2.87 d (14.8, 1H)	–0.02
6β	2.97 d (14.9, 1H)	2.98 d (14.7, 1H)	–0.01
8	4.40 dd (7.0, 1.6, 1H)	4.41 dd (7.0, 1.7, 1H)	–0.01
9α	1.63 ddd (14.6, 1.6, 1.6, 1H)	1.64 dt (14.6, 1.5, 1H)	–0.01
9β	2.02 m (1H)	2.03–1.98 m (1H)	-
13	1.94 m (1H)	1.97–1.94 m (1H)	-
13	2.31 dd (13.2, 5.8, 1H)	2.32 dd (13.2, 5.9, 1H)	–0.01
14	1.74 t (1.6, 3H)	1.76 t (1.7, 3H)	–0.02
15	1.42 s (3H)	1.43 s (3H)	–0.01
1’	2.42 m (1H)	2.44 – 2.40 m, (1H)	-
1’	2.22 m (1H)	2.27 – 2.19 m, (1H)	-
2’	5.62 brs (1H)	5.63 s (1H)	–0.01
4’	3.20 brd (10.3, 1H)	3.22 d (10.1, 1H)	–0.02
5’	5.79 dd (15.1, 10.3)	5.80 dd (15.1, 10.4, 1H)	–0.01
6’	5.71 d (15.1, 1H)	5.73 d (15.1, 1H)	–0.02
8’	1.23 s (3H)	1.24 s (3H)	–0.01
9’	1.26 s (3H)	1.28 s (3H)	–0.02
10’	1.72 brs (3H)	1.74 s, (3H)	–0.02

Table S6. Comparison of the ^{13}C NMR spectroscopic data (methanol-d_4) of natural and synthetic orientanoid A (1)

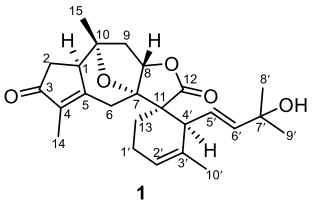

1

position	Natural δ_C (ppm) 125 MHz	Synthetic δ_C (ppm) 125 MHz	Err (Natural–Synthetic) $\Delta\delta_C$ (ppm)
1	50.43	50.43	0
2	37.03	37.03	0
3	210.02	209.97	+0.05
4	137.77	137.76	+0.01
5	170.20	170.16	+0.04
6	34.99	34.99	0
7	91.30	91.29	+0.01
8	85.97	85.95	+0.02
9	39.74	39.74	0
10	86.69	86.68	+0.01
11	56.14	56.14	0
12	181.94	181.91	+0.03
13	27.51	27.50	+0.01
14	7.89	7.89	0
15	24.91	24.91	0
1’	23.64	23.64	0
2’	123.97	123.96	+0.01
3’	134.03	134.01	+0.02
4’	50.37	50.37	0
5’	123.45	123.45	0
6’	146.07	146.07	0
7’	71.08	71.06	+0.02
8’	29.63	29.64	–0.01
9’	30.17	30.18	–0.01
10’	22.26	22.25	+0.01

Table S7. Comparison of the ^{1}H NMR spectroscopic data (methanol-d_4) of natural and synthetic orientanoid B (2)

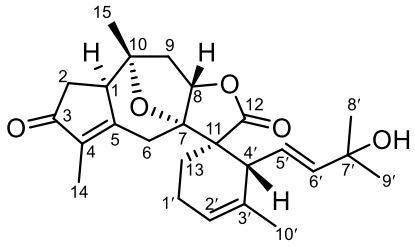

2

position	Natural δ_H [ppm, mult, *J* (Hz)] 500 MHz	Synthetic δ_H [ppm, mult, *J* (Hz)] 400 MHz	Err (Natural–Synthetic) $\Delta\delta_H$ (ppm)
1	2.87 m (1H)	2.92 – 2.83 m (1H)	-
2α	2.46 dd (19.1, 6.7, 1H)	2.46 dd (19.0, 6.7, 1H)	0
2β	1.92 dd (19.1, 2.6, 1H)	1.92 dd (19.1, 2.7, 1H)	0
6α	2.69 d (14.8, 1H)	2.69 d (14.2, 1H)	0
6β	2.76 d (14.8, 1H)	2.76 d (14.7, 1H)	0
8	4.70 dd (6.8, 1.4, 1H)	4.70 dd (6.9, 1.5, 1H)	0
9α	1.62 ddd (*J* = 14.7, 1.4, 1.4, 1H)	1.61 ddd (14.6, 1.5, 1.5, 1H)	+0.01
9β	2.02 m (1H)	2.02 – 1.96 m (1H)	-
13	2.05 – 1.98 m (2H)	2.05 – 1.98 m (2H)	-
14	1.72 t (1.5, 3H)	1.71 t (1.7, 3H)	+0.01
15	1.41 s (3H)	1.41 s (3H)	0
1’	2.31 – 2.24 m (2H)	2.32 – 2.21 m (2H)	-
2’	5.63 brs (1H)	5.63 s (1H)	0
4’	2.67 d (9.1, 1H)	2.67 d (9.4, 1H)	0
5’	5.45 dd (15.4, 9.1, 1H)	5.45 dd (15.4, 9.1, 1H)	0
6’	5.67 d (15.4, 1H)	5.67 d (15.5, 1H)	0
8’	1.24 s (3H)	1.24 s (3H)	0
9’	1.25 s (3H)	1.25 s (3H)	0
10’	1.74 dd (3.1, 1.8, 3H)	1.74 d (1.8, 3H)	0

Table S8. Comparison of the ^{13}C NMR spectroscopic data (methanol-d_4) of natural and synthetic orientanoid B (2)

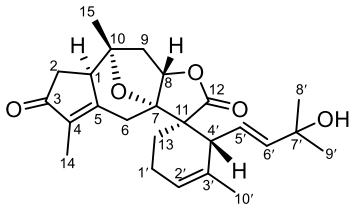

2

position	**Natural** δ_C (ppm) 125 MHz	**Synthetic** δ_C (ppm) 125 MHz	**Err** (Natural–Synthetic) $\Delta\delta_C$ (ppm)
1	50.40	50.44	–0.04
2	37.01	37.05	–0.04
3	210.08	210.10	–0.02
4	138.04	138.07	–0.03
5	170.25	170.26	–0.01
6	32.97	33.01	–0.04
7	91.97	92.01	–0.04
8	85.55	85.58	–0.03
9	39.51	39.54	–0.03
10	87.33	87.36	–0.03
11	54.00	54.04	–0.04
12	179.86	179.88	–0.02
13	21.06	21.09	–0.03
14	7.78	7.81	–0.03
15	24.91	24.95	–0.04
1’	23.02	23.05	–0.03
2’	124.36	124.39	–0.03
3’	133.73	133.74	–0.01
4’	45.74	45.79	–0.05
5’	126.30	126.31	–0.01
6’	142.33	142.37	–0.04
7’	71.06	71.10	–0.04
8’	29.57	29.61	–0.04
9’	29.77	29.81	–0.04
10’	22.56	22.59	–0.03

Table S9. Comparison of the ^{1}H NMR spectroscopic data (methanol-d_4) of natural and synthetic orientanoid C (3)

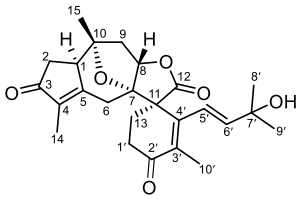

3

position	Natural δ_H [ppm, mult, *J* (Hz)] 500 MHz	Synthetic δ_H [ppm, mult, *J* (Hz)] 600 MHz	Err (Natural–Synthetic) $\Delta\delta_H$ (ppm)
1	2.93 m (1H)	2.96 – 2.89 m (1H)	-
2α	2.48 dd (19.1, 6.7, 1H)	2.47 dd (19.0, 6.8, 1H)	+0.01
2β	1.95 dd (19.1, 2.4, 1H)	1.94 dd (19.1, 2.8, 1H)	+0.01
6α	2.59 d (14.9, 1H)	2.59 d (14.6, 1H)	0
6β	2.75 d (14.9, 1H)	2.75 d (14.7, 1H)	0
8	4.45 dd (7.1, 1.9, 1H)	4.45 dd (7.2, 2.0, 1H)	0
9α	1.72 ddd (14.6, 1.9, 1.9, 1H)	1.72 dt (14.7, 1.7, 1H)	0
9β	2.11 dd (14.6, 7.2, 1H)	2.11 dd (14.7, 7.2, 1H)	0
13	2.59 m (1H)	2.62 – 2.59 m (1H)	-
13	2.39 m (1H)	2.41 – 2.34 m (1H)	-
14	1.67 t (1.6, 3H)	1.67 t (1.6, 3H)	0
15	1.47 s (3H)	1.47 s (3H)	0
1’	2.76 m (1H)	2.80 – 2.77 m (1H)	-
1’	2.63 m (1H)	2.67 – 2.62 m (1H)	-
5’	6.06 dd (16.1, 1.0, 1H)	6.06 dd (16.1, 1.2, 1H)	0
6’	6.17 d (16.1, 1H)	6.18 d (16.0, 1H)	–0.01
8’	1.34 s (3H)	1.34 s (3H)	0
9’	1.32 s (3H)	1.32 s (3H)	0
10’	1.97 d (0.9, 3H)	1.96 d (1.1, 3H)	+0.01

Table S10. Comparison of the ^{13}C NMR spectroscopic data (methanol-d_4) of natural and synthetic orientanoid C (3)

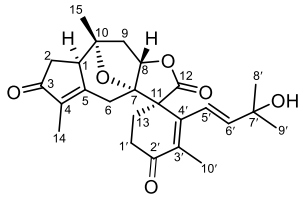

3

position	Natural δ_C (ppm) 125 MHz	Synthetic δ_C (ppm) 125 MHz	Err (Natural–Synthetic) $\Delta\delta_C$ (ppm)
1	50.18	50.13	+0.05
2	36.98	36.94	+0.04
3	209.75	209.64	+0.11
4	138.51	138.45	+0.06
5	168.94	168.85	+0.09
6	34.19	34.16	+0.03
7	90.83	90.76	+0.07
8	86.67	86.61	+0.06
9	39.47	39.43	+0.04
10	87.87	87.82	+0.05
11	57.50	57.43	+0.07
12	178.90	178.81	+0.09
13	27.56	27.52	+0.04
14	8.07	8.07	0
15	24.84	24.83	+0.01
1’	34.55	34.51	+0.03
2’	199.47	199.37	+0.10
3’	136.66	136.59	+0.07
4’	148.19	148.11	+0.08
5’	122.21	122.15	+0.06
6’	150.71	150.66	+0.05
7’	71.47	71.41	+0.06
8’	29.60	29.58	+0.02
9’	29.64	29.62	+0.02
10’	13.62	13.62	0

Table S11. Comparison of the ^{1}H NMR spectroscopic data ($CDCl_3$) of natural and synthetic hedyosumin B (6)

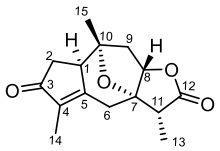

hedyosumin B

position	Natural δ_H [ppm, mult, *J* (Hz)] 400 MHz	Synthetic δ_H [ppm, mult, *J* (Hz)] 400 MHz	Err (Natural–Synthetic) $\Delta\delta_H$ (ppm)
1	2.81 m (1H)	2.85 – 2.79 m (1H)	-
2α	2.48 dd (18.8, 7.0, 1H)	2.48 dd, (19.0, 6.9, 1H)	0
2β	1.82 dd (18.8, 2.8, 1H)	1.81 dd, (19.0, 2.8, 1H)	+0.01
6α	2.80 d (14.4, 1H)	2.76 d, (14.3, 1H)	+0.04
6β	2.68 d (14.4, 1H)	2.68 d (14.3, 1H)	0
8	4.38 dd (7.0, 1.8, 1H)	4.38 dd (7.0, 1.5, 1H)	0
9α	1.74 dd (14.5, 1.8, 1H)	1.77 – 1.73 m (1H)	-
9β	1.98 dd (14.5, 7.0, 1H)	1.98 dd (14.6, 7.1, 1H)	0
11	2.62 q (7.0, 1H)	2.61 q (7.5, 1H),	+0.01
13	1.34 d (7.0, 3H)	1.34 d (7.3, 3H)	0
14	1.72 s (3H)	1.72 s (3H)	0
15	1.42 s (3H)	1.41 s (3H)	+0.01

Table S12. Comparison of the ^{13}C NMR spectroscopic data ($CDCl_3$) of natural and synthetic hedyosumin B (6)

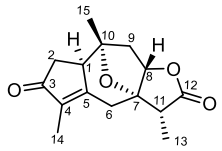

hedyosumin B

position	**Natural** δ_C (ppm) 100 MHz	**Synthetic** δ_C (ppm) 125 MHz	**Err** (Natural–Synthetic) $\Delta\delta_C$ (ppm)
1	48.7	48.8	-0.1
2	36.1	36.2	-0.1
3	206.8	206.8	0
4	137.7	137.7	0
5	166.6	166.6	0
6	33.9	34.0	-0.1
7	86.5	86.5	0
8	85.0	85.1	-0.1
9	38.8	38.9	-0.1
10	87.6	87.6	0
11	43.4	43.5	-0.1
12	176.8	176.8	0
13	8.2	8.2	0
14	8.0	8.0	0
15	24.6	24.7	-0.1

Table S13. Comparison of the ^{1}H NMR spectroscopic data ($CDCl_3$) of natural and synthetic hedyosumin C (10)

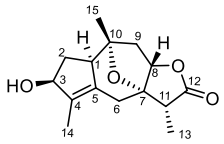

hedyosumin C

position	Natural δ_H [ppm, mult, *J* (Hz)] 400 MHz	Synthetic δ_H [ppm, mult, *J* (Hz)] 400 MHz	Err (Natural–Synthetic) $\Delta\delta_H$ (ppm)
1	2.51 m (1H)	2.50 – 2.47 m (1H)	-
2α	2.42 m (1H)	2.46 – 2.35 m (2H)	-
2β	1.02 m (1H)	1.05 – 0.95 m (1H)	-
3	4.71 brt (1H)	4.76 – 4.60 m (1H)	-
6α	2.42 d (13.6, 1H)	2.46 – 2.35 m (2H)	-
6β	2.28 d (13.6, 1H)	2.27 d, (14.3, 1H)	+0.01
8	4.45 brd (7.1, 1H)	4.44 dd (7.1, 1.8, 1H)	+0.01
9α	1.63 brd (14.2, 1H)	1.69 – 1.60 m (1H)	-
9β	2.34 dd (14.2, 7.1, 1H)	2.34 dd (14.3, 7.1,1H)	0
11	2.53 q (7.2, 1H)	2.52 q (7.2, 1H)	+0.01
13	1.33 d (7.2, 3H)	1.29 d, (7.3, 3H)	+0.04
14	1.69 s (3H)	1.67 s (3H)	+0.02
15	1.31 s (3H)	1.29 s (3H)	+0.02

Table S14. Comparison of the ^{13}C NMR spectroscopic data ($CDCl_3$) of natural and synthetic hedyosumin C (10)

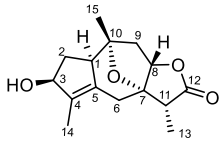

hedyosumin C

position	**Natural** δ_C (ppm) 100 MHz	**Synthetic** δ_C (ppm) 125 MHz	**Err** (Natural–Synthetic) $\Delta\delta_C$ (ppm)
1	52.6	52.6	0
2	34.7	34.6	+0.1
3	79.2	79.2	0
4	136.2	136.3	-0.1
5	133.0	132.9	+0.1
6	31.7	31.7	0
7	87.3	87.2	+0.1
8	86.0	86.0	0
9	38.9	38.9	0
10	86.6	86.6	0
11	43.7	43.7	0
12	177.8	177.8	0
13	8.2	8.2	0
14	10.6	10.5	+0.1
15	24.2	24.1	+0.1

3. Synthetic Procedures and Product Characterization

Synthesis of compound 9

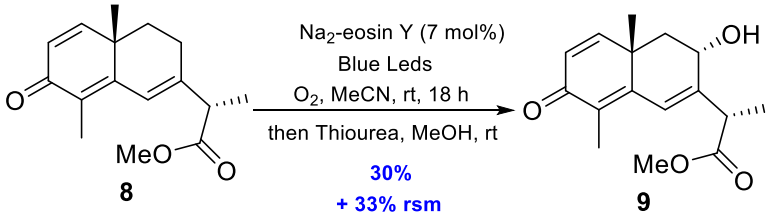

Procedure:

Enone **8** (530 mg, 2.04 mmol, 1 equiv; **8** was made from santonin in one step in 58% yield according to the reported procedure),[6] Na_2-eosin Y (99 mg, 0.14 mmol, 7 mol%) and MeCN (80 mL) were added to a 200 mL eggplant-shaped bottle. After purging the flask with vacuum, O_2 from a balloon was bubbled through the reaction mixture for 3 min. Then the reaction mixture was stirred for 18 h under 50 W 455 nm LED irradiation (PLS-100C, Beijing Perfectlight®, distance ~ 5 cm) under an O_2 atmosphere at room temperature. The reaction solution was concentrated in vacuo, then thiourea (187 mg, 2.45 mmol, 1.2 equiv) and MeOH (30 mL) were added to the mixture and stirred for 4 h. Then the reaction solution was concentrated in vacuo and water (10 mL) was added. Finally, the mixture was extracted with EtOAc (3 x 15 mL). The combined organic layers were washed with brine, dried over anhydrous Na_2SO_4, filtered, and concentrated under reduced pressure. The resulting crude product was then purified by column chromatography (petroleum ether:EtOAc = 2:1) afford starting material **8** (174 mg, 33%) and product **9** as a white solid (168 mg, 30% yield).

Characterization data of 9

R_f = 0.50 (silica, petroleum ether/EtOAc = 1:1);

^{1}H NMR (400 MHz, $CDCl_3$) δ 6.75 (d, J = 9.8 Hz, 1H), 6.57 (s, 1H), 6.23 (d, J = 9.8 Hz, 1H), 4.56 (t, J = 8.0 Hz, 1H), 3.69 (s, 3H), 3.68 (q, J = 8.1 Hz, 1H), 2.24 (dd, J = 12.5, 6.0 Hz, 1H), 1.94 (s, 3H), 1.50 (dd, J = 12.8, 2.0 Hz, 1H), 1.45 (d, J = 7.3 Hz,

3H), 1.13 (s, 3H);

^{13}C NMR (100 MHz, $CDCl_3$) δ 186.60, 175.20, 154.72, 152.66, 146.54, 129.84, 127.19, 123.46, 65.97, 52.38, 42.37, 42.24, 40.10, 25.79, 15.57, 10.36;

$[\alpha]_D^{21}$: +110.25 (c = 0.40 in $CHCl_3$);

IR (KBr) ν_{max} 3442, 2926, 1736, 1649, 1604, 1404, 1201, 1074, 836 cm^{-1};

HRMS (ESI): Calculated for $C_{16}H_{21}O_4$ $(M+H)^+$: 277.1434, Found: 277.1435.

Table S15. Screening of conditions for allylic hydroxylation of enone 8[a]

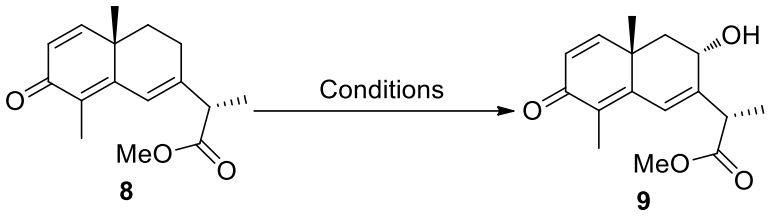

Entry	Conditions	Yield[b]
1	SeO_2, *t*-BuOOH, DCM, r.t. to reflux	n.d.
2	SeO_2, dioxane, reflux	16% (36% rsm)
3	SeO_2, *t*-BuOH/Py, 120 °C	n.d.
4	O_2, AIBN, NHPI, MeCN, 75 °C	n.d.
5	O_2, 9,10-DBA, MeCN, blue LEDs	n.d.
6	O_2, AQ, MeCN, blue LEDs	n.d.
7	H_2-eosin Y, O_2, blue LEDs, MeCN, then thiourea, MeOH	trace
8	Na_2-eosin Y, O_2, blue LEDs, MeCN, then thiourea, MeOH	42% (24% rsm)
9[c]	**Na_2-eosin Y, O_2, blue LEDs, MeCN, then thiourea, MeOH**	**30% (33% rsm)**

[a]Reactions were carried out on a 1.0 mmol scale. [b]Isolated yield. [c]on a 2.0 mmol scale. n.d. = not detected. rsm = recovered starting material. r. t. = room temperature. Py = pyridine. AIBN = 2,2'-azobis (isobutyronitrile). NHPI = N-hydroxyphthalimide. 9,10-DBA = 9,10-dibromoanthracene. AQ = anthraquinone.

Synthesis of compound 7

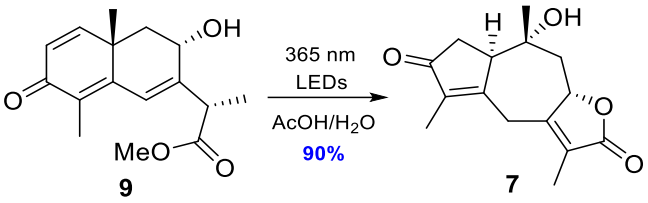

Procedure:

Compound **9** (400 mg, 1.45 mmol, 1 equiv) was dissolved in H_2O (80 mL) and AcOH (20 mL) in a 200 mL round bottom flask. The reaction mixture was degassed by a flow of Ar for 15 min and was then irradiated with 50 W 365nm LEDs at room temperature for 8.5 h. The solution was concentrated under reduced pressure after addition of EtOH and the residue was purified by column chromatography (petroleum ether:EtOAc = 1:2) to yield **7** (343 mg, 90% yield) as a white solid.

Table S16. Screening of conditions for photochemical rearrangement/lactonization/alkene migration cascade reaction

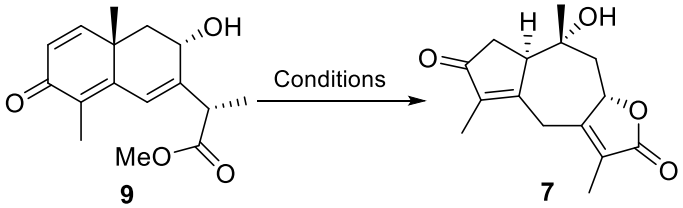

Entry	Conditons	Yield[a]
1	250W high-pressure Hg lamp, AcOH/H_2O, rt, 12 h	74%
2	50 W 420 nm LEDs, AcOH/H_2O, rt, 8.5 h	n.d.
3	50 W 420 nm LEDs, AcOH/H_2O, $Ir(ppy)_3$, rt, 8.5 h	trace
4	**50 W 365 nm LEDs, AcOH/H_2O, rt, 8.5 h**	**90%**

[a]Isolated yield after flash chromatography. n.d. = not detected.

Characterization data of 7

R_f = 0.23 (silica, petroleum ether/EtOAc = 1:2);

^{1}H NMR (400 MHz, $CDCl_3$) δ 4.82 – 4.73 (m, 1H), 3.81 (d, J = 20.8 Hz, 1H), 3.57 (d, J = 20.4 Hz, 1H), 2.99 (dt, J = 6.6, 1.8 Hz, 1H), 2.74 – 2.56 (m, 2H), 2.47 (ddd, J = 19.3, 6.6, 1.1 Hz, 1H), 1.88 (s, 3H), 1.76 (d, J = 1.5 Hz, 3H), 1.71 (d, J = 12.3 Hz,

1H), 1.08 (s, 3H);

^{13}C NMR (100 MHz, $CDCl_3$) δ 207.40, 173.36, 164.61, 157.79, 140.02, 125.45, 79.22, 71.81, 53.11, 50.00, 37.97, 29.01, 21.24, 8.69, 8.39;

$[\alpha]_D^{21}$: +35.83 (c = 0.60 in Methanol);

IR (KBr) ν_{max} 3445, 2925, 1755, 1697, 1384, 1338, 1095, 1018 cm^{-1};

HRMS (ESI): Calculated for $C_{15}H_{19}O_4$ $(M+H)^+$: 263.1278, Found: 263.1277.

Synthesis of compound 6

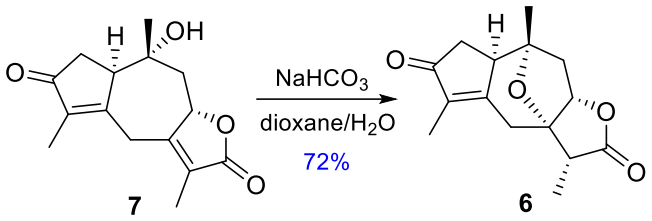

Procedure:

To a solution of compound **7** (195 mg, 0.74 mmol, 1 equiv) in H_2O (22 mL) and dioxane (11 mL) was added $NaHCO_3$ (75 mg, 0.89 mmol, 1.2 equiv) and the mixture was stirred under argon at room temperature for 4 h. Then the reaction was quenched with 1M aqueous HCl and extracted with EtOAc. The combined organic layers were washed with brine, dried over anhydrous Na_2SO_4, filtered, and concentrated under reduced pressure. The crude material was purified by column chromatography (petroleum ether:EtOAc = 1:1) to yield **6** (138 mg, 72%) as a white solid.

Characterization data of 6

R_f = 0.49 (silica, petroleum ether/EtOAc = 1:1);

^{1}H NMR (400 MHz, $CDCl_3$) δ 4.38 (dd, J = 7.0, 1.5 Hz, 1H), 2.85 – 2.79 (m, 1H), 2.76 (d, J = 14.3 Hz, 1H), 2.68 (d, J = 14.3 Hz, 1H), 2.61 (q, J = 7.5 Hz, 1H), 2.48 (dd, J = 19.0, 6.9 Hz, 1H), 1.98 (dd, J = 14.6, 7.1 Hz, 1H), 1.81 (dd, J = 19.0, 2.8 Hz, 1H), 1.77 – 1.73 (m, 1H), 1.72 (s, 3H), 1.41 (s, 3H), 1.34 (d, J = 7.3 Hz, 3H);

^{13}C NMR (125 MHz, $CDCl_3$) δ 206.79, 176.83, 166.58, 137.70, 87.63, 86.54, 85.06, 48.80, 43.48, 38.91, 36.17, 33.96, 24.68, 8.20, 8.02;

$[\alpha]_D^{21}$: +106.53 (c = 0.50 in Methanol);

IR (KBr) ν_{max} 2976, 2942, 1777, 1702, 1655, 1381, 1198, 1509, 1014 cm^{-1};

HRMS (ESI): Calculated for $C_{15}H_{19}O_4$ $(M+H)^+$: 263.1278, Found: 263.1283.

Table S17. Screening of conditions for oxa-Michael reaction

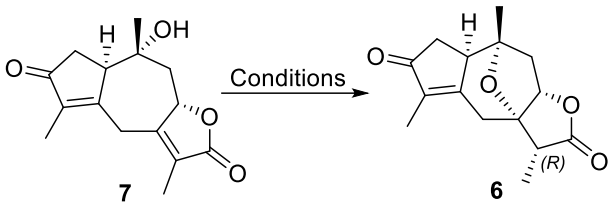

Entry	Conditons	Yield[a]
1	*p*-TsOH·H_2O, CH_2Cl_2, rt	n.d.
2	CSA, CH_2Cl_2, rt	n.d.
3	9% HCl(aq), EtOH, reflux	trace
4	Imidazole, H_2O/dioxane, rt, 12 h	40%
5	**$NaHCO_3$, H_2O/dioxane, rt, 4 h**	**72%**

[a]Isolated yield after flash chromatography. n.d. = not detected. CSA = camphorsulfonic acid

Synthesis of compound 10 and 11

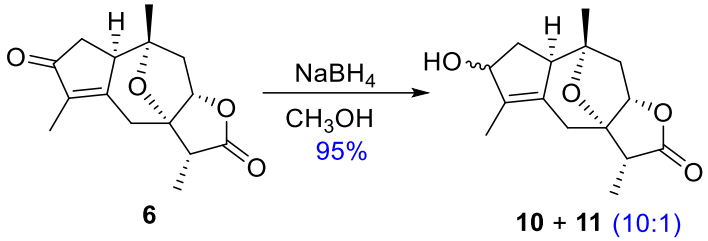

Procedure:

To a stirred solution of **6** (240 mg, 0.91 mmol, 1 equiv) in MeOH (13 mL) at 0 °C in an ice/water bath was added $NaBH_4$ (69 mg, 1.83 mmol, 2.0 equiv). The resulting mixture was stirred at the same temperature for 30 min before quenched with saturated NH_4Cl solution. The aqueous layer was extracted with EtOAc (3 x 15 mL). The combined organic fractions were dried with Na_2SO_4, filtered, and concentrated. The crude material was purified by column chromatography (petroleum ether: EtOAc = 1:1) to yield **10** (209 mg, 87% yield) as a white foam and **11** (21mg, 8% yield) as a white foam.

Characterization data of 10:

R_f = 0.38 (silica, petroleum ether/EtOAc = 1:1);

^{1}H NMR (400 MHz, $CDCl_3$) δ 4.76 – 4.60 (m, 1H), 4.44 (dd, *J* = 7.1, 1.8 Hz, 1H), 2.52 (q, *J* = 7.3 Hz, 1H), 2.50 – 2.47 (m, 1H), 2.46 – 2.35 (m, 2H), 2.34 (dd, *J* = 14.3, 7.1 Hz, 1H), 2.27 (d, *J* = 14.3 Hz, 1H), 1.67 (s, 3H), 1.69 – 1.60 (m, 1H), 1.29 (s, 3H), 1.29 (d, *J* = 7.3 Hz, 3H), 1.05 – 0.95 (m, 1H);

^{13}C NMR (125 MHz, $CDCl_3$) δ 177.80, 136.26, 132.88, 87.23, 86.57, 86.00, 79.17, 52.56, 43.67, 38.89, 34.64, 31.66, 24.12, 10.54, 8.17;

$[\alpha]_D^{21}$: -1.05 (c = 0.20 in Methanol);

IR (KBr) ν_{max} 3444, 2940, 1774, 1448, 1378, 1360, 1203, 1164, 1092, 1043, 1016, 991 cm^{-1};

HRMS (ESI): Calculated for $C_{15}H_{21}O_4$ $(M+H)^+$: 265.1434, Found: 265.1432.

Characterization data of 11:

R_f = 0.35 (silica, petroleum ether/EtOAc = 1:1);

^{1}H NMR (400 MHz, $CDCl_3$) δ 4.54 (d, *J* = 7.6 Hz, 1H), 4.32 (dd, *J* = 7.1, 1.9 Hz, 1H), 2.83 (s, 1H), 2.53 (q, *J* = 7.3 Hz, 1H), 2.45 (dq, *J* = 14.3, 1.6 Hz, 1H), 2.30 (dd, *J* = 14.3, 0.7 Hz, 1H), 1.99 (dd, *J* = 14.3, 7.0 Hz, 1H), 1.87 (ddd, *J* = 14.7, 8.0, 1.4 Hz, 1H), 1.74 (t, *J* = 2.0 Hz, 3H), 1.61 (dt, *J* = 14.3, 1.6 Hz, 2H), 1.55 (dd, *J* = 14.6, 7.2 Hz, 1H), 1.32 (s, 3H), 1.30 (d, *J* = 7.3 Hz, 3H);

^{13}C NMR (125 MHz, $CDCl_3$) δ 177.86, 135.91, 135.51, 87.31, 87.02, 85.85, 80.19, 52.93, 43.71, 38.86, 34.93, 32.22, 24.50, 11.40, 8.40;

$[\alpha]_D^{21}$: +50.78 (c = 0.34 in Methanol);

IR (KBr) ν_{max} 3440, 2926, 2854, 1775, 1447, 1378, 1202, 1165, 1144, 1092, 1017, 984 cm^{-1};

HRMS (ESI): Calculated for $C_{15}H_{21}O_4$ $(M+H)^+$: 265.1434, Found: 265.1427.

Synthesis of compound 5

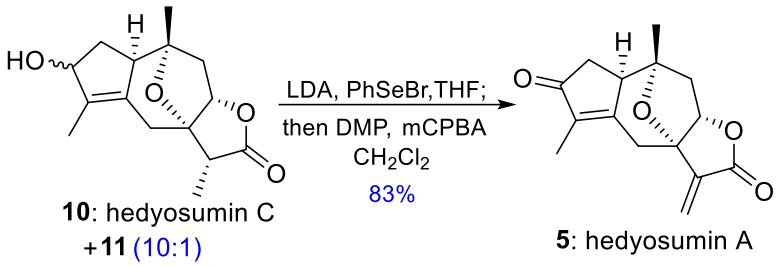

Procedure:

LDA (2.0 M solution in THF, 1.01 mL, 2.02 mmol, 3.5 equiv) was added to a stirred solution of **10** and **11** (152 mg, 0.58 mmol, 1.0 equiv) in 24 mL dry THF at -78 °C under argon. After stirring at -78 °C for 40 min, a solution of PhSeBr (546 mg, 2.31 mmol, 4.0 equiv) in 5 mL dry THF was added. After an additional 2 h, the reaction mixture was quenched by the addition of saturated NH_4Cl solution and extracted with EtOAc. The combined organic layers were washed with brine, dried over anhydrous $NaSO_4$, filtered and concentrated by rotary evaporation. The crude selenylated lactones were used directly into next reaction without further purification.

To a solution of the above selenylated lactone in 19 mL DCM was added DMP (366 mg, 0.86 mmol, 1.5 equiv) at room temperature. After stirred for 20 min at the same temperature, the reaction mixture was cooled to 0 °C and to the stirred solution was added *m*-CPBA (667 mg, 75 wt% 2.90 mmol, 5.0 equiv). After stirred at 0 °C for 20 min, the reaction mixture was quenched with saturated $Na_2S_2O_3$ solution and extracted with EtOAc. The combined organic fractions were dried with Na_2SO_4, filtered, and concentrated. The crude material was purified by column chromatography (petroleum ether:EtOAc = 1:1) to yield **5** (126 mg, 83% yield) as a colorless solid.

Characterization data of 5:

R_f = 0.43 (silica, petroleum ether/EtOAc = 1:1);

^{1}H NMR (400 MHz, $CDCl_3$) δ 6.51 (s, 1H), 6.03 (s, 1H), 4.40 (dd, J = 7.3, 2.6 Hz, 1H), 2.99 (d, J = 14.3 Hz, 1H), 2.94 – 2.87 (m, 1H), 2.79 (d, J = 14.2 Hz, 1H), 2.53 (dd, J = 19.0, 6.9 Hz, 1H), 2.12 (dd, J = 14.5, 7.3 Hz, 1H), 1.90 – 1.81 (m, 2H), 1.75

(s, 3H), 1.46 (s, 3H);

^{13}C NMR (125 MHz, $CDCl_3$) δ 206.50, 168.47, 165.54, 138.27, 136.56, 125.55, 87.92, 85.30, 84.30, 48.83, 39.20, 36.17, 33.10, 24.60, 8.08;

$[\alpha]_D^{21}$: +190.08 (c = 0.64 in Methanol);

IR (KBr) ν_{max} 2920, 1769, 1703, 1383, 1332, 1126, 1030 cm^{-1};

HRMS (ESI): Calculated for $C_{15}H_{15}O_4$ $(M-H)^-$: 259.0976, Found: 259.0975.

Synthesis of compound 1, 2, 14 and 15

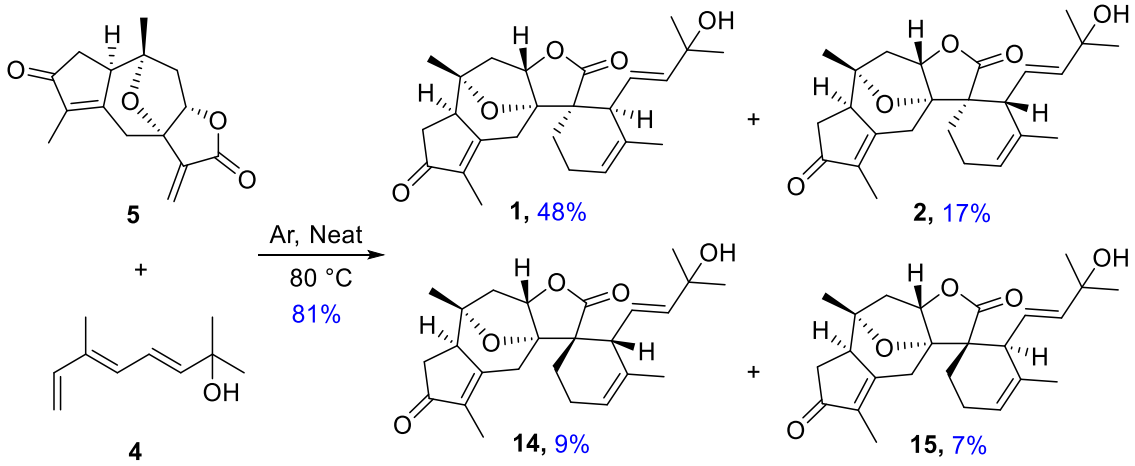

The ratios of **1**: **2**: **14**: **15** =6.9: 2.5: 1.3: 1.0

Orientanoid A (**1**), **Orientanoid B** (**2**), **14**, and **15:** To the solution of **5** (110 mg, 0.42 mmol, 1.0 equiv) in DCM (4 mL) was added a solution of **4** (232 mg, 1.52 mmol, 3.6 equiv) in 3 mL DCM at room temperature. After removal of the solvent under vacuum, the residue was heated to 80 °C under Ar and kept at that temperature for 18 h before it was cooled to room temperature. The resultant mixture was directly purified by column chromatography (petroleum ether:EtOAc = 1:1) to yield **1** (83 mg, 48%) as a colorless solid and a mixture of **2**, **14** and **15** as a colorless oil.

This mixture was subjected to HPLC for purification using MeOH/water (70:30, 3.0 mL/min) as eluent to give **2** (30 mg, 17%, colorless oil), **14** (15 mg, 9%, colorless oil), and **15** (12 mg, 7%, colorless oil).

Characterization data of 4:

R_f = 0.22 (silica, petroleum ether/EtOAc = 10:1);

^{1}H NMR (400 MHz, $CDCl_3$) δ 6.56 (ddd, J = 15.2, 11.1, 0.9 Hz, 1H), 6.39 (dd, J =

17.4, 10.6 Hz, 1H), 6.04 (d, *J* = 11.1 Hz, 1H), 5.87 (d, *J* = 15.2 Hz, 1H), 5.20 (d, *J* = 17.3 Hz, 1H), 5.03 (d, *J* = 10.6 Hz, 1H), 1.87 (d, *J* = 1.1 Hz, 3H), 1.35 (s, 6H);

^{13}C NMR (100 MHz, $CDCl_3$) δ 142.32, 141.27, 135.48, 130.79, 122.97, 112.68, 71.14, 29.99, 12.15;

IR (KBr) ν_{max} 3385, 2972, 1616, 1360, 1148, 986, 967, 890 cm^{-1};

HRMS (EI): Calculated for $C_{10}H_{16}O$ (M): 152.1196, Found: 152.1204.

Characterization data of synthetic 1:

R_f = 0.47 (silica, petroleum ether/EtOAc = 1:1.5);

^{1}H NMR (600 MHz, Methanol-*d*$_4$) δ 5.80 (dd, *J* = 15.1, 10.4 Hz, 1H), 5.73 (d, *J* = 15.1 Hz, 1H), 5.63 (s, 1H), 4.41 (dd, *J* = 7.0, 1.7 Hz, 1H), 3.22 (d, *J* = 10.1 Hz, 1H), 2.98 (d, *J* = 14.7 Hz, 1H), 2.90 – 2.88 (m, 1H), 2.87 (d, *J* = 14.8 Hz, 1H), 2.47 (dd, *J* = 19.1, 6.7 Hz, 1H), 2.44 – 2.40 (m, 1H), 2.32 (dd, *J* = 13.2, 5.9 Hz, 1H), 2.27 – 2.19 (m, 1H), 2.03 – 1.98 (m, 1H), 1.97 – 1.94 (m, 1H), 1.94 – 1.91 (m, 1H), 1.76 (t, *J* = 1.7 Hz, 3H), 1.74 (s, 3H), 1.64 (dt, *J* = 14.6, 1.5 Hz, 1H), 1.43 (s, 3H), 1.28 (s, 3H), 1.24 (s, 3H);

^{13}C NMR (125 MHz, Methanol-*d*$_4$) δ 209.97, 181.91, 170.16, 146.07, 137.76, 134.01, 123.96, 123.45, 91.29, 86.68, 85.95, 71.06, 56.14, 50.43, 50.37, 39.74, 37.03, 34.99, 30.18, 29.64, 27.50, 24.91, 23.64, 22.25, 7.89.;

$[\alpha]_D^{21}$: +41.67 (c = 0.66 in Methanol);

IR (KBr) ν_{max} 3464, 2971, 2929, 1769, 1702, 1655, 1382, 1340, 1274, 1211, 1022 cm^{-1};

HRMS (ESI): Calculated for $C_{25}H_{33}O_5$ $(M+H)^+$: 413.2323, Found: 413.2326.

Characterization data of synthetic 2:

R_f = 0.38 (silica, petroleum ether/EtOAc = 1:1.5);

^{1}H NMR (400 MHz, Methanol-*d*$_4$) δ 5.67 (d, *J* = 15.5 Hz, 1H), 5.63 (s, 1H), 5.45 (dd, *J* = 15.4, 9.1 Hz, 1H), 4.70 (dd, *J* = 6.9, 1.5 Hz, 1H), 2.92 – 2.83 (m, 1H), 2.76 (d, *J* = 14.7 Hz, 1H), 2.69 (d, *J* = 14.2 Hz, 1H), 2.67 (d, *J* = 9.4 Hz, 1H), 2.46 (dd, *J* = 19.0, 6.7 Hz, 1H), 2.32 – 2.21 (m, 2H), 2.05 – 1.98 (m, 2H), 2.02 – 1.96 (m, 1H), 1.92 (dd,

J = 19.1, 2.7 Hz, 1H), 1.74 (d, *J* = 1.8 Hz, 3H), 1.71 (t, *J* = 1.7 Hz, 3H), 1.61 (ddd, *J* = 14.6, 1.5 Hz, 1H), 1.41 (s, 3H), 1.25 (s, 3H), 1.24 (s, 3H);

^{13}C NMR (125 MHz, Methanol-*d*$_4$) δ 210.10, 179.88, 170.26, 142.37, 138.07, 133.74, 126.31, 124.39, 92.01, 87.36, 85.58, 71.10, 54.04, 50.44, 45.79, 39.54, 37.05, 33.01, 29.81, 29.61, 24.95, 23.05, 22.59, 21.09, 7.81;

$[\alpha]_D^{21}$: -78.00 (c = 0.30 in Methanol);

IR (KBr) ν_{max} 3446, 2969, 2924, 2852, 1769, 1703, 1656, 1382, 1338, 1017 cm^{-1};

HRMS (ESI): Calculated for $C_{25}H_{31}O_5$ $(M-H)^-$: 411.2177, Found: 411.2171.

Characterization data of 14:

R_f = 0.38 (silica, petroleum ether/EtOAc = 1:1.5);

^{1}H NMR (500 MHz, Methanol-*d*$_4$): See Table S4;

^{13}C NMR (125 MHz, Methanol-*d*$_4$): See Table S4;

$[\alpha]_D^{21}$: -36.36 (c = 0.22 in Methanol);

IR (KBr) ν_{max} 3360, 2922, 2851, 1703, 1658, 1633, 1469, 1411, 1271, 1164, 1075, 1035 cm^{-1};

HRMS (ESI): Calculated for $C_{25}H_{32}NaO_5$ $(M+Na)^+$: 435.2142, Found: 435.2137.

Characterization data of 15:

R_f = 0.38 (silica, petroleum ether/EtOAc = 1:1.5);

^{1}H NMR (500 MHz, Methanol-*d*$_4$): See Table S4;

^{13}C NMR (125 MHz, Methanol-*d*$_4$): See Table S4;

$[\alpha]_D^{21}$: +210.00 (c = 0.10 in Methanol);

IR (KBr) ν_{max} 3359, 2922, 2851, 1771, 1703, 1657, 1633, 1468, 1381, 1339, 1273, 1157, 1130, 1075 cm^{-1};

HRMS (ESI): Calculated for $C_{25}H_{32}NaO_5$ $(M+Na)^+$: 435.2142, Found: 435.2136.

Synthesis of compound 3

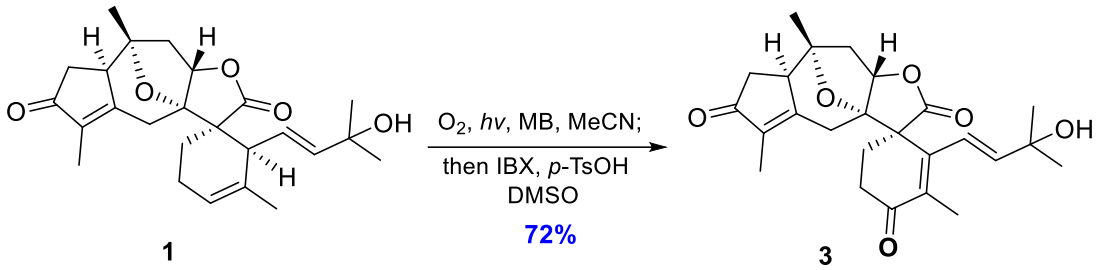

Orientanoid C (3): To an oxygen bubbled solution of orientanoid A **(1)** (31 mg, 0.073 mmol, 1.0 equiv) in MeCN (10.5 mL) at 0 °C was added methylene blue (3.4 mg, 0.01 mmol, 0.14 equiv). The reaction mixture was irradiated with an U-shaped fluorescent lamp (Essential 23 W, PHILIPS®, distance ~ 2 cm) at 0 °C until TLC showed complete consumption of the starting material. The reaction solution was concentrated in vacuo. To a stirred solution of the above residue in DMSO (1.8 mL) at room temperature was added sequentially *p*-toluenesulfonic acid (3.7 mg, 0.019 mmol, 0.27 equiv) and 2-Iodoxybenzoic acid (15.4 mg, 0.055 mmol, 0.75 equiv). The resulting mixture was stirred for 24 h at room temperature before it was quenched with H_2O. The aqueous layer was extracted with EtOAc. The combined organic layers were washed with brine, dried over anhydrous $NaSO_4$, filtered and concentrated by rotary evaporation. The residue was purified by FCC (petroleum ether:EtOAc = 1:1.5) to afford orientanoid C (**3**) (23 mg, 72% yield) as colorless solid.

Characterization data of synthetic 3:

R_f = 0.52 (silica, petroleum ether/EtOAc = 1:2);

^{1}H NMR (600 MHz, Methanol-*d*$_4$) δ 6.18 (d, J = 16.0 Hz, 1H), 6.06 (dd, J = 16.1, 1.2 Hz, 1H), 4.45 (dd, J = 7.2, 2.0 Hz, 1H), 2.96 – 2.89 (m, 1H), 2.80 – 2.77 (m, 1H), 2.75 (d, J = 14.7 Hz, 1H), 2.67 – 2.62 (m, 1H), 2.62 – 2.59 (m, 1H), 2.59 (d, J = 14.6 Hz, 1H), 2.47 (dd, J = 19.0, 6.8 Hz, 1H), 2.41 – 2.34 (m, 1H), 2.11 (dd, J = 14.7, 7.2 Hz, 1H), 1.96 (d, J = 1.1 Hz, 3H), 1.94 (dd, J = 19.1, 2.8 Hz, 1H), 1.72 (dt, J = 14.7, 1.7 Hz, 1H), 1.67 (t, J = 1.6 Hz, 3H), 1.47 (s, 3H), 1.34 (s, 3H), 1.32 (s, 3H);

^{13}C NMR (125 MHz, Methanol-*d*$_4$) δ 209.64, 199.37, 178.81, 168.85, 150.66, 148.11, 138.45, 136.59, 122.15, 90.76, 87.82, 86.61, 71.41, 57.43, 50.13, 39.43, 36.94, 34.51, 34.16, 29.62, 29.58, 27.52, 24.83, 13.62, 8.07;

[α]$_D^{21}$: +173.07 (c=0.32 in Methanol);

IR (KBr) ν_{max} 3446, 2971, 2925, 2854, 1771, 1704, 1660, 1382, 1353, 1338, 1208, 1072 cm^{-1};

HRMS (ESI): Calculated for $C_{25}H_{31}O_6$ $(M+H)^+$: 427.2115, Found: 427.2121.

4. Biological Assays and Data

Materials and methods

Cell culture. RAW 264.7, E0771 and Hepa1-6 cells were obtained from the American Type Culture Collection (USA). All cell lines in this study were maintained in the appropriate medium as suppliers suggested and were authenticated via single-nucleotide polymorphism (SNP) analysis with the latest test in December 2022 (Crown Bioscience, China).

Macrophages culture and stimulation. The protocols for animal handling were approved by the Institutional Animal Care and Use Committee at Shanghai Institute of Materia Medica and performed according to the institutional ethical guidelines on animal care. Bone marrow cells were isolated from the tibia and femur of 6–8 weeks old female C57BL/6 mice, seeded at a density of 2×10^6 cells/well in a 6-well plate and differentiated in the presence of M-CSF (20 ng/mL) and 10% fetal bovine serum in IMDM growth medium for 7 days. The medium was changed every three days. To fully polarize M2 macrophages, macrophages were stimulated with 20 ng/mL IL-4/IL-13. In certain experiments, macrophages were treated with different concentrations of compounds.

Quantitative real-time PCR (RT-PCR). Total RNA was isolated from cells using the EZ-press RNA Purification Kit (EZBioscience, China) and subjected to reverse transcription with 5×HiScript II qRT SuperMix II (Vazyme, China). PCR was performed with 2×ChamQ Universal SYBR qPCR Master Mix (Vazyme, China). All primers for qRT-PCR are described in Table S18.

Table S18. RT-PCR primer sequences.

Primer[a]	Sequence (5' to 3' direction)
ARG1-F	CATATCTGCCAAAGACATCGTG
ARG1-R	GACATCAAAGCTCAGGTGAATC
MRC1-F	CCTATGAAAATTGGGCTTACGG
MRC1-R	CTGACAAATCCAGTTGTTGAGG
CD163-F	GTTTGTGGAGCCATTCTATTGG
CD163-R	GGAAACTGTAAGTCGCTGAATC
β-actin-F	ATCACTATTGGCAACGAGCGGTTC
β-actin-R	CAGCACTGTGTTGGCATAGAGGTC
VEGF-F	GCACATAGAGAGAATGAGCTTCC
VEGF-R	CTCCGCTCTGAACAAGGCT

[a]F = Forward Primer, R = Reverse Primer.

Cell proliferation assay. Cells were seeded in 96-well tissue culture plates. On the next day, cells were exposed to various concentrations of compounds and further cultured for indicated period. Finally, cell proliferation was determined by using Cell Counting Kit (CCK-8) assay.

$CD8^+$ T cells suppression assay. Spleen cells were isolated from C57BL/6 mice, followed by red blood cell (RBC) lysis. BMDMs were induced to M2-like macrophages and treated with different concentrations of compound 1 for 48 h. Then, 1.5×10^5 spleen cells/well were stimulated with αCD3/αCD28 /IL-2 and co-cultured with 1×10^4 pro-treated BMDMs in 96-well plates in LCM (RPMI 1640 with 50 mM 2-mercaptoethanol and 10% fetal bovine serum) at 37 °C. After 72 h, the spleen cells were treated with eBioscience™ Cell Stimulation Cocktail (plus protein transport inhibitors) for 4 h, and cells activation was then determined by the proportion of $IFN\gamma^+$ $CD8^+$ T cells and $granzymeB^+$ $CD8^+$ T cells in $CD8^+$ T cells by flow cytometry.

Cell proliferation was determined by the proportion of $Ki67^+$ $CD8^+$ T cells in $CD8^+$ T cells by flow cytometry.

In vivo antitumor efficacy. Animal procedures were approved by the Institutional Animal Care and Use Committee of the Shanghai Institute of Materia Medica (approval No. 2022-06-DJ-68 and No. 2022-06-DJ-69). Mice (4–6 weeks-old) were housed five or six mice per cage in a specific pathogen-free room with a 12 h light/dark schedule at 25°C ± 1°C and were fed an autoclaved chow diet and water ad libitum. E0771 cells ($2x10^6$ cells) and Hepa1-6 cells ($2x10^6$ cells) were subcutaneously implanted in the right flank of C57 BL/6 mice. Hepa1-6 cells ($2x10^6$ cells) were subcutaneously implanted in the right flank of BALB/c nu/nu mice. When the tumors reached a volume of around 50 mm^3, mice were randomized into each treatment group, vehicle groups were given vehicle alone, and treatment groups received compound **1** as indicated doses via intratumoral injection once daily for indicated days. The tumor volumes and body weights were measured twice per week. Tumor volume (TV) was calculated as follows: $TV = (\text{length} \times \text{width}^2)/2$, and the individual relative tumor volume (RTV) was calculated as follows: $RTV = V_t / V_0$, where V_t is the volume on a particular day and V_0 is the volume at the beginning of the treatment. Significant differences between the treated versus the vehicle groups were determined using Student's *t*-test.

For analyses of tumor-infiltrating immune cells, E0771 tumor tissues were minced and digested using a Mouse Tumor Dissociation Kit (Miltenyi, Germany). In analysis of the tumor infiltration immune cell as shown in panels **c-i**, due to the limited tumor size, five individual tumor samples were merged as two samples in the compound **1**-treated group and two individual tumor tissues were merged into one sample in the vehicle group. In addition, the cell viability of two individual tumor in vehicle group is too low that was below the analytical limit of detection, so they were excluded. Thus, the samples number in Fig. 6c shown as 6 per group. The cells were passed through a 70 μm cell strainer, stained with a fluorescent antibody or the matching isotype controls for 30 min at room temperature and then tested using a BD LSRFortessa^{TM}. Antibodies specific for the following proteins and the matching

isotype control or FMO control were used to analyze the leukocyte infiltrate: CD45, CD11b, F4/80, CD206, CD3e, CD8a, CD4, IFNγ, and TNFα (BD, eBioscience and Biolegend). Viability was determined by staining with either the LIVE/DEAD® Fixable Violet Dead Cell Stain Kit (Invitrogen) or the Zombie Aqua™ Fixable Viability Kit (Biolegend). Data were analyzed using FlowJo10.4 software.

Statistical Analysis. Statistical analysis in this paper was conducted using GraphPad Prism 9 software (version 9.0.0; GraphPad Software, La Jolla, CA, USA).

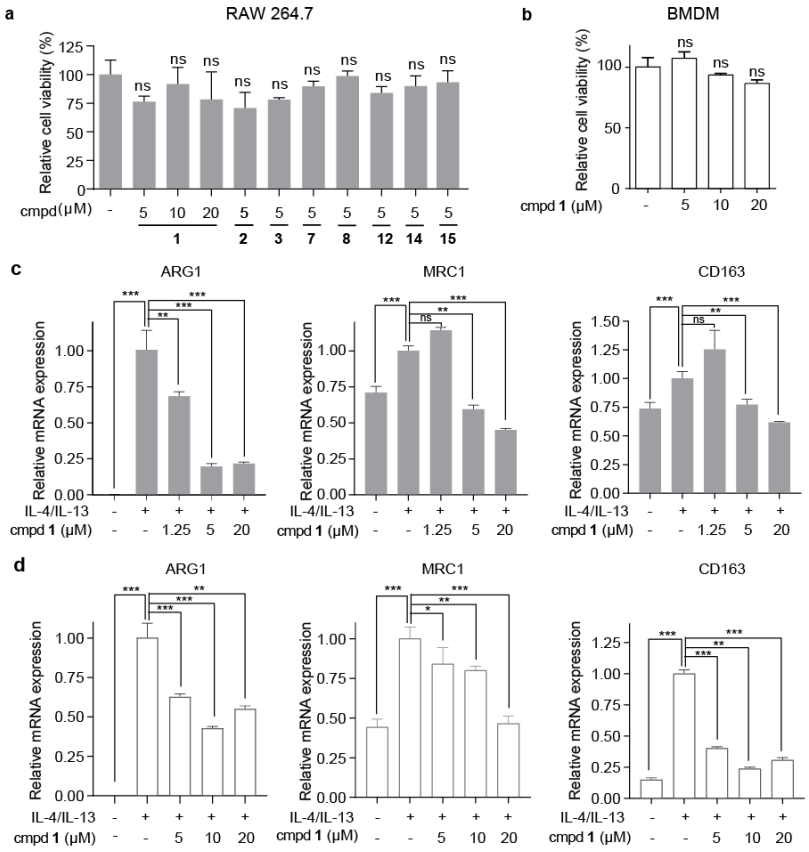

Fig. S7. (**a**, **b**) The effect of compounds on cell viability of RAW 264.7 cells and BMDMs. RAW 264.7 cells (**a**) and BMDM (**b**) were treated with indicated compounds for 48 h and cell viability was detected by CCK8 assay. ns, $P > 0.05$ vs vehicle control group. (**c**, **d**) qRT-PCR analysis of ARG1, MRC1, CD163 mRNA level in RAW264.7 cells (**c**) and BMDMs (**d**) stimulated with IL-4/IL-13 alone or combined with compound **1** for 12 h. Data represent means ± SD from triplicates. *$P < 0.05$, **$P < 0.01$, ***$P < 0.001$, ns, $P > 0.05$, determined by Student's *t*-test.

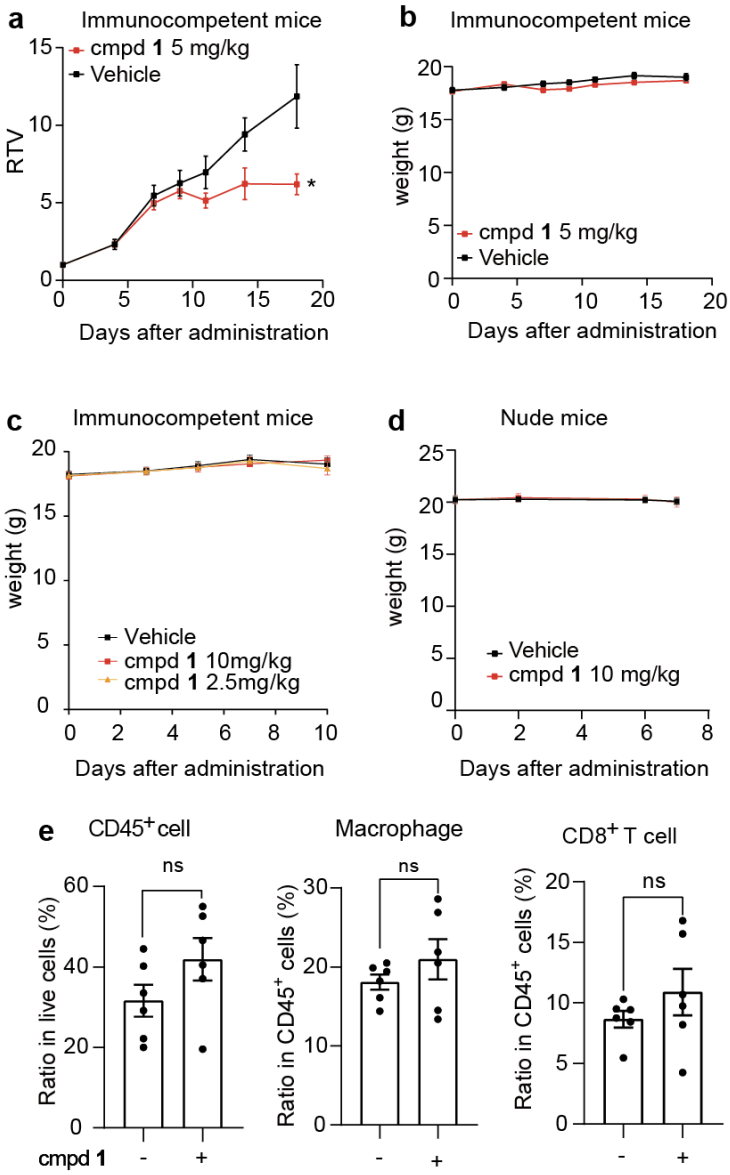

Fig. S8. *In vivo* antitumor effect of compound 1. (**a**, **b**) Immune-competent mice bearing E0771 xenograft were intratumorally administrated with compound **1** at 5 mg/kg or vehicle daily for 18 days (n = 9 per group). The relative tumor volume (RTV) **(a)** and body weight **(b)** shown as the mean ± SEM. (**c**, **d**) Body weights of immune-competent mice bearing Hepa1-6 xenograft (**c**) and nude mice bearing Hepa1-6 xenograft (**d**) related to the **Fig. 5a**,**b**. Data are shown as mean ± SEM. (**e**) Flow cytometric analysis of tumor infiltrated immune cell subsets in the E0771 tumor model treated with compound **1** (5 mg/kg) (n = 6 per group). Data are shown as the mean ± SEM. *P < 0.05, ns P > 0.05 vs the vehicle group, determined by Student's *t*-test.

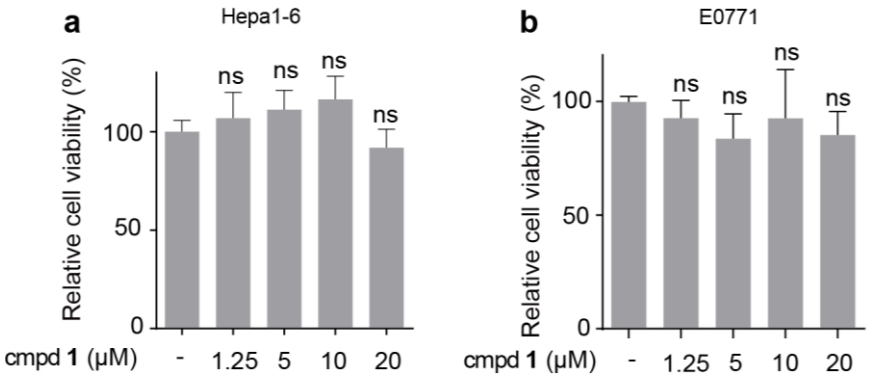

Fig. S9. The effect of compound 1 on Hepa1-6 cells and E0771 cells viability. Hepa1-6 cells (**a**) and E0771 cells (**b**) were treated with compound **1** for 72 h and cell viability was detected by CCK8 assay. Data represent means ± SD from triplicates. ns, $P > 0.05$ vs control vehicle group. P values were determined by Student's *t*-test.

Gating strategy. The gating strategy in flow cytometry experiments is shown as below (Figs. S10–S11). Data were analyzed using FlowJo10.4 software.

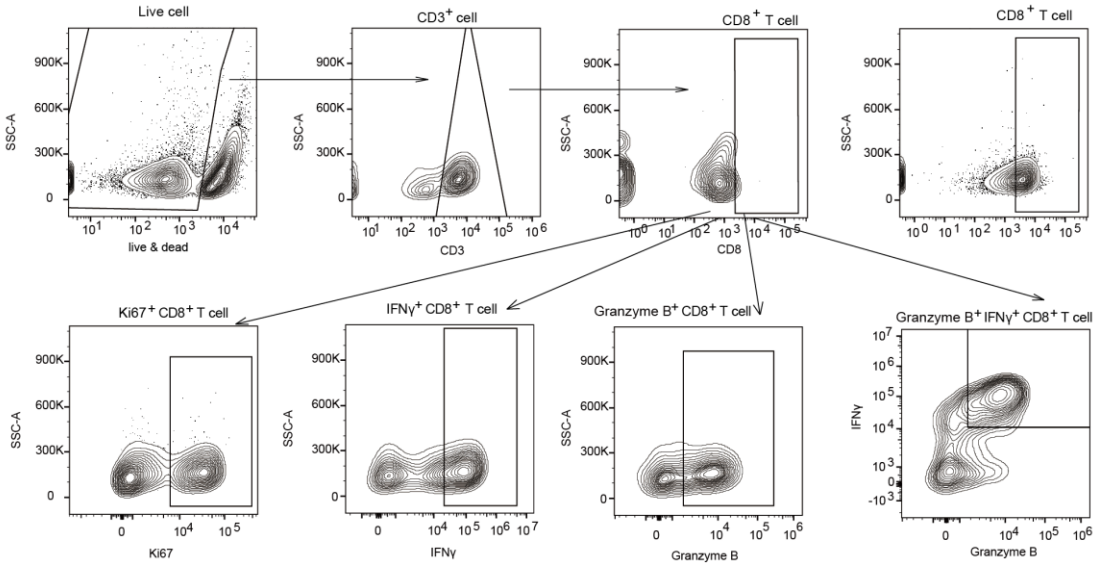

Fig. S10. The gating strategy for CD8$^+$ T cells in Fig. 9. CD8$^+$ T cells were identified by FMO control.

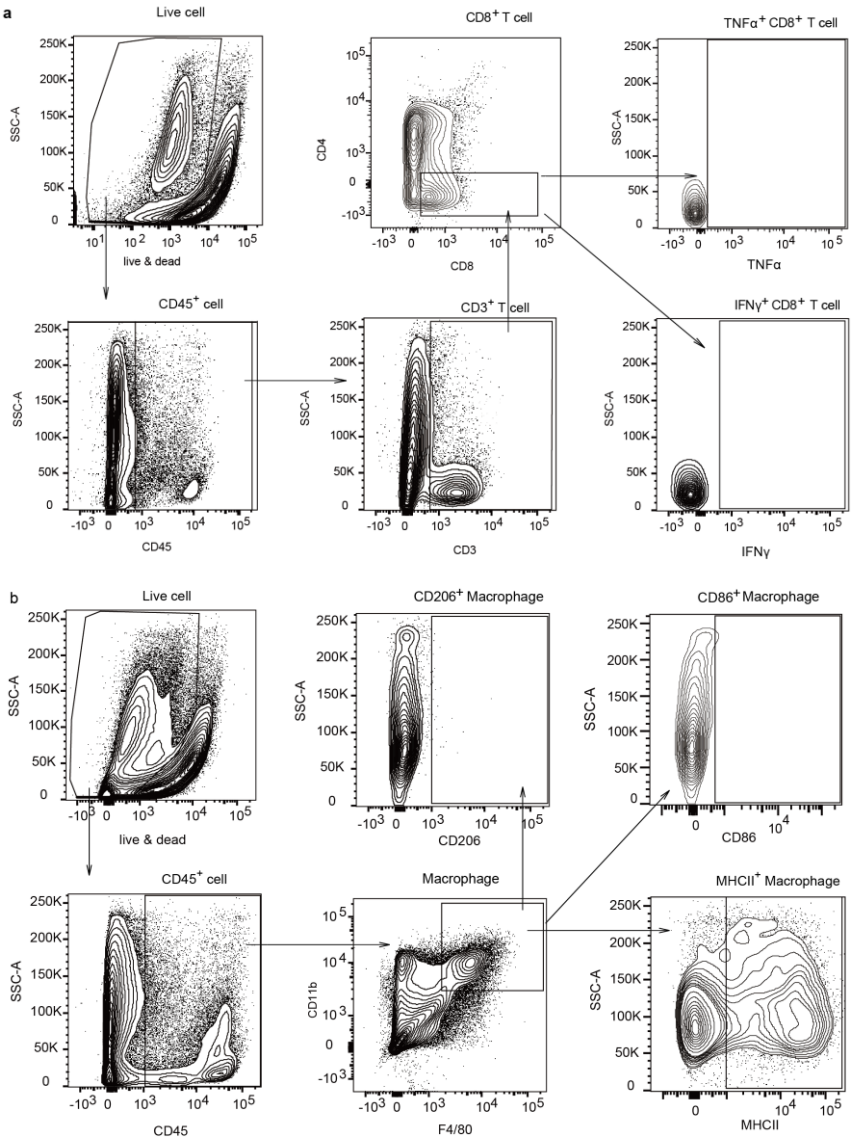

Fig. S11. The gating strategies for CD8$^+$ T cell (a) and Macrophage (b) in flow cytometry analyses of tumor-infiltrating immune cells in Fig. 5. TNFα$^+$ CD8$^+$ T cell, IFNγ$^+$ CD8 T cell, CD206$^+$ Macrophage, CD86$^+$ Macrophage were identified by FMO control.

5. X-Ray Crystallographic Data for Synthetic Compounds

Table S19. Crystal data and structure refinement for compound 9

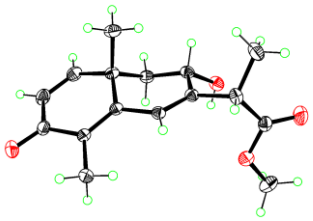

X-ray Crystal Structure for compound **9** (CCDC 2216319)

Identification code	ZZ
Empirical formula	$C_{16}H_{20}O_4$
Formula weight	276.32
Temperature/K	170.00
Crystal system	orthorhombic
Space group	$P2_12_12_1$
a/Å	10.2733(2)
b/Å	10.3627(2)
c/Å	13.3957(3)
α/°	90
β/°	90
γ/°	90
Volume/Å^3	1426.09(5)
Z	4
ρ_{calc}g/cm^3	1.287
μ/mm^{-1}	0.748
F(000)	592.0
Crystal size/mm^3	0.15 × 0.08 × 0.05
Radiation	CuKα (λ = 1.54178)
2Θ range for data collection/°	10.794 to 149.438
Index ranges	-12 ≤ h ≤ 12, -12 ≤ k ≤ 12, -16 ≤ l ≤ 16
Reflections collected	14626
Independent reflections	2912 [R_{int} = 0.0411, R_{sigma} = 0.0277]
Data/restraints/parameters	2912/0/186
Goodness-of-fit on F^2	1.066
Final R indexes [I>=2σ (I)]	R_1 = 0.0325, wR_2 = 0.0849
Final R indexes [all data]	R_1 = 0.0342, wR_2 = 0.0869
Largest diff. peak/hole / e Å^{-3}	0.22/-0.18
Flack parameter	-0.07(9)

Table S20. Crystal data and structure refinement for compound 6

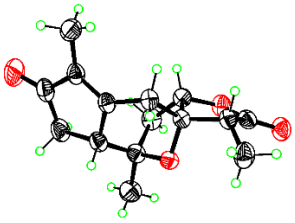

X-ray Crystal Structure for compound **6** (CCDC 2002637)

Identification code	cu_22020154_0m
Empirical formula	$C_{15}H_{18}O_4$
Formula weight	262.29
Temperature/K	298.0
Crystal system	monoclinic
Space group	$P2_1$
a/Å	6.4115(5)
b/Å	6.9501(5)
c/Å	15.4228(12)
α/°	90
β/°	100.540(4)
γ/°	90
Volume/Å^3	675.65(9)
Z	2
ρ_{calc}g/cm^3	1.289
μ/mm^{-1}	0.763
F(000)	280.0
Crystal size/mm^3	0.16 × 0.09 × 0.06
Radiation	CuKα (λ = 1.54178)
2Θ range for data collection/°	5.828 to 149.586
Index ranges	$-8 \le h \le 8$, $-8 \le k \le 8$, $-19 \le l \le 19$
Reflections collected	17282
Independent reflections	2732 [R_{int} = 0.0384, R_{sigma} = 0.0245]
Data/restraints/parameters	2732/1/175
Goodness-of-fit on F^2	1.059
Final R indexes [I>=2σ (I)]	R_1 = 0.0320, wR_2 = 0.0794
Final R indexes [all data]	R_1 = 0.0332, wR_2 = 0.0807
Largest diff. peak/hole / e Å^{-3}	0.14/-0.13
Flack parameter	-0.05(6)

Table S21. Crystal data and structure refinement for compound 10

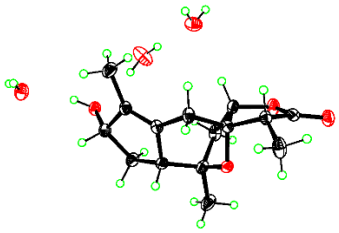

X-ray Crystal Structure for compound **10** (CCDC 2022064)

Identification code	cu_22020479_0m
Empirical formula	$C_{15}H_{26}O_7$
Formula weight	318.36
Temperature/K	170.0
Crystal system	orthorhombic
Space group	$P2_12_12_1$
a/Å	6.7959(2)
b/Å	10.8224(3)
c/Å	22.5827(6)
α/°	90
β/°	90
γ/°	90
Volume/Å^3	1660.91(8)
Z	4
ρ_{calc}g/cm^3	1.273
μ/mm^{-1}	0.841
F(000)	688.0
Crystal size/mm^3	0.15 × 0.08 × 0.05
Radiation	CuKα (λ = 1.54178)
2Θ range for data collection/°	7.83 to 149.248
Index ranges	$-8 \le h \le 8$, $-13 \le k \le 13$, $-27 \le l \le 28$
Reflections collected	14858
Independent reflections	3388 [R_{int} = 0.0586, R_{sigma} = 0.0424]
Data/restraints/parameters	3388/3/221
Goodness-of-fit on F^2	1.052
Final R indexes [I>=2σ (I)]	R_1 = 0.0456, wR_2 = 0.1138
Final R indexes [all data]	R_1 = 0.0519, wR_2 = 0.1200
Largest diff. peak/hole / e Å^{-3}	0.25/-0.25
Flack parameter	-0.08(11)

Table S22. Crystal data and structure refinement for compound 11

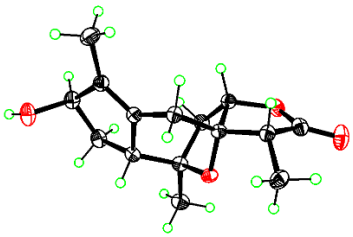

X-ray Crystal Structure for compound **11** (CCDC 2022065)

Identification code	cu_22020436_0m
Empirical formula	$C_{15}H_{20}O_4$
Formula weight	264.31
Temperature/K	150.0
Crystal system	tetragonal
Space group	$P4_3$
a/Å	13.0969(2)
b/Å	13.0969(2)
c/Å	8.2344(2)
α/°	90
β/°	90
γ/°	90
Volume/Å^3	1412.44(6)
Z	4
ρ_{calc}g/cm^3	1.243
μ/mm^{-1}	0.730
F(000)	568.0
Crystal size/mm^3	0.15 × 0.12 × 0.08
Radiation	CuKα (λ = 1.54178)
2Θ range for data collection/°	6.748 to 144.562
Index ranges	-16 ≤ h ≤ 16, -16 ≤ k ≤ 16, -9 ≤ l ≤ 10
Reflections collected	17538
Independent reflections	2714 [R_{int} = 0.0372, R_{sigma} = 0.0223]
Data/restraints/parameters	2714/1/179
Goodness-of-fit on F^2	1.070
Final R indexes [I>=2σ (I)]	R_1 = 0.0273, wR_2 = 0.0716
Final R indexes [all data]	R_1 = 0.0274, wR_2 = 0.0716
Largest diff. peak/hole / e Å^{-3}	0.16/-0.13
Flack parameter	0.03(4)

Table S23. Crystal data and structure refinement for compound 5

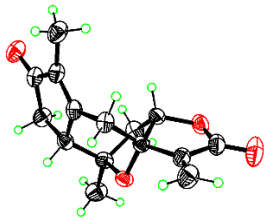

X-ray Crystal Structure for compound **5** (CCDC 2002638)

Identification code	cu_22020155_0m
Empirical formula	$C_{15}H_{16}O_4$
Formula weight	260.28
Temperature/K	298
Crystal system	orthorhombic
Space group	$P2_12_12_1$
a/Å	10.4619(19)
b/Å	10.6895(19)
c/Å	11.617(2)
α/°	90
β/°	90
γ/°	90
Volume/Å^3	1299.1(4)
Z	4
ρ_{calc}g/cm^3	1.331
μ/mm^{-1}	0.793
F(000)	552.0
Crystal size/mm^3	0.16 × 0.08 × 0.05
Radiation	CuKα (λ = 1.54178)
2Θ range for data collection/°	11.248 to 149.816
Index ranges	$-12 \le h \le 12$, $-13 \le k \le 12$, $-14 \le l \le 14$
Reflections collected	22909
Independent reflections	2651 [R_{int} = 0.0647, R_{sigma} = 0.0327]
Data/restraints/parameters	2651/0/174
Goodness-of-fit on F^2	1.053
Final R indexes [I>=2σ (I)]	R_1 = 0.0438, wR_2 = 0.1129
Final R indexes [all data]	R_1 = 0.0455, wR_2 = 0.1151
Largest diff. peak/hole / e Å^{-3}	0.20/-0.23
Flack parameter	0.09(8)

Table S24. Crystal data and structure refinement for synthetic compound 1

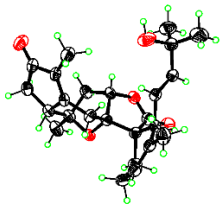

X-ray Crystal Structure for synthetic compound **1** (CCDC 2002639)

Identification code	mj20178_0m
Empirical formula	$C_{25}H_{32}O_5$
Formula weight	412.50
Temperature/K	200
Crystal system	orthorhombic
Space group	$P2_12_12_1$
a/Å	9.1292(6)
b/Å	9.1825(6)
c/Å	26.7030(16)
α/°	90
β/°	90
γ/°	90
Volume/Å^3	2238.5(2)
Z	4
ρ_{calc}g/cm^3	1.224
μ/mm^{-1}	0.435
F(000)	888.0
Crystal size/mm^3	0.12 × 0.08 × 0.06
Radiation	GaKα (λ = 1.34139)
2Θ range for data collection/°	5.758 to 110.134
Index ranges	$-11 \leq h \leq 8$, $-11 \leq k \leq 11$, $-32 \leq l \leq 32$
Reflections collected	19853
Independent reflections	4207 [R_{int} = 0.0426, R_{sigma} = 0.0321]
Data/restraints/parameters	4207/0/277
Goodness-of-fit on F^2	1.072
Final R indexes [I>=2σ (I)]	R_1 = 0.0546, wR_2 = 0.1217
Final R indexes [all data]	R_1 = 0.0718, wR_2 = 0.1352
Largest diff. peak/hole / e Å^{-3}	0.20/-0.25
Flack parameter	-0.03(10)

Table S25. Crystal data and structure refinement for compound 14

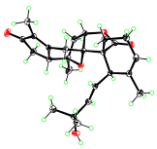

X-ray Crystal Structure for compound **14** (CCDC 2181591)

Identification code	cu_2022538_0m
Empirical formula	$C_{25}H_{32}O_5$
Formula weight	412.50
Temperature/K	150.0
Crystal system	orthorhombic
Space group	$P2_12_12_1$
a/Å	6.9481(2)
b/Å	15.6259(4)
c/Å	20.1605(4)
α/°	90
β/°	90
γ/°	90
Volume/Å^3	2188.83(9)
Z	4
ρ_{calc}g/cm^3	1.252
μ/mm^{-1}	0.692
F(000)	888.0
Crystal size/mm^3	0.12 × 0.08 × 0.05
Radiation	CuKα (λ = 1.54178)
2Θ range for data collection/°	7.158 to 160.046
Index ranges	$-8 \le h \le 8$, $-19 \le k \le 19$, $-25 \le l \le 25$
Reflections collected	38753
Independent reflections	4706 [R_{int} = 0.0529, R_{sigma} = 0.0254]
Data/restraints/parameters	4706/0/277
Goodness-of-fit on F^2	1.049
Final R indexes [I>=2σ (I)]	R_1 = 0.0320, wR_2 = 0.0738
Final R indexes [all data]	R_1 = 0.0353, wR_2 = 0.0763
Largest diff. peak/hole / e Å^{-3}	0.22/-0.18
Flack parameter	0.08(7)

Table S26. Crystal data and structure refinement for synthetic compound 3

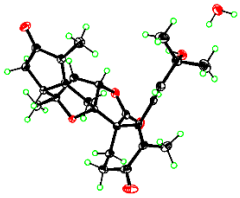

X-ray Crystal Structure for synthetic compound **3** (CCDC 2013505)

Identification code	mj20335_0m
Empirical formula	$C_{25}H_{31}O_{6.5}$
Formula weight	435.50
Temperature/K	172.99
Crystal system	orthorhombic
Space group	$P2_12_12$
a/Å	12.2867(14)
b/Å	21.497(3)
c/Å	9.6289(11)
α/°	90
β/°	90
γ/°	90
Volume/Å^3	2543.2(5)
Z	4
ρ_{calc}g/cm^3	1.137
μ/mm^{-1}	0.429
F(000)	932.0
Crystal size/mm^3	0.18 × 0.09 × 0.08
Radiation	GaKα (λ = 1.34139)
2Θ range for data collection/°	7.21 to 109.73
Index ranges	$-13 \leq h \leq 14$, $-26 \leq k \leq 26$, $-11 \leq l \leq 11$
Reflections collected	27725
Independent reflections	4808 [R_{int} = 0.0442, R_{sigma} = 0.0275]
Data/restraints/parameters	4808/0/291
Goodness-of-fit on F^2	1.086
Final R indexes [I>=2σ (I)]	R_1 = 0.0278, wR_2 = 0.0728
Final R indexes [all data]	R_1 = 0.0282, wR_2 = 0.0733
Largest diff. peak/hole / e Å^{-3}	0.15/-0.20
Flack parameter	-0.02(4)

6. Spectral Data

Fig. S12. ^{1}H NMR spectrum of natural orientanoid A (**1**) in Methanol-d_4.

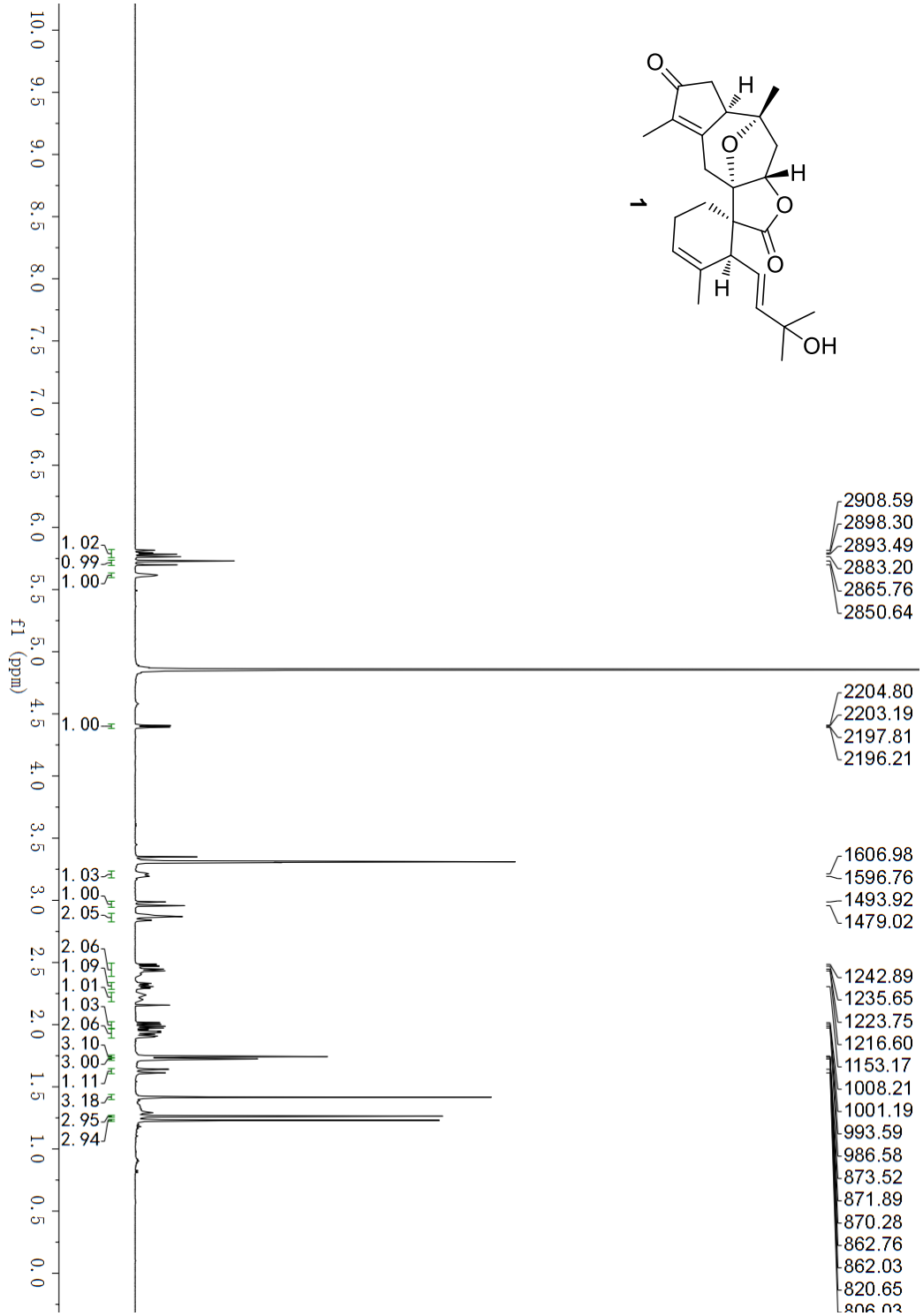

Fig. S13. ^{13}C NMR spectrum of natural orientanoid A (**1**) in Methanol-d_4.

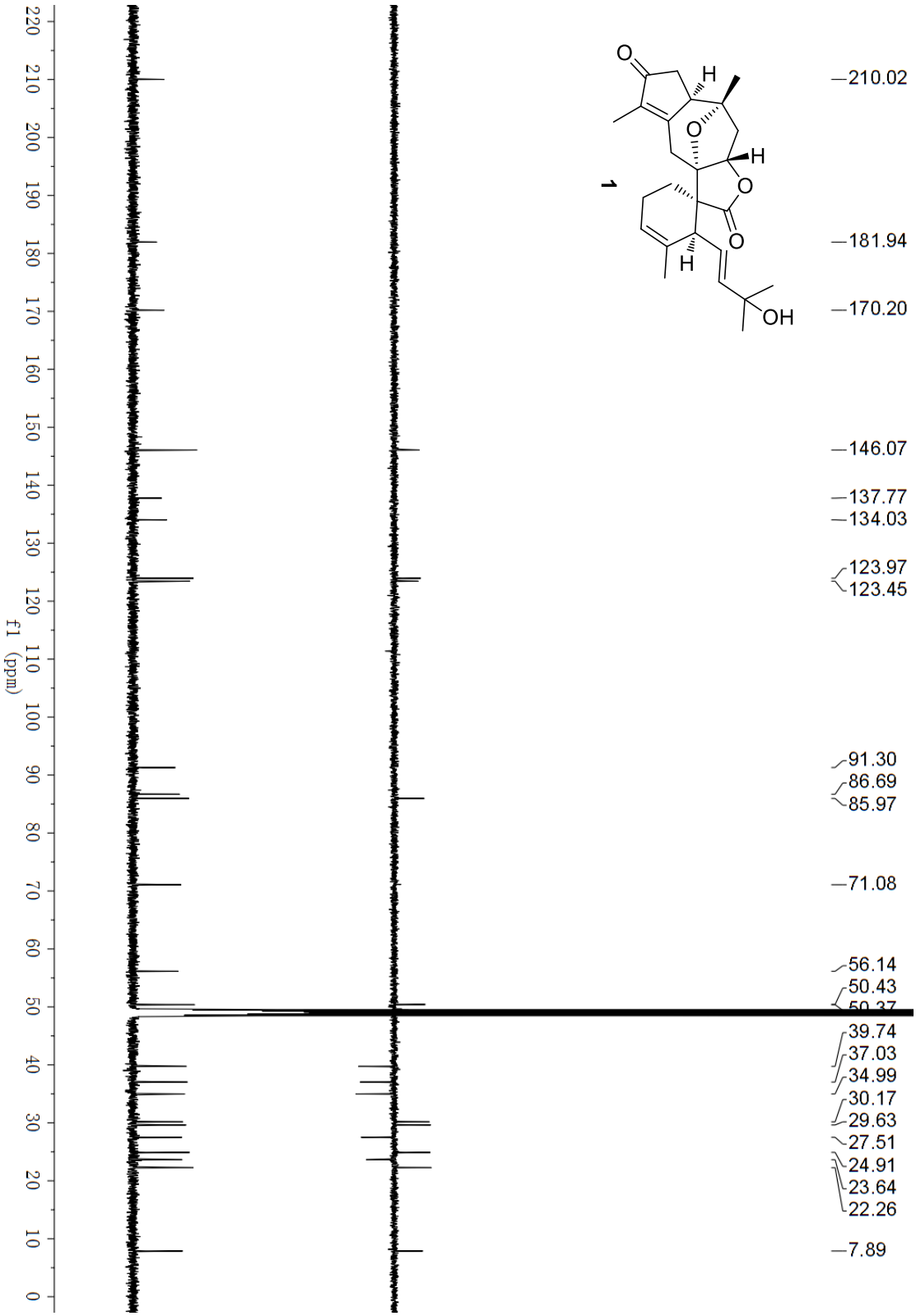

Fig. S14. ^{1}H–^{1}H COSY spectrum of natural orientanoid A (**1**) in Methanol-d_4.

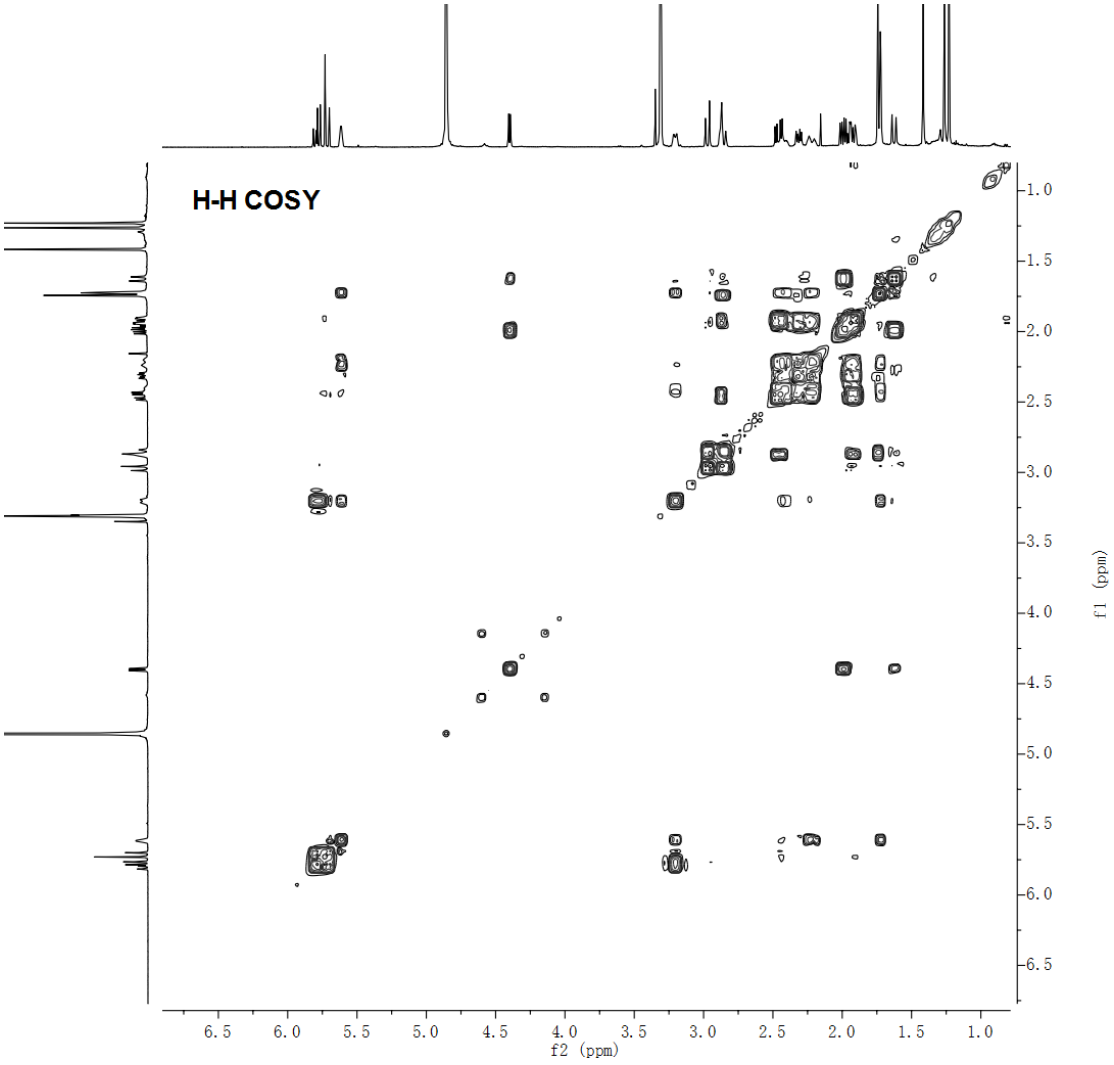

Fig. S15. HSQC spectrum of natural orientanoid A (**1**) in Methanol-d_4.

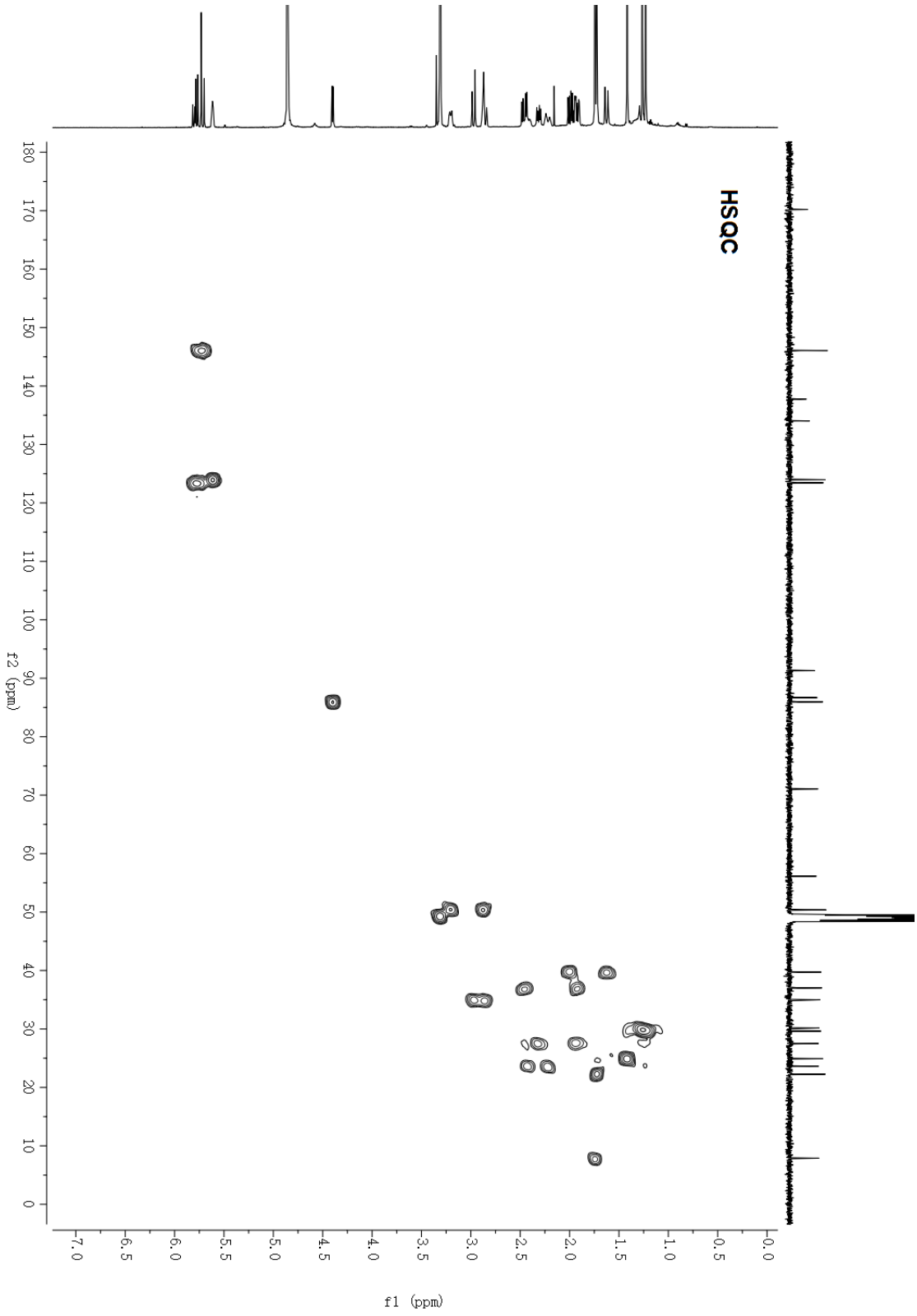

Fig. S16. HMBC spectrum of natural orientanoid A (**1**) in Methanol-d_4.

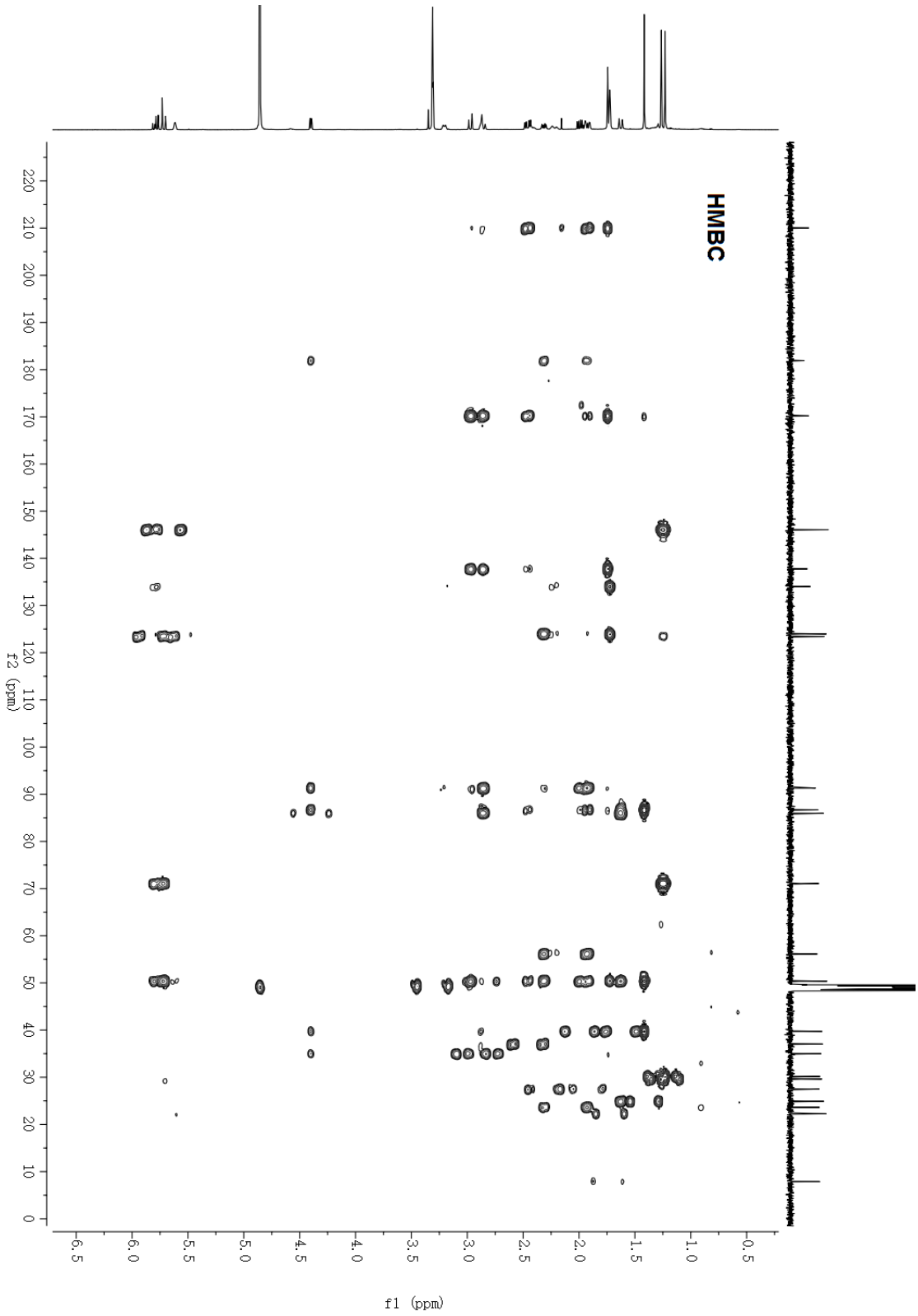

Fig. S17. NOESY spectrum of natural orientanoid A (**1**) in Methanol-d_4.

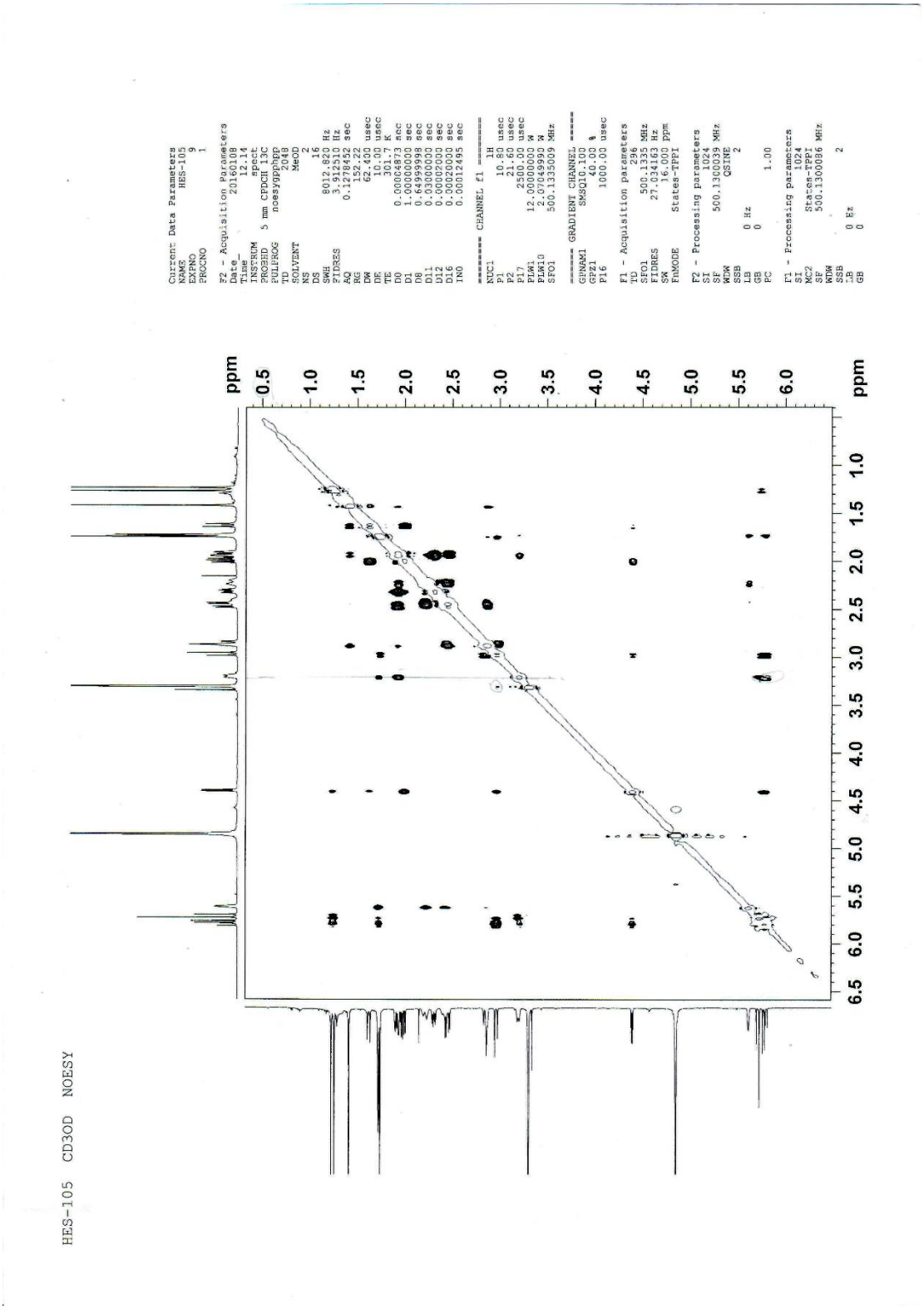

Fig. S18. (+)-ESIMS spectrum of natural orientanoid A (**1**).

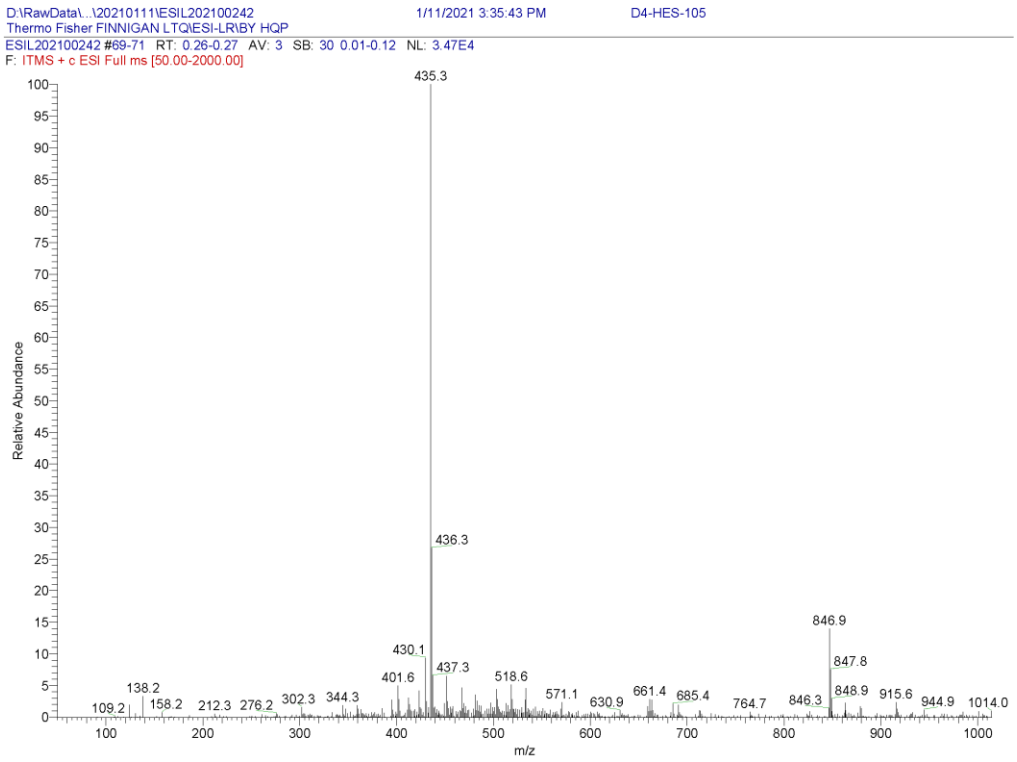

Fig. S19. (+)-HRESIMS spectrum of natural orientanoid A (**1**).

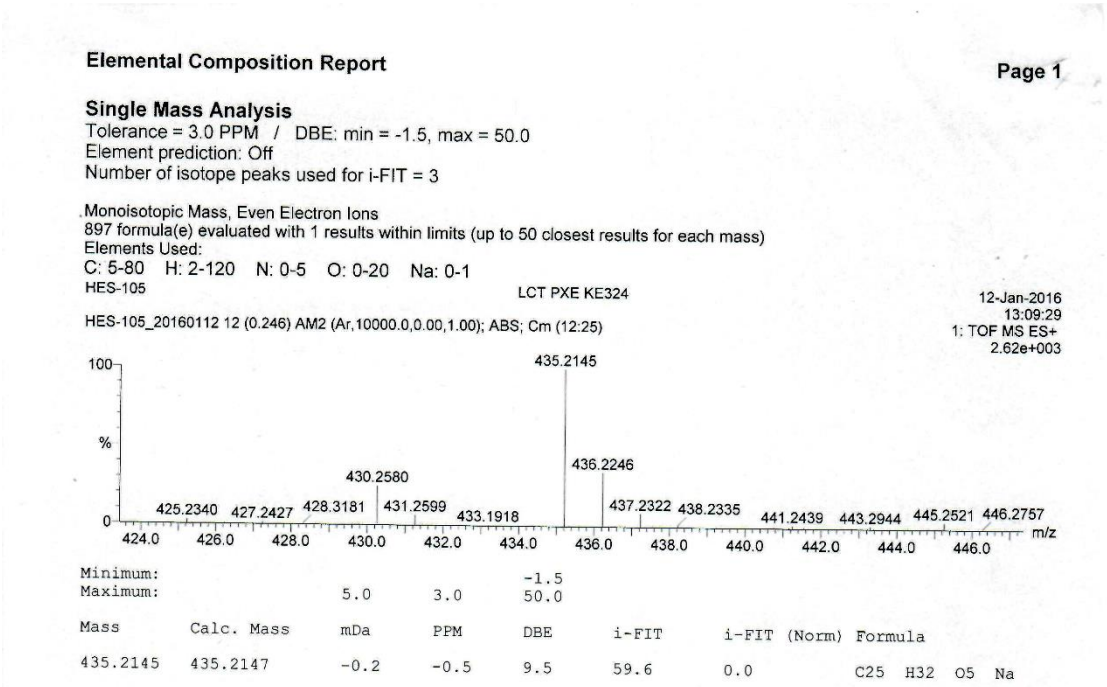

Fig. S20. IR spectrum of natural orientanoid A (**1**).

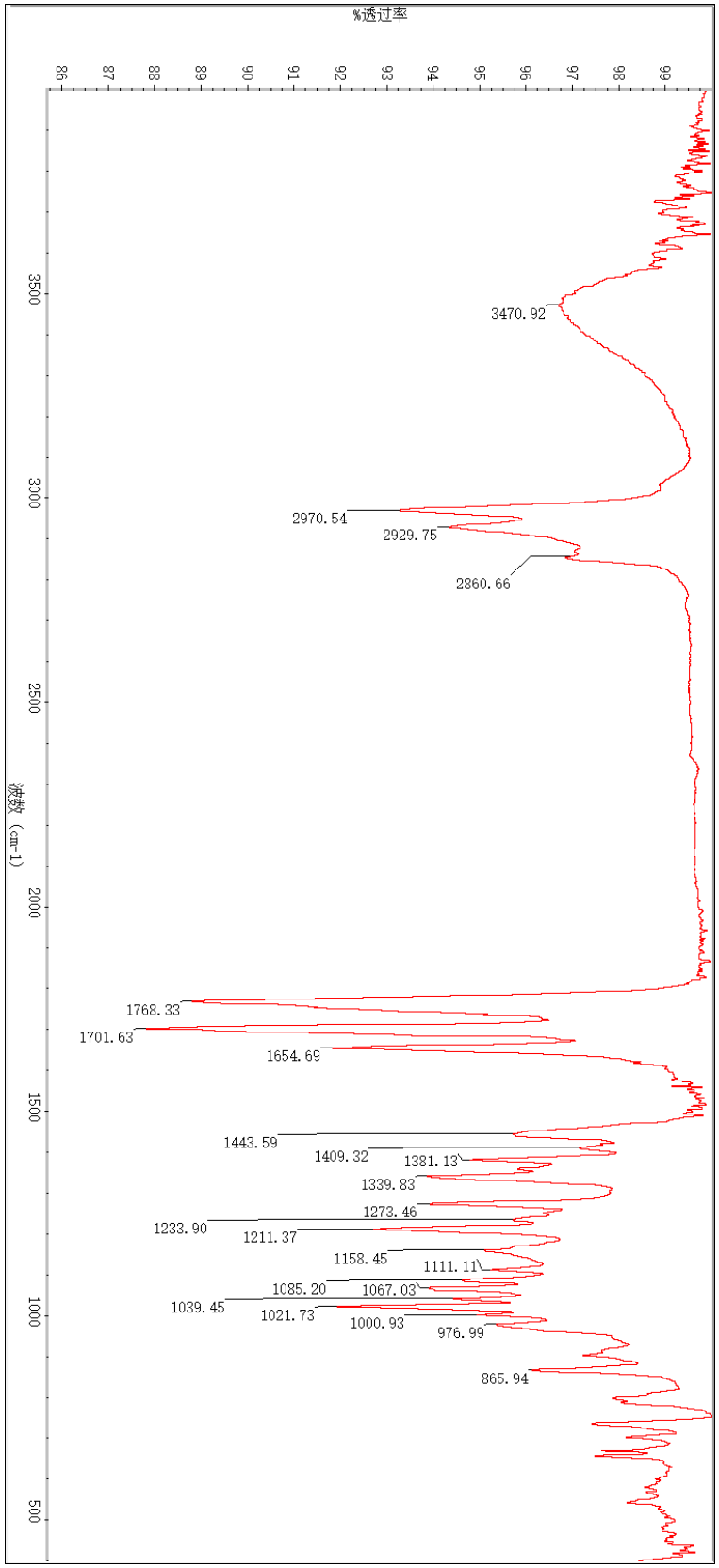

Fig. S21. [1]H NMR spectrum of natural orientanoid B (**2**) in Methanol-d_4.

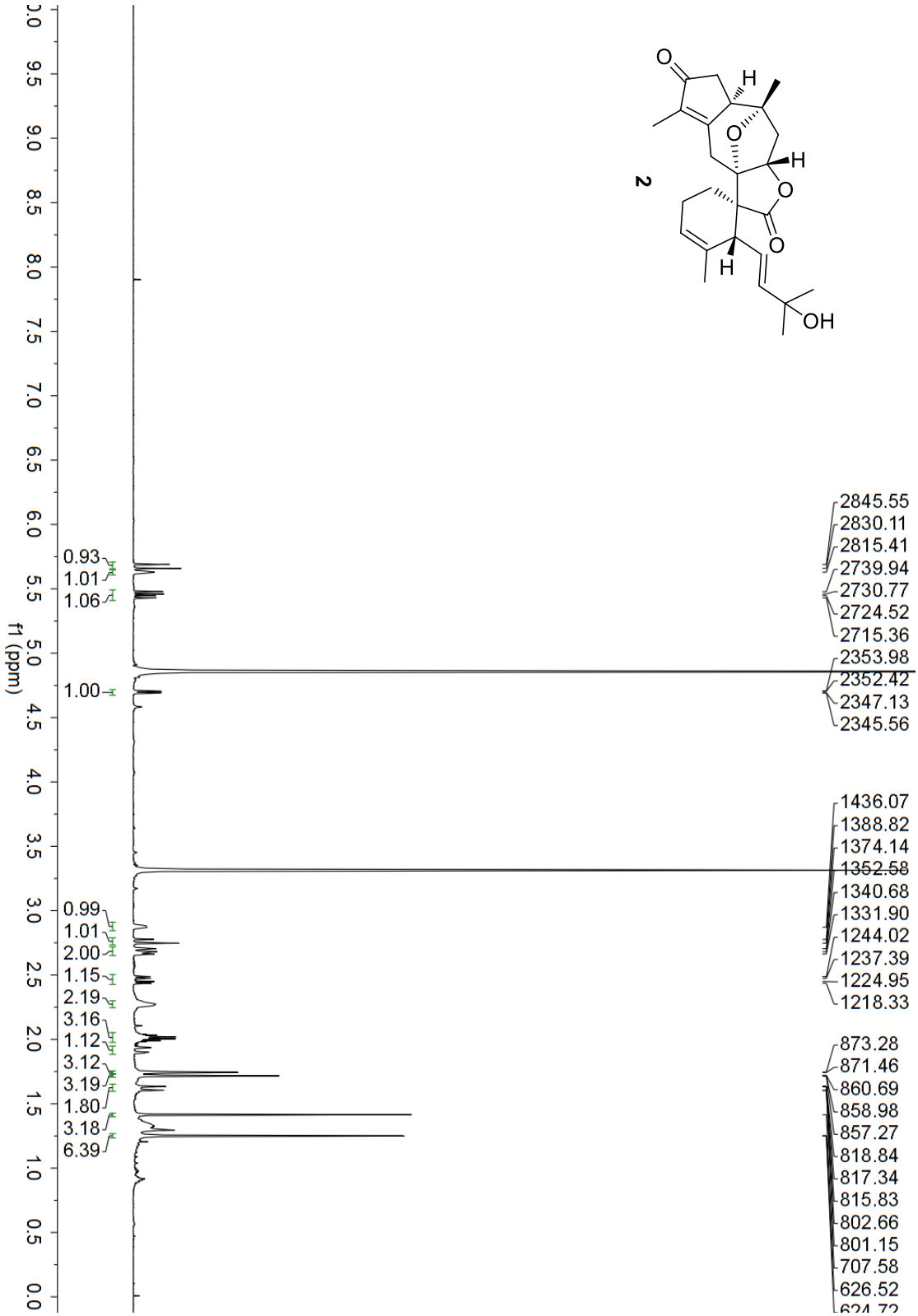

Fig. S22. ^{13}C NMR spectrum of natural orientanoid B (**2**) in Methanol-d_4.

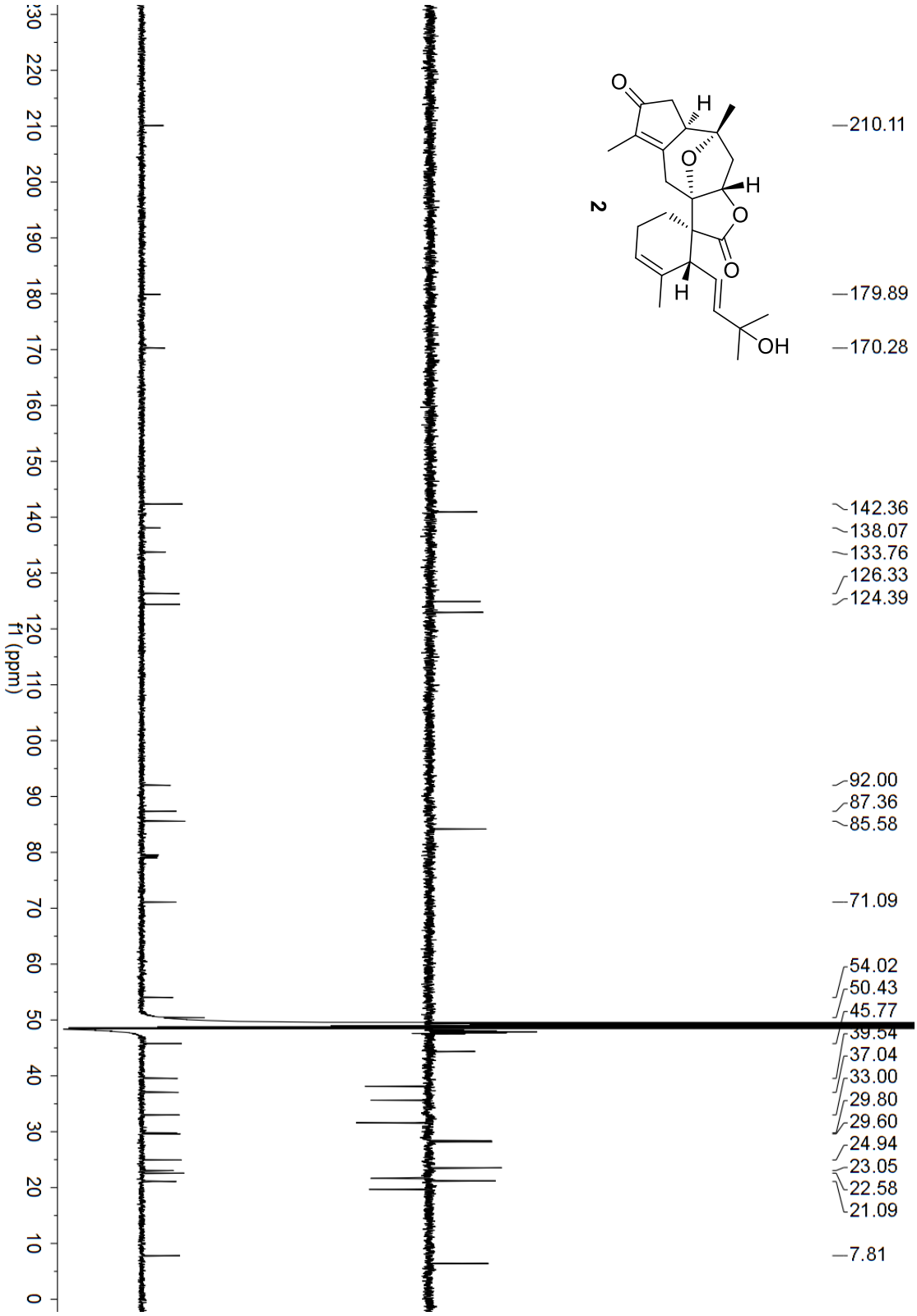

Fig. S23. ^{1}H–^{1}H COSY spectrum of natural orientanoid B (**2**) in Methanol-d_4.

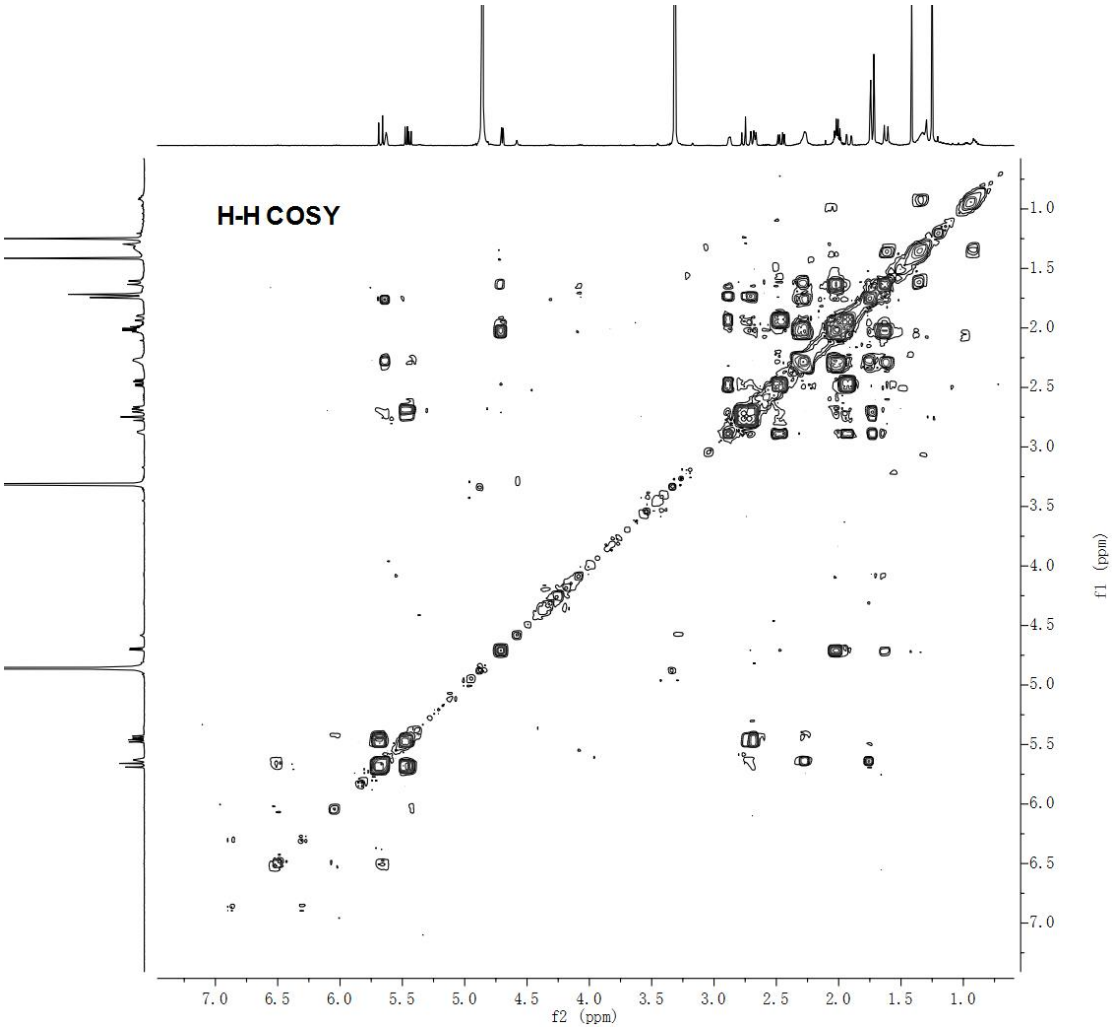

Fig. S24. HSQC spectrum of natural orientanoid B (**2**) in Methanol-d_4.

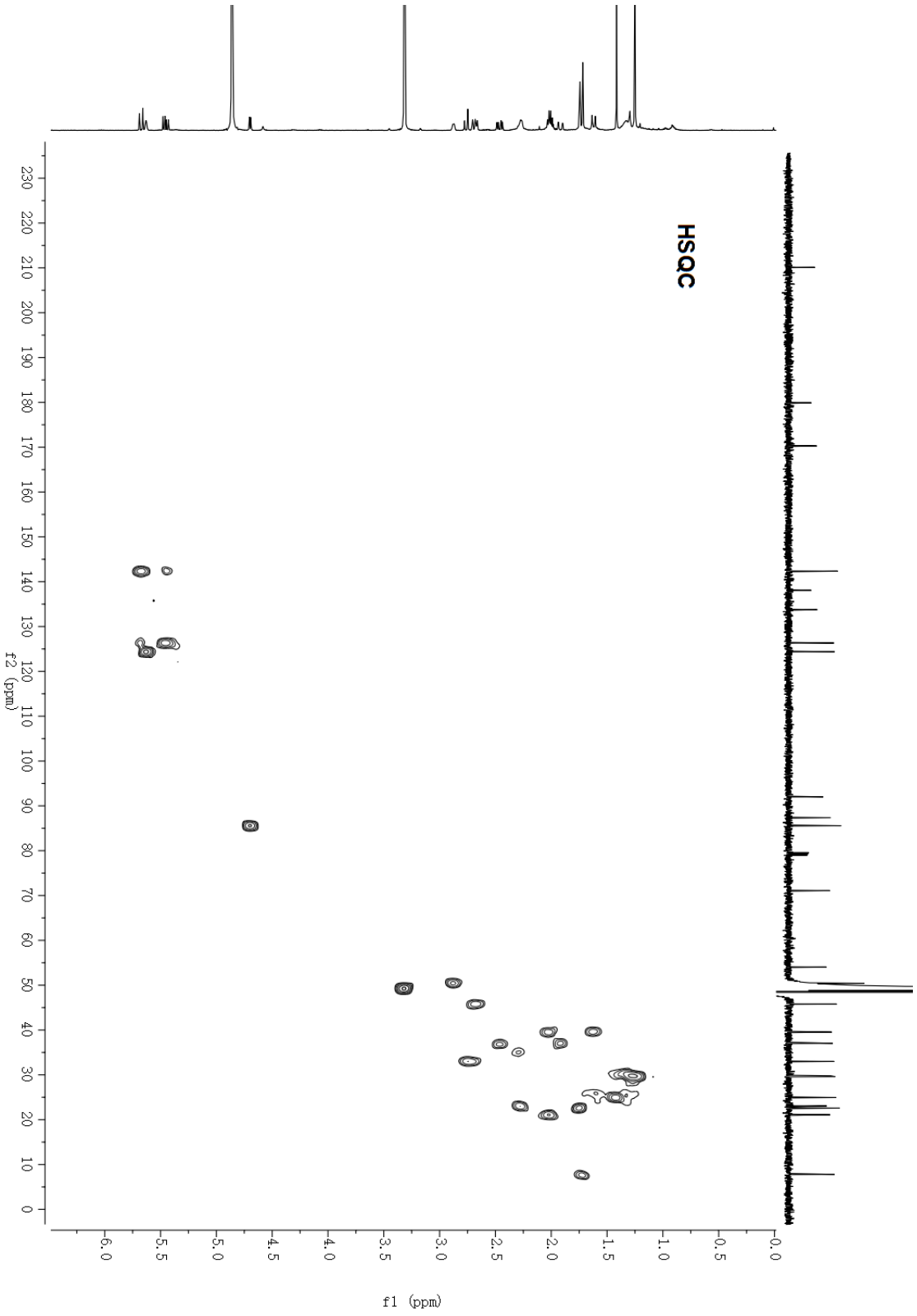

Fig. S25. HMBC spectrum of natural orientanoid B (**2**) in Methanol-d_4.

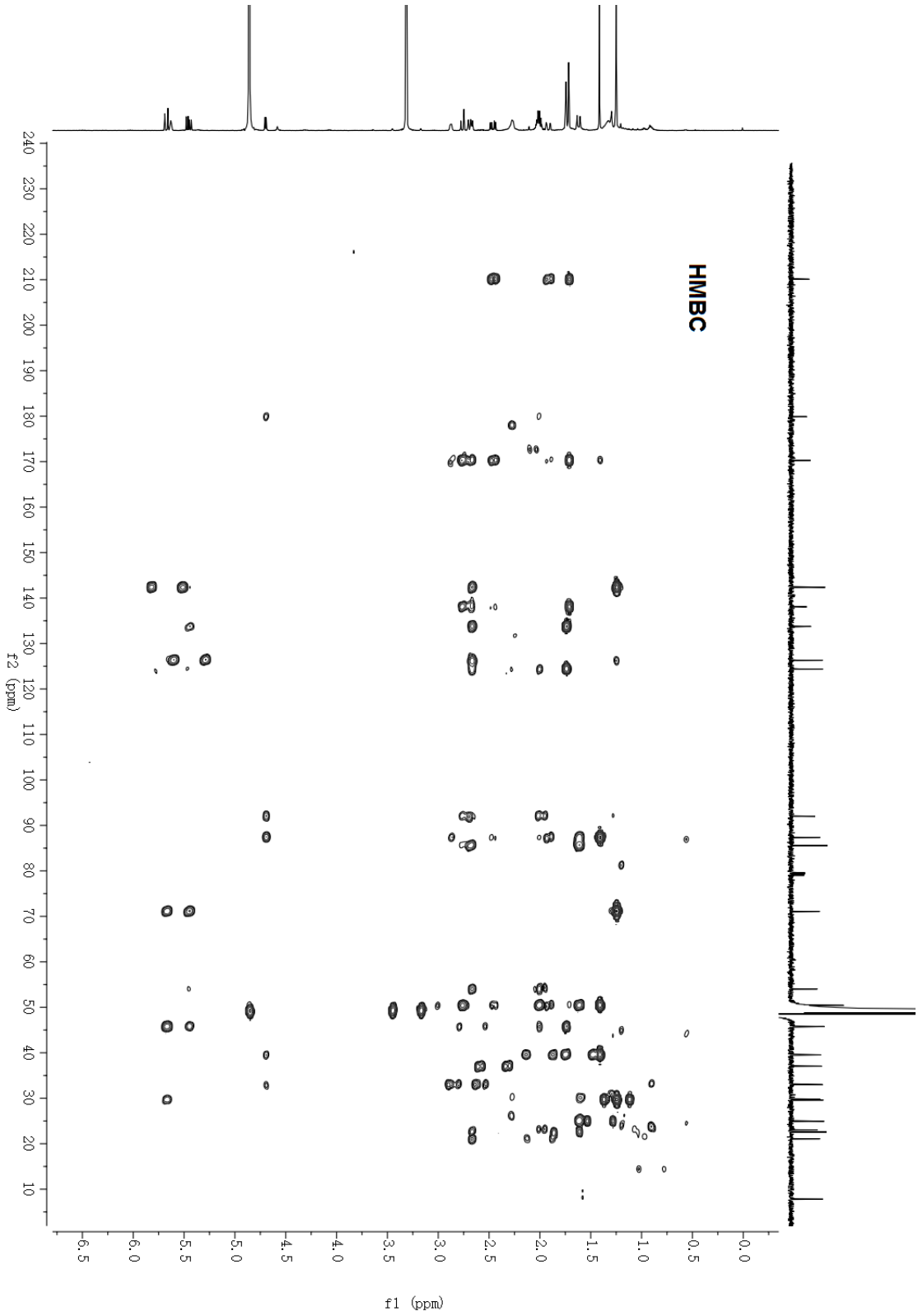

Fig. S26. NOESY spectrum of natural orientanoid B (**2**) in Methanol-d_4.

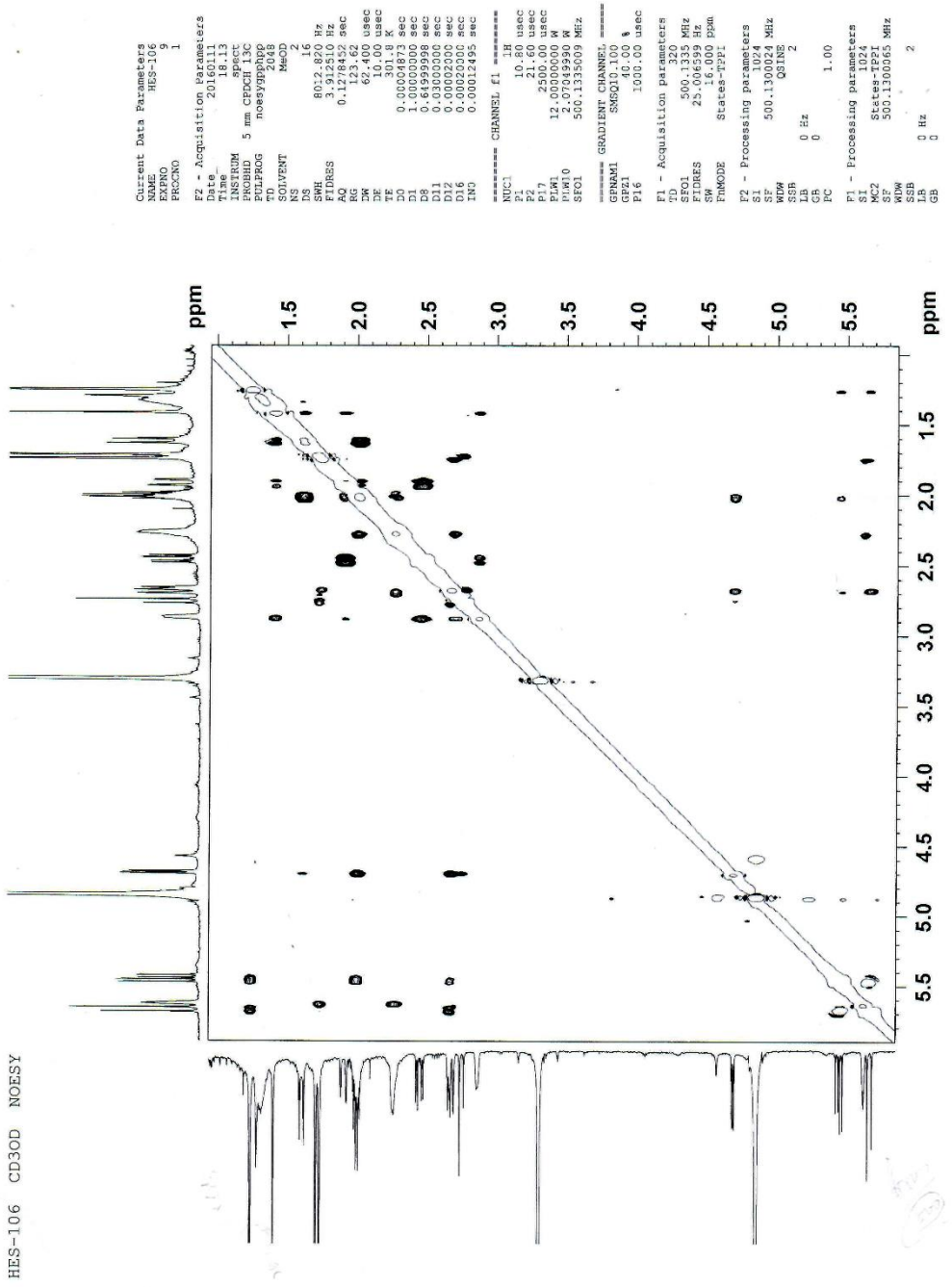

Fig. S27. ESIMS spectra of natural orientanoid B (**2**).

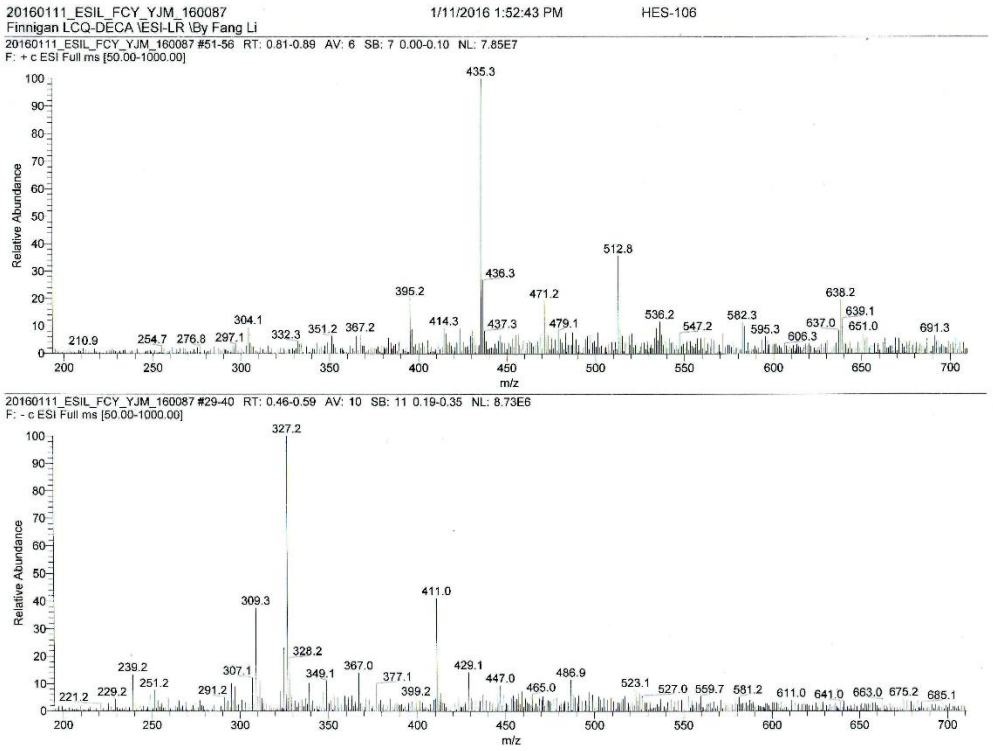

Fig. S28. (+)-HRESIMS spectrum of natural orientanoid B (**2**).

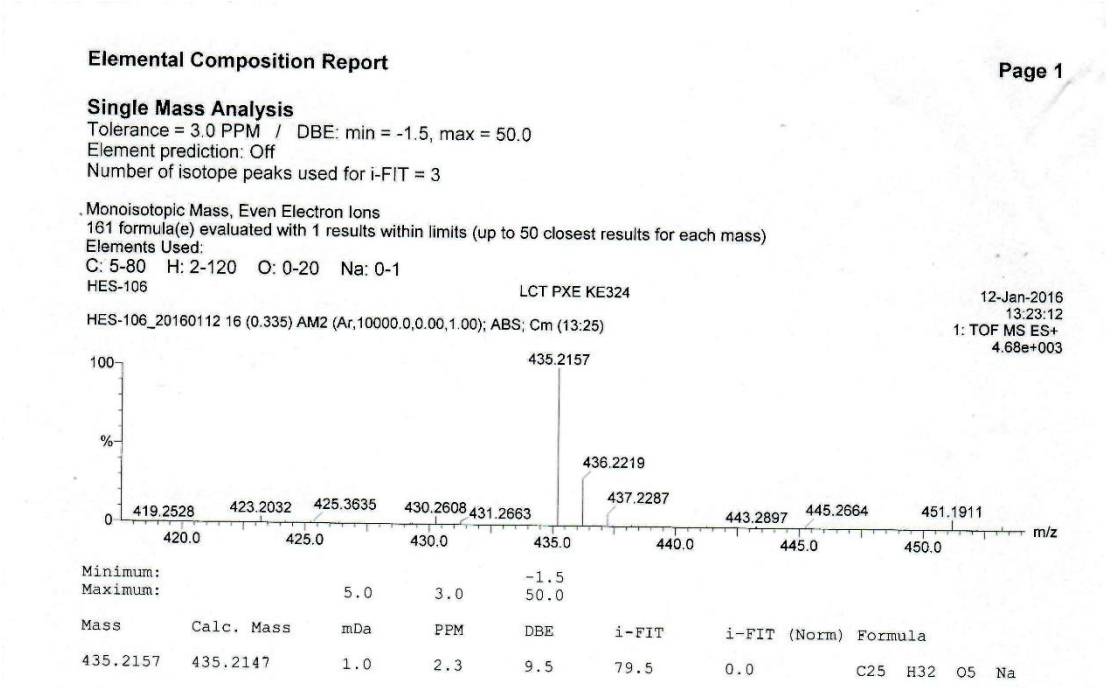

Elemental Composition Report Page 1

Single Mass Analysis
Tolerance = 3.0 PPM / DBE: min = -1.5, max = 50.0
Element prediction: Off
Number of isotope peaks used for i-FIT = 3

Monoisotopic Mass, Even Electron Ions
161 formula(e) evaluated with 1 results within limits (up to 50 closest results for each mass)
Elements Used:
C: 5-80 H: 2-120 O: 0-20 Na: 0-1

HES-106 LCT PXE KE324 12-Jan-2016 13:23:12

HES-106_20160112 16 (0.335) AM2 (Ar,10000.0,0.00,1.00); ABS; Cm (13:25) 1: TOF MS ES+ 4.68e+003

Minimum:				-1.5			
Maximum:		5.0	3.0	50.0			
Mass	Calc. Mass	mDa	PPM	DBE	i-FIT	i-FIT (Norm)	Formula
435.2157	435.2147	1.0	2.3	9.5	79.5	0.0	C25 H32 O5 Na

Fig. S29. IR spectrum of natural orientanoid B (**2**).

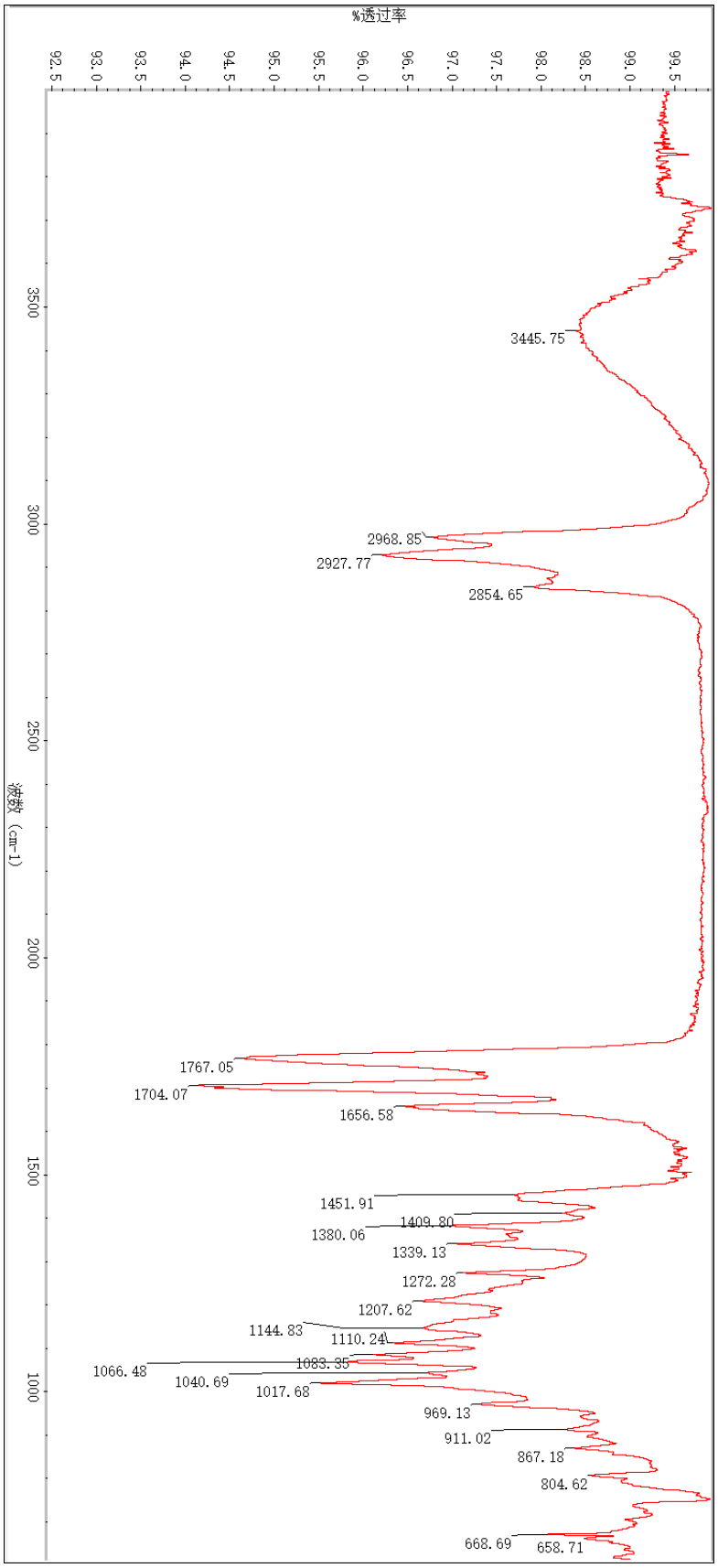

Fig. S30. [1]H NMR spectrum of natural orientanoid C (**3**) in Methanol-d_4.

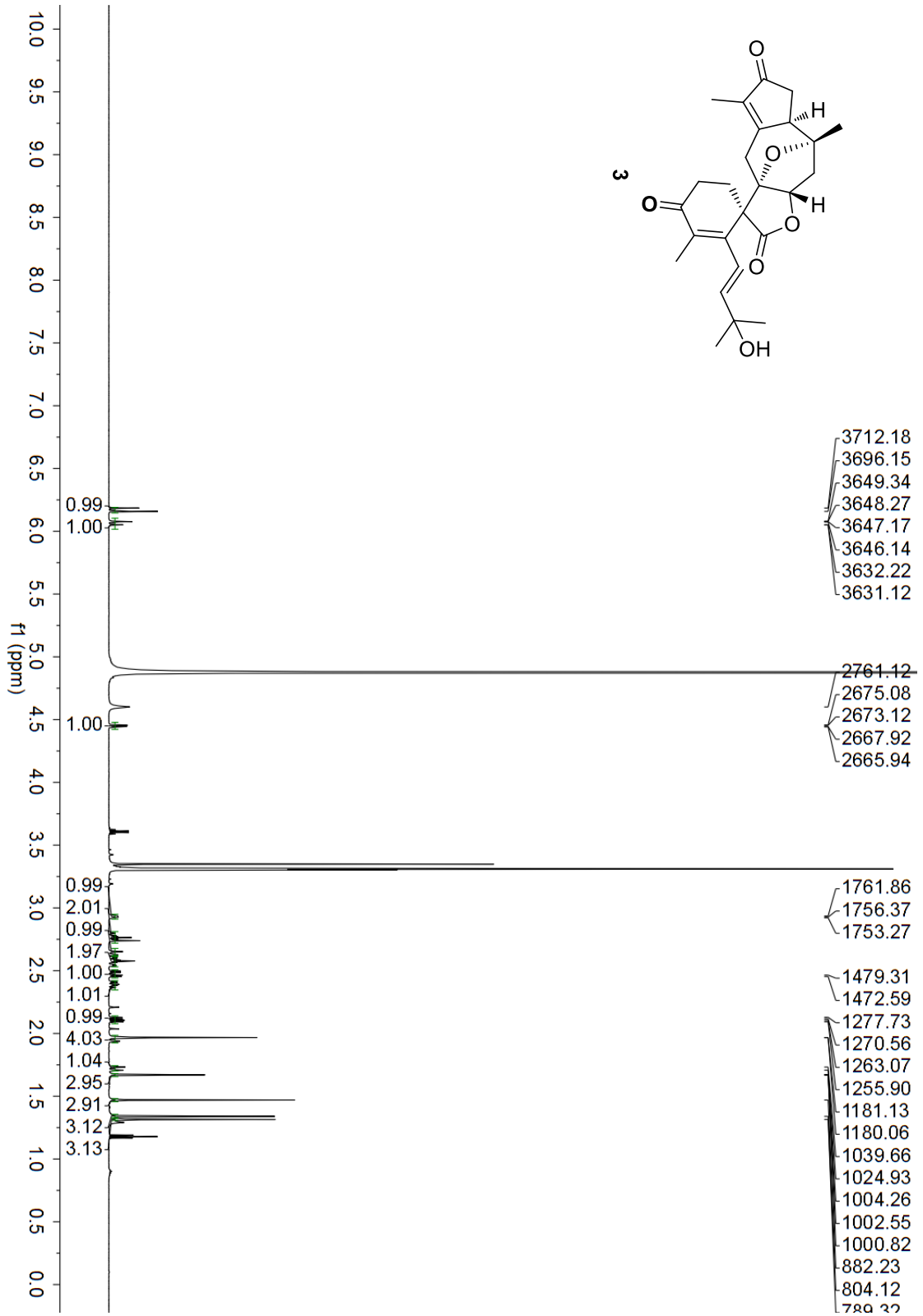

Fig. S31. ^{13}C NMR spectrum of natural orientanoid C (**3**) in Methanol-d_4.

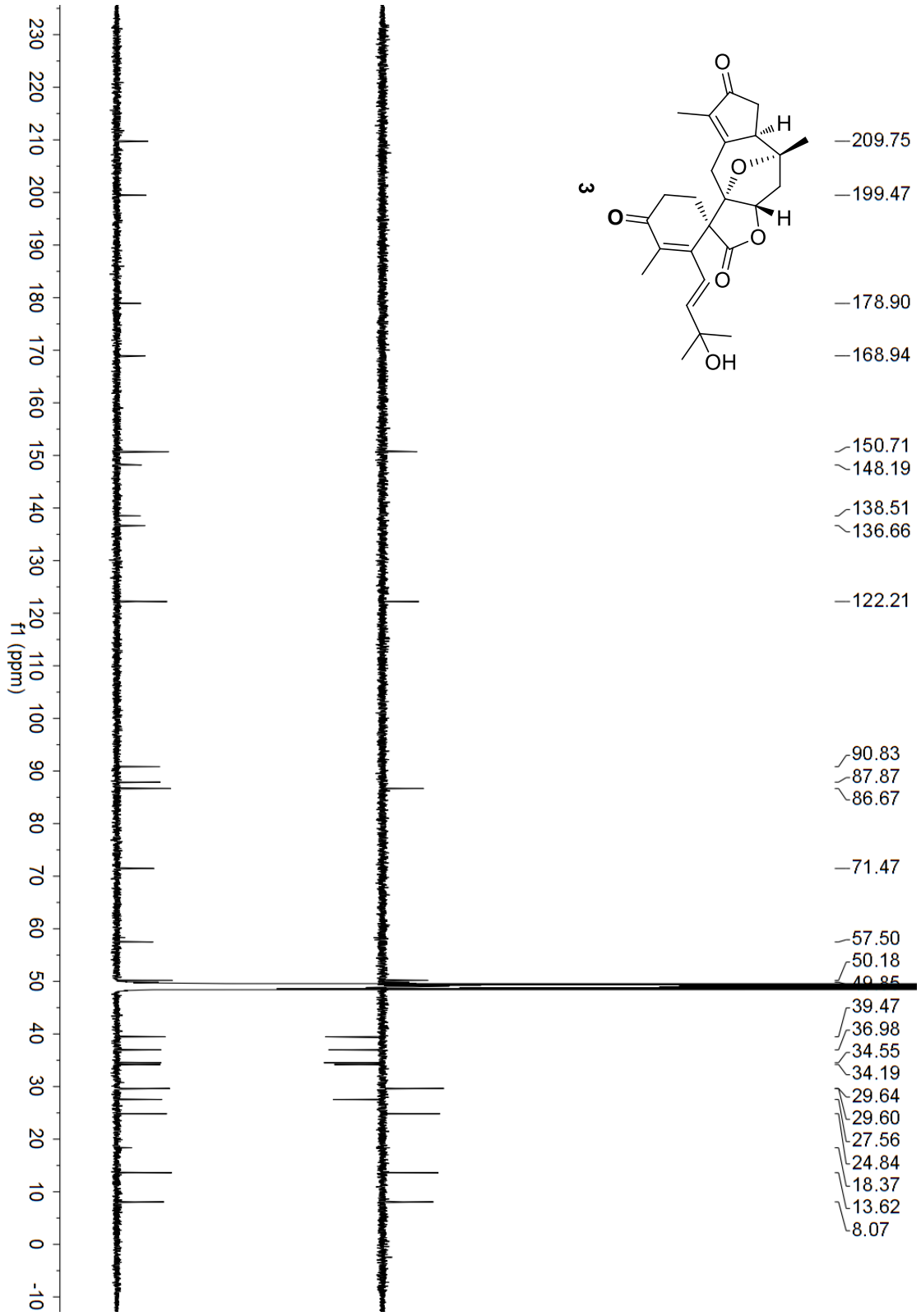

Fig. S32. ^{1}H–^{1}H COSY spectrum of natural orientanoid C (**3**) in Methanol-d_4.

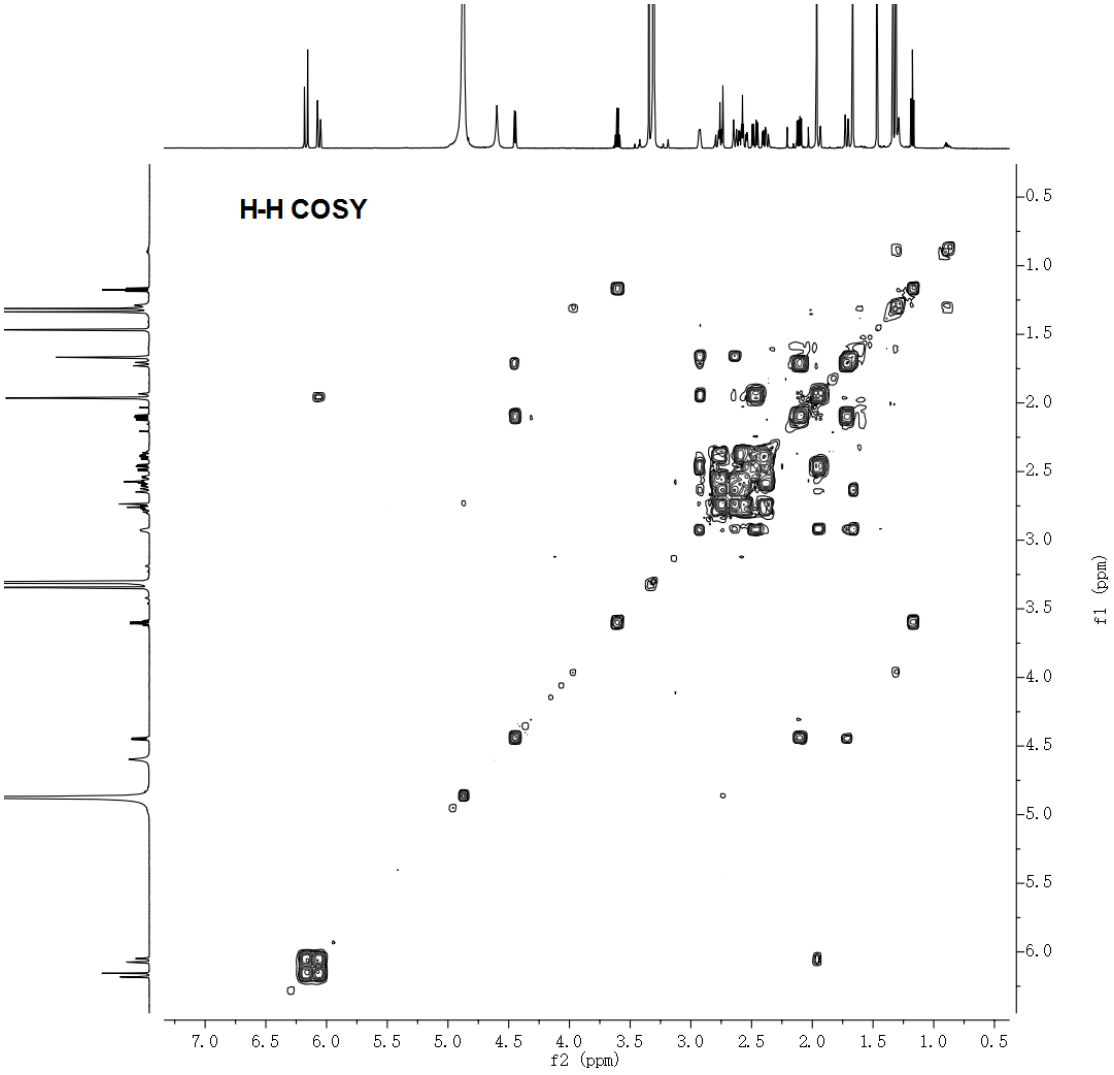

Fig. S33. HSQC spectrum of natural orientanoid C (**3**) in Methanol-d_4.

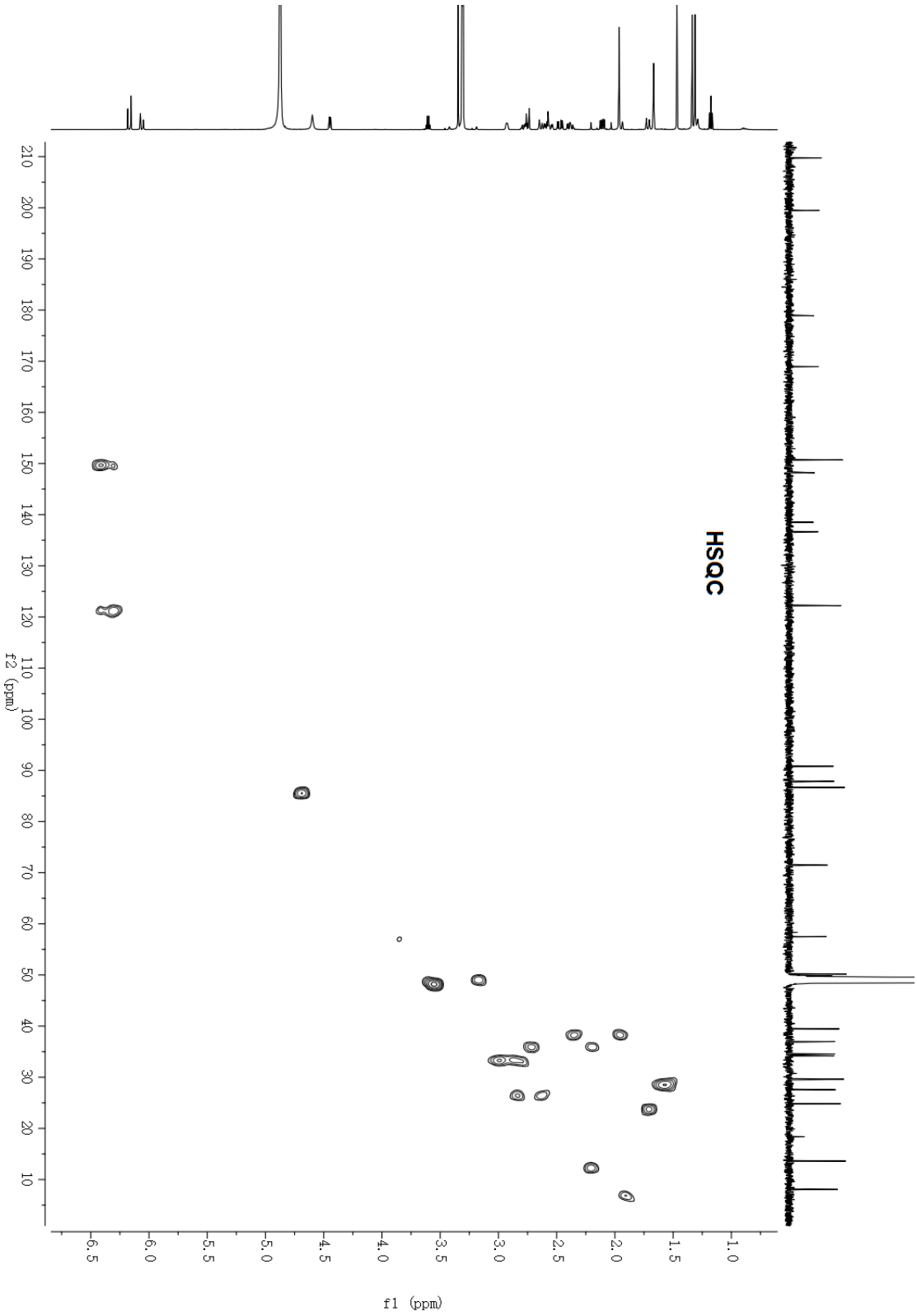

Fig. S34. HMBC spectrum of natural orientanoid C (**3**) in Methanol-d_4.

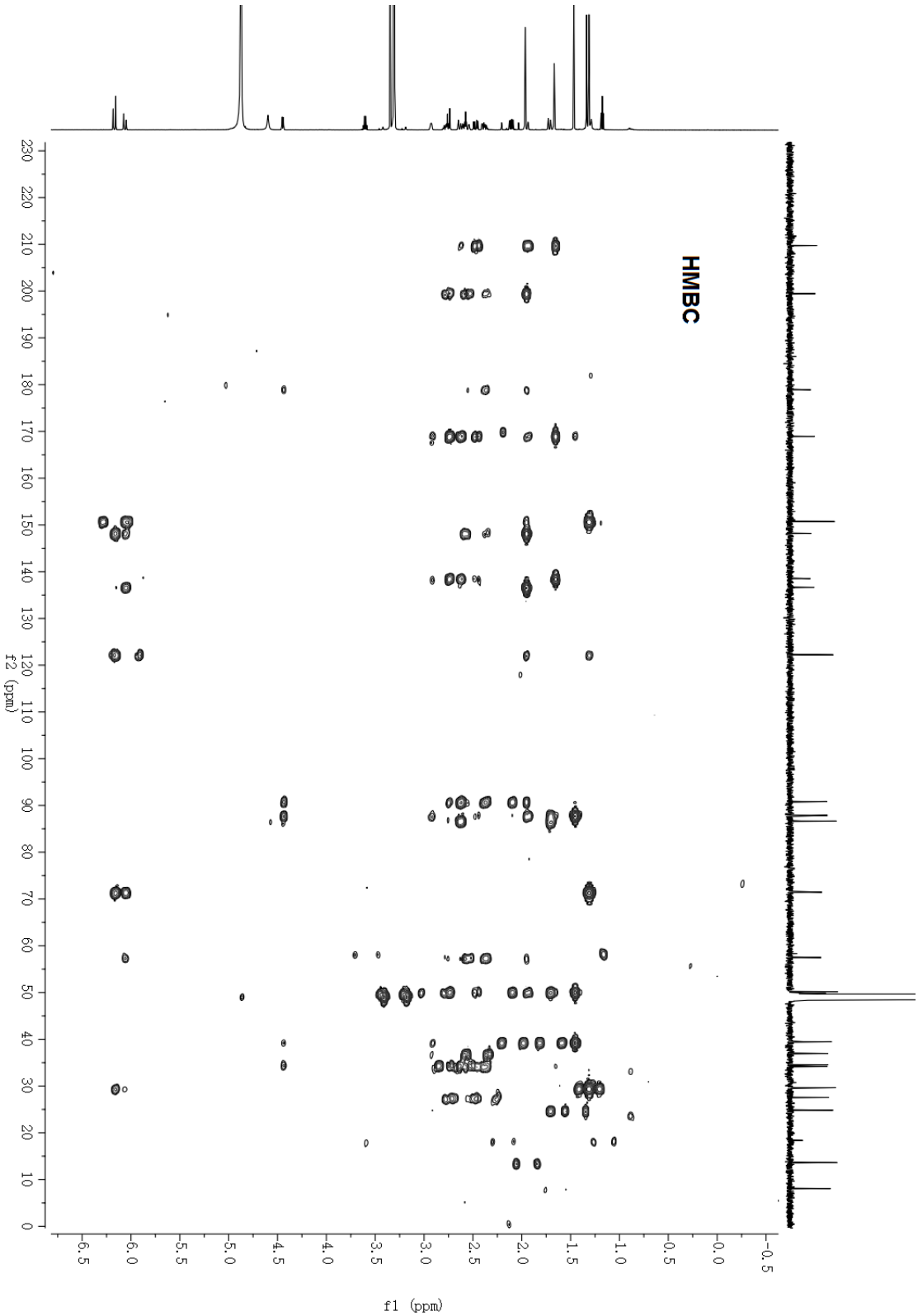

Fig. S35. NOESY spectrum of natural orientanoid C (**3**) in Methanol-d_4.

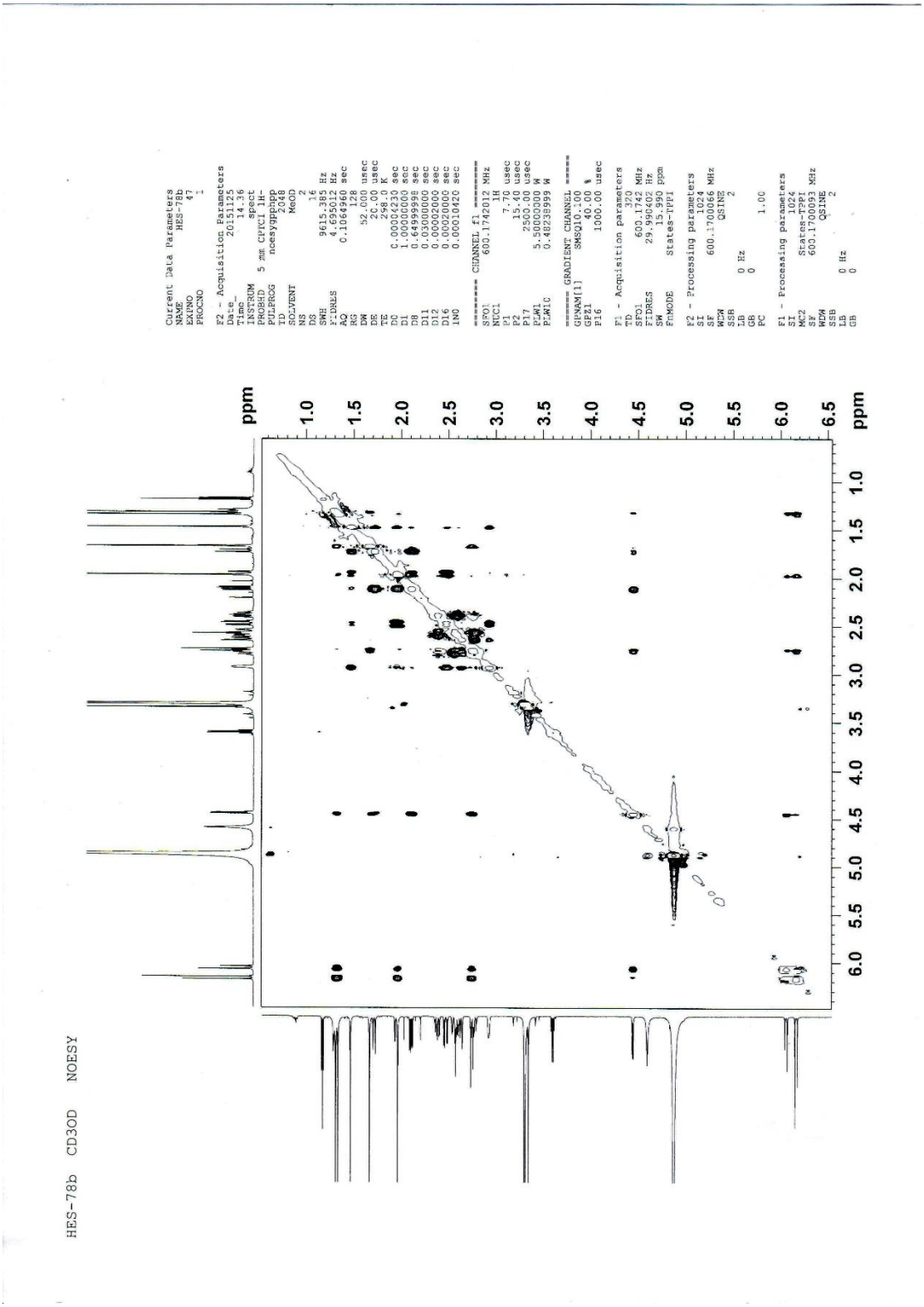

Fig. S36. (–)-ESIMS spectrum of natural orientanoid C (**3**).

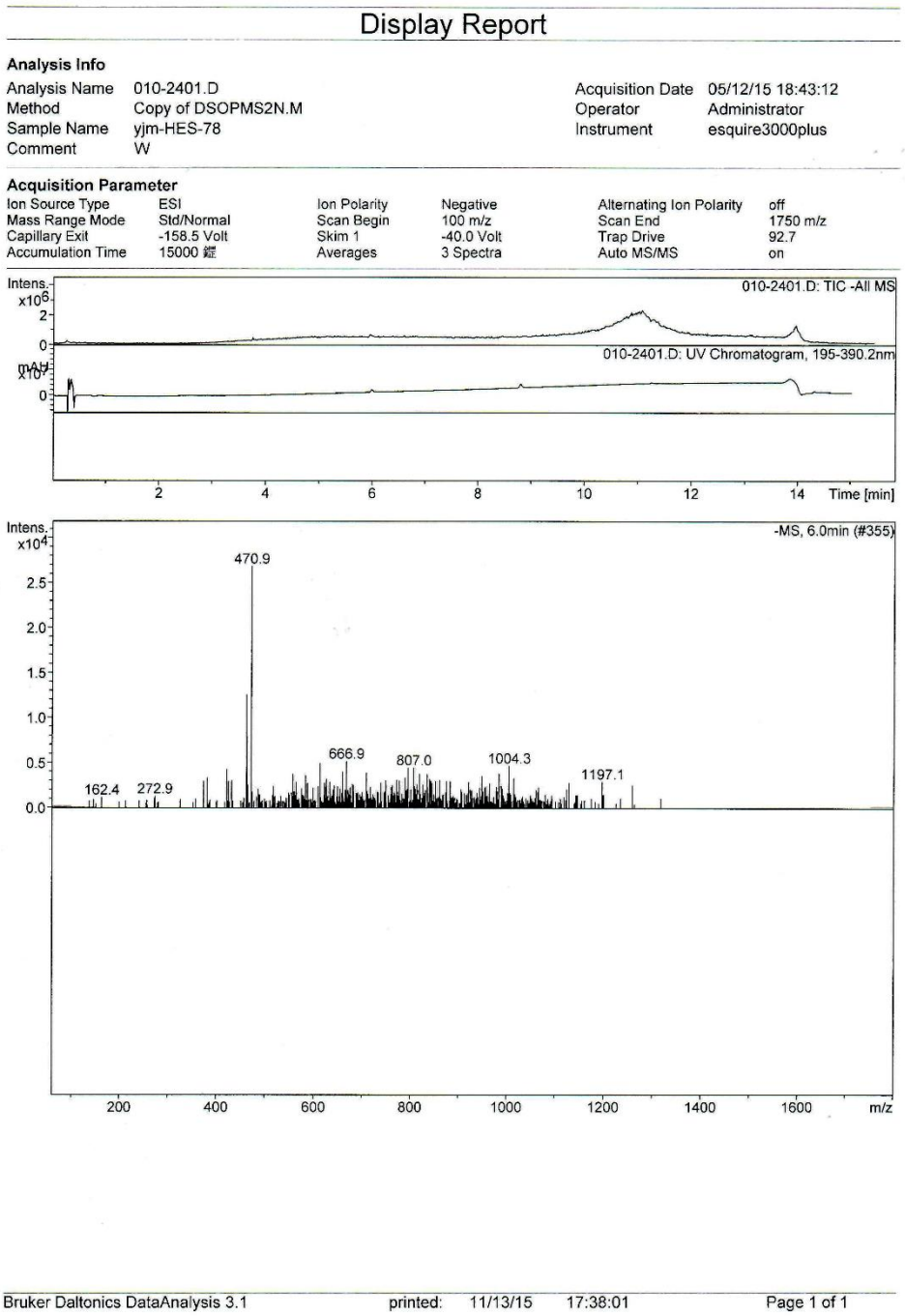

Fig. S37. (–)-HRESIMS spectrum of natural orientanoid C (**3**).

Elemental Composition Report **Page 1**

Single Mass Analysis
Tolerance = 3.0 PPM / DBE: min = -1.5, max = 50.0
Element prediction: Off
Number of isotope peaks used for i-FIT = 3

Monoisotopic Mass, Even Electron Ions
179 formula(e) evaluated with 1 results within limits (up to 50 closest results for each mass)
Elements Used:
C: 5-80 H: 2-120 O: 0-20 Na: 0-1

HES-78 LCT PXE KE324 17-Nov-2015 14:40:29

HES-78_20151117 59 (1.288) AM2 (Ar,10000.0,0.00,1.00); ABS; Cm (50:66) 1: TOF MS ES- 1.43e+004

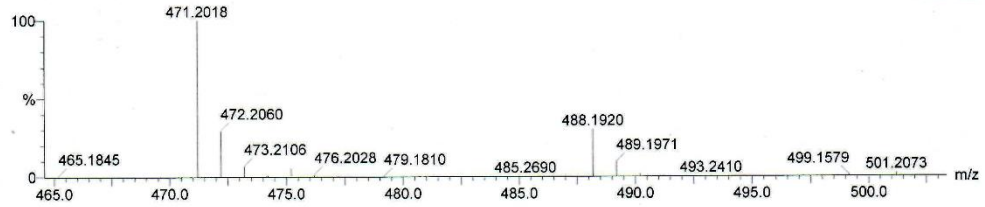

Minimum:				-1.5			
Maximum:		5.0	3.0	50.0			
Mass	Calc. Mass	mDa	PPM	DBE	i-FIT	i-FIT (Norm)	Formula
471.2018	471.2019	-0.1	-0.2	11.5	102.1	0.0	C26 H31 O8

Fig. S38. IR spectrum of natural orientanoid C (**3**).

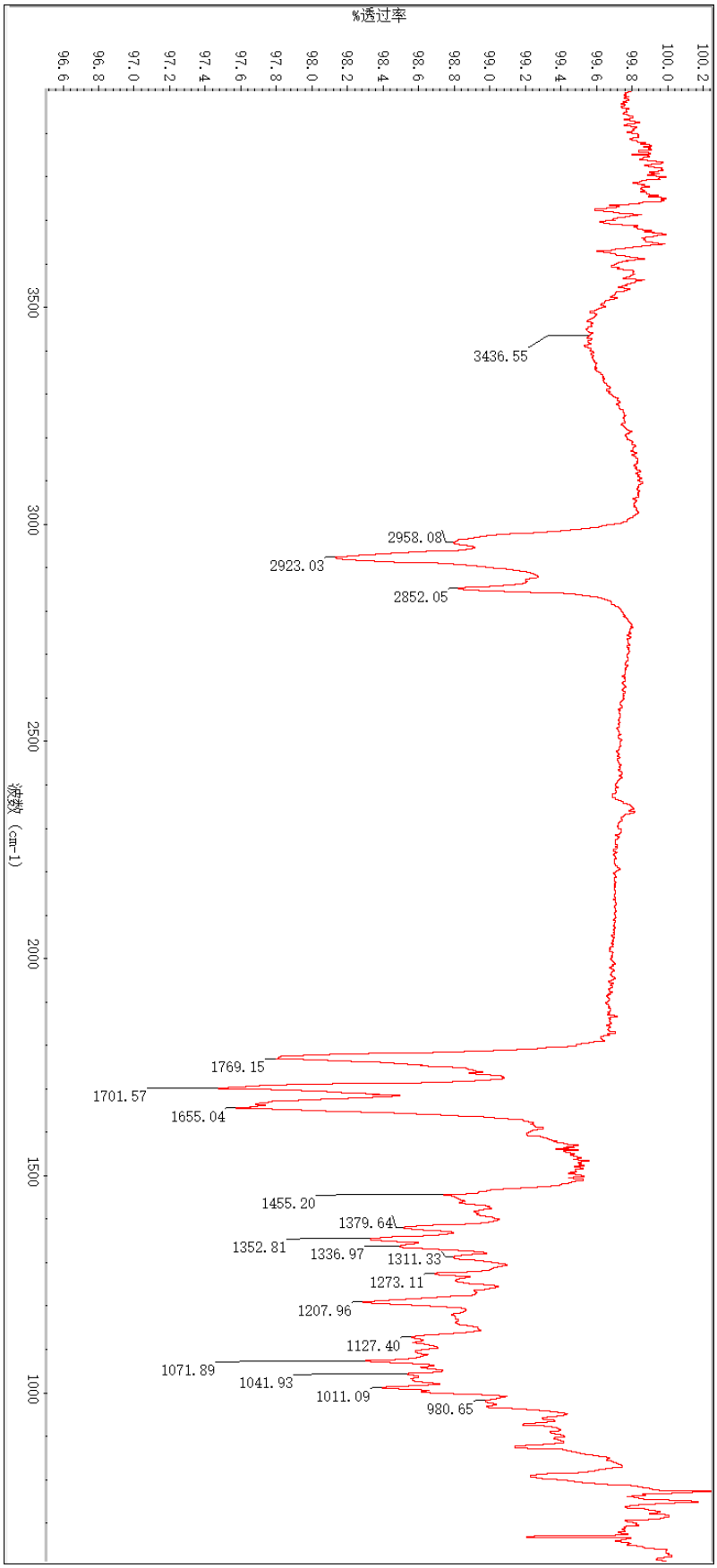

Fig. S39. [1]H NMR spectrum of compound **14** in Methanol-d_4.

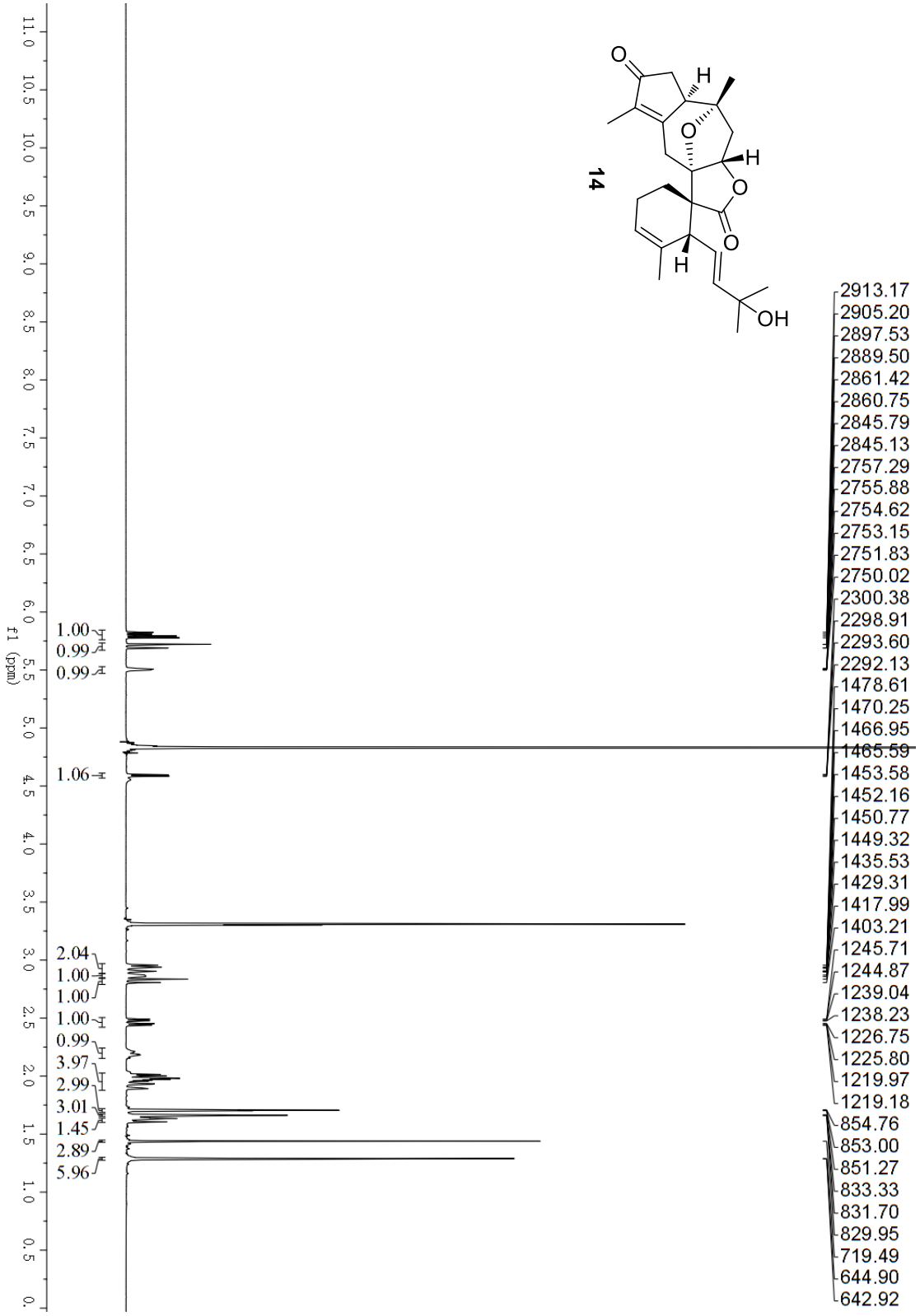

Fig. S40. ^{13}C NMR spectrum of compound **14** in Methanol-d_4.

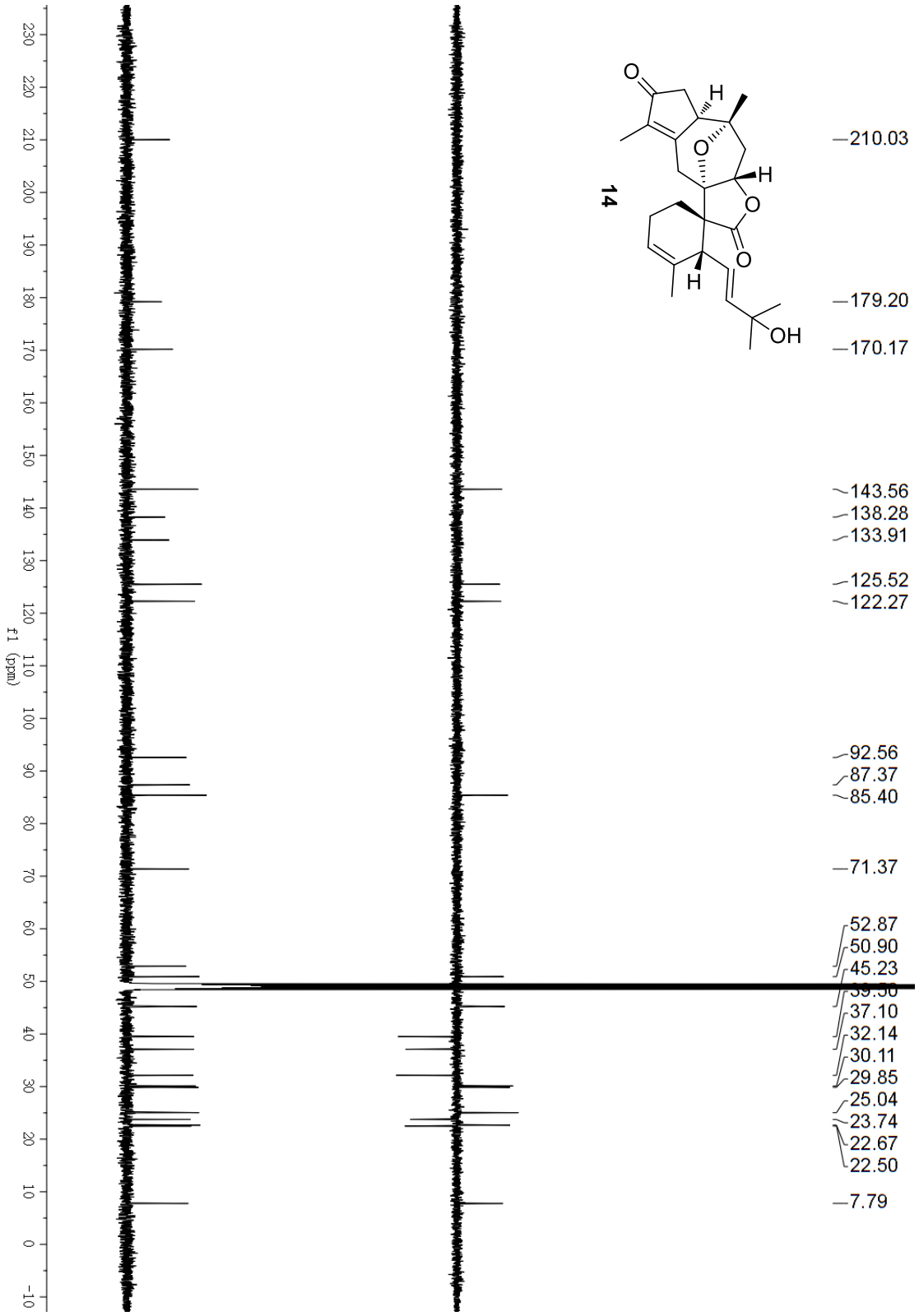

Fig. S41. ^{1}H–^{1}H COSY spectrum of compound **14** in Methanol-d_4.

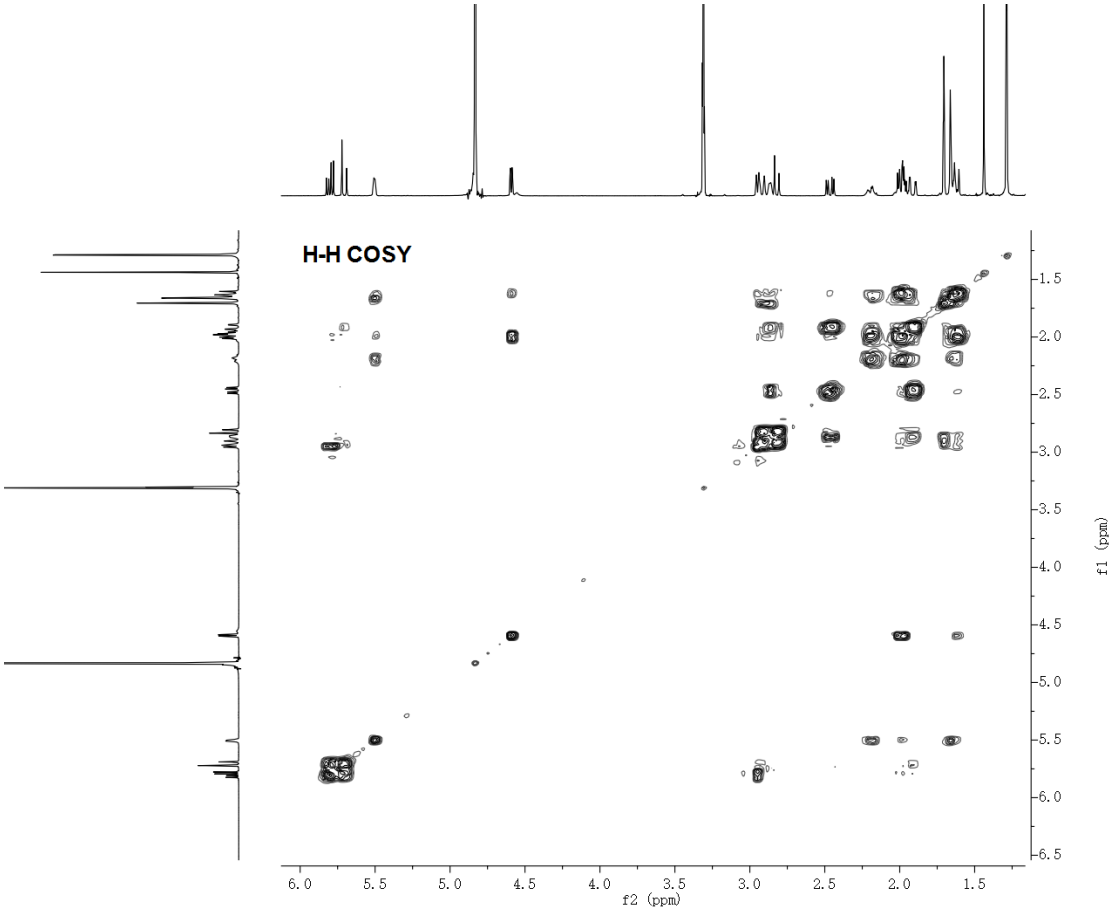

Fig. S42. HSQC spectrum of compound **14** in Methanol-d_4.

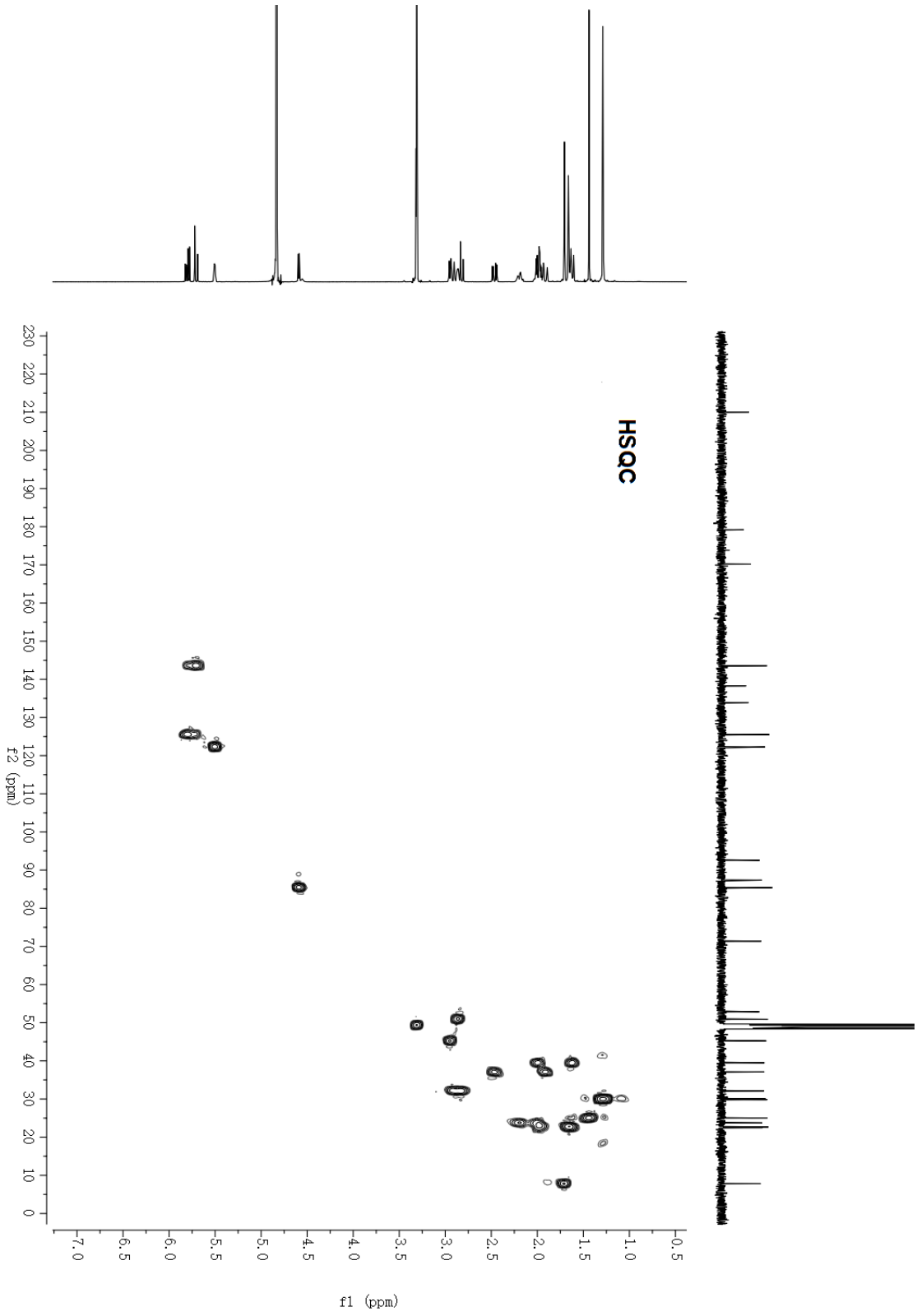

Fig. S43. HMBC spectrum of compound **14** in Methanol-d_4.

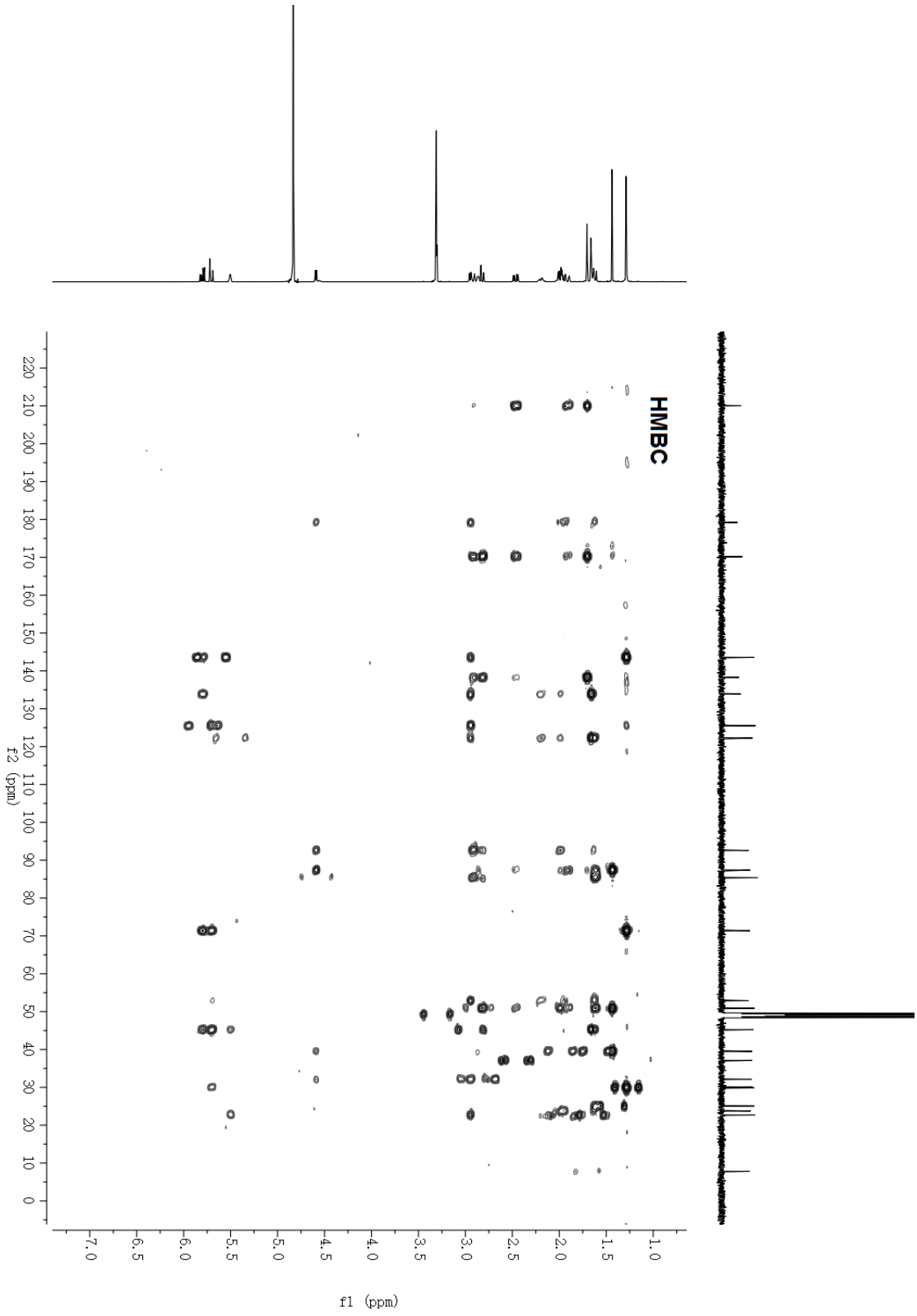

Fig. S44. NOESY spectrum of compound **14** in Methanol-d_4.

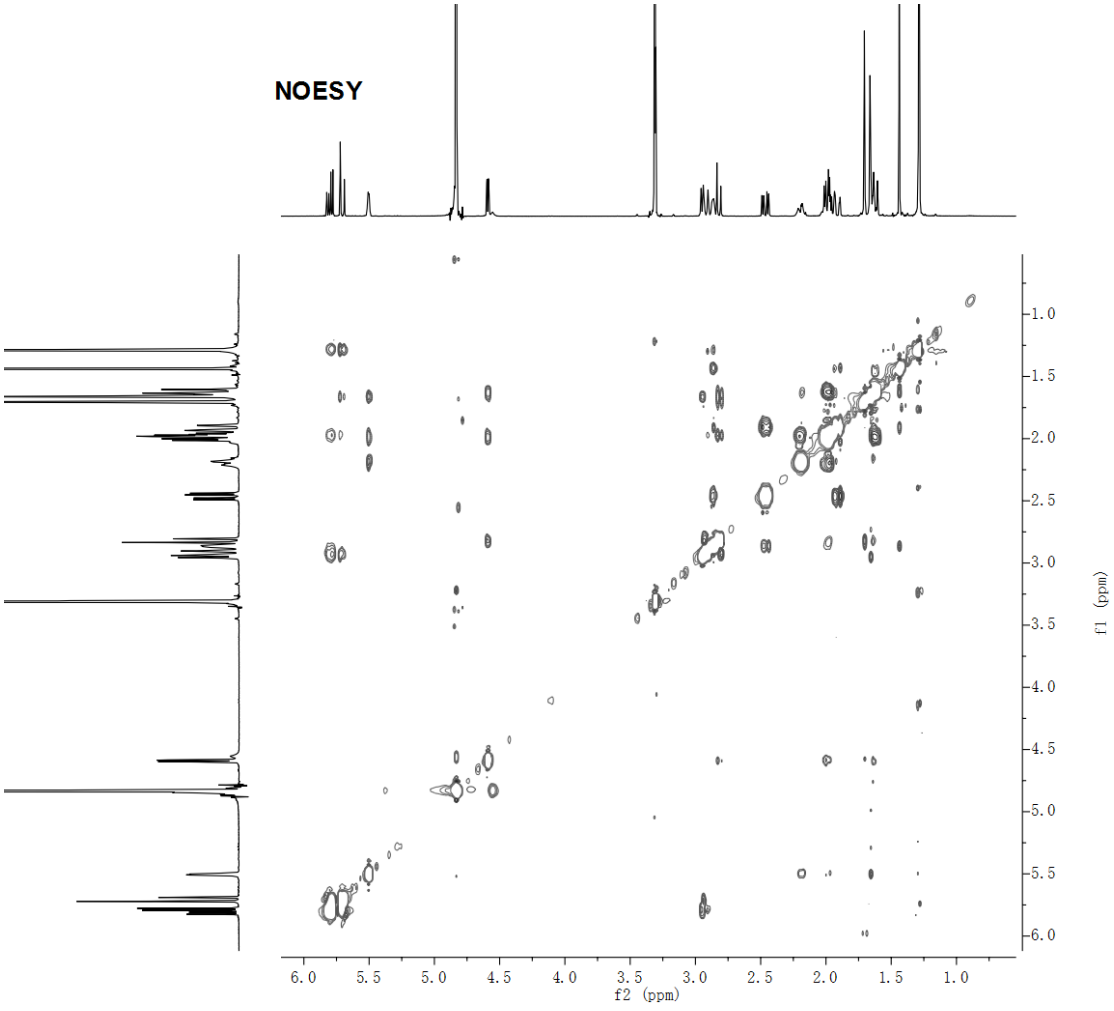

Fig. S45. [1]H NMR spectrum of compound **15** in Methanol-d_4.

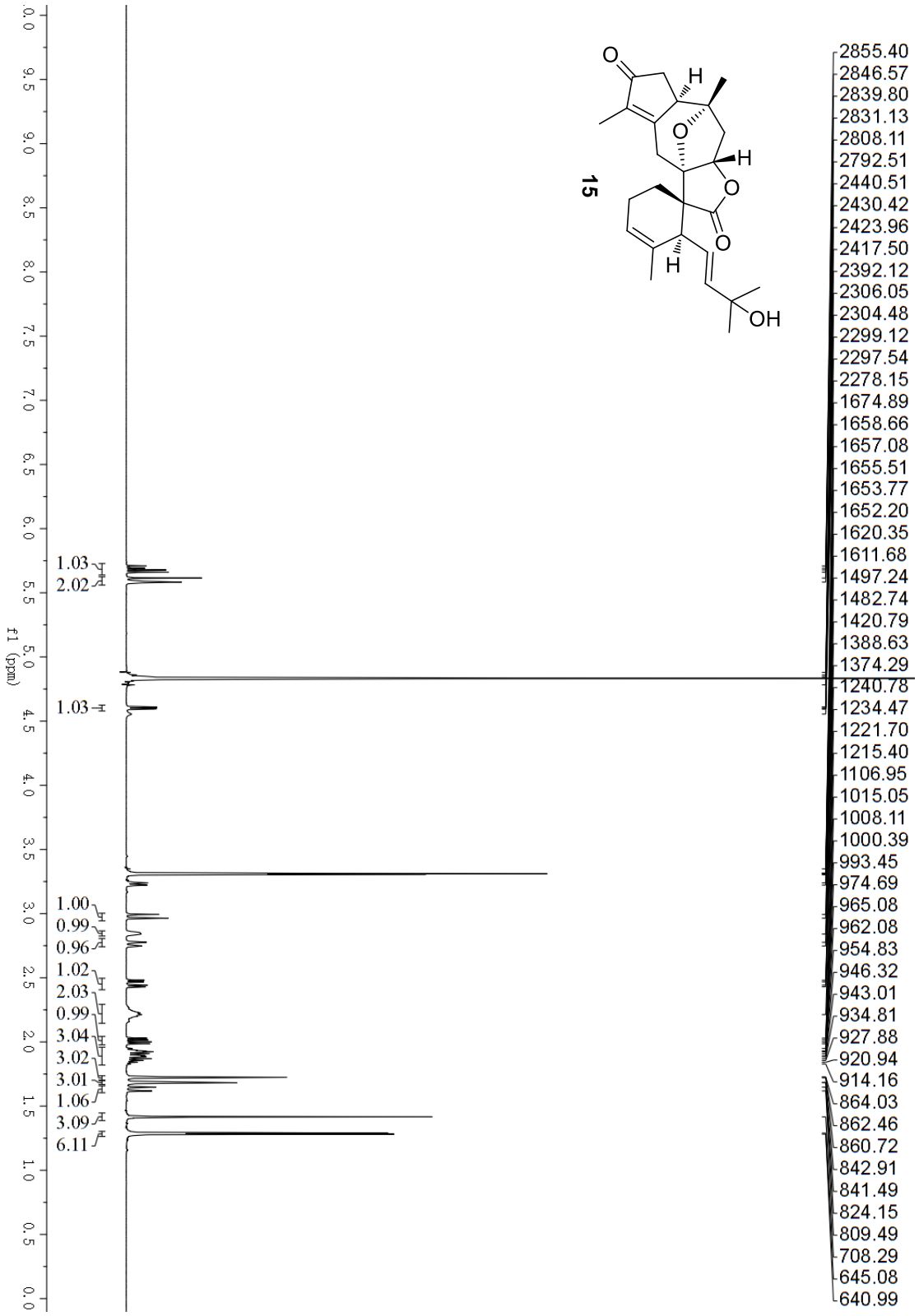

Fig. S46. ^{13}C NMR spectrum of compound **15** in Methanol-d_4.

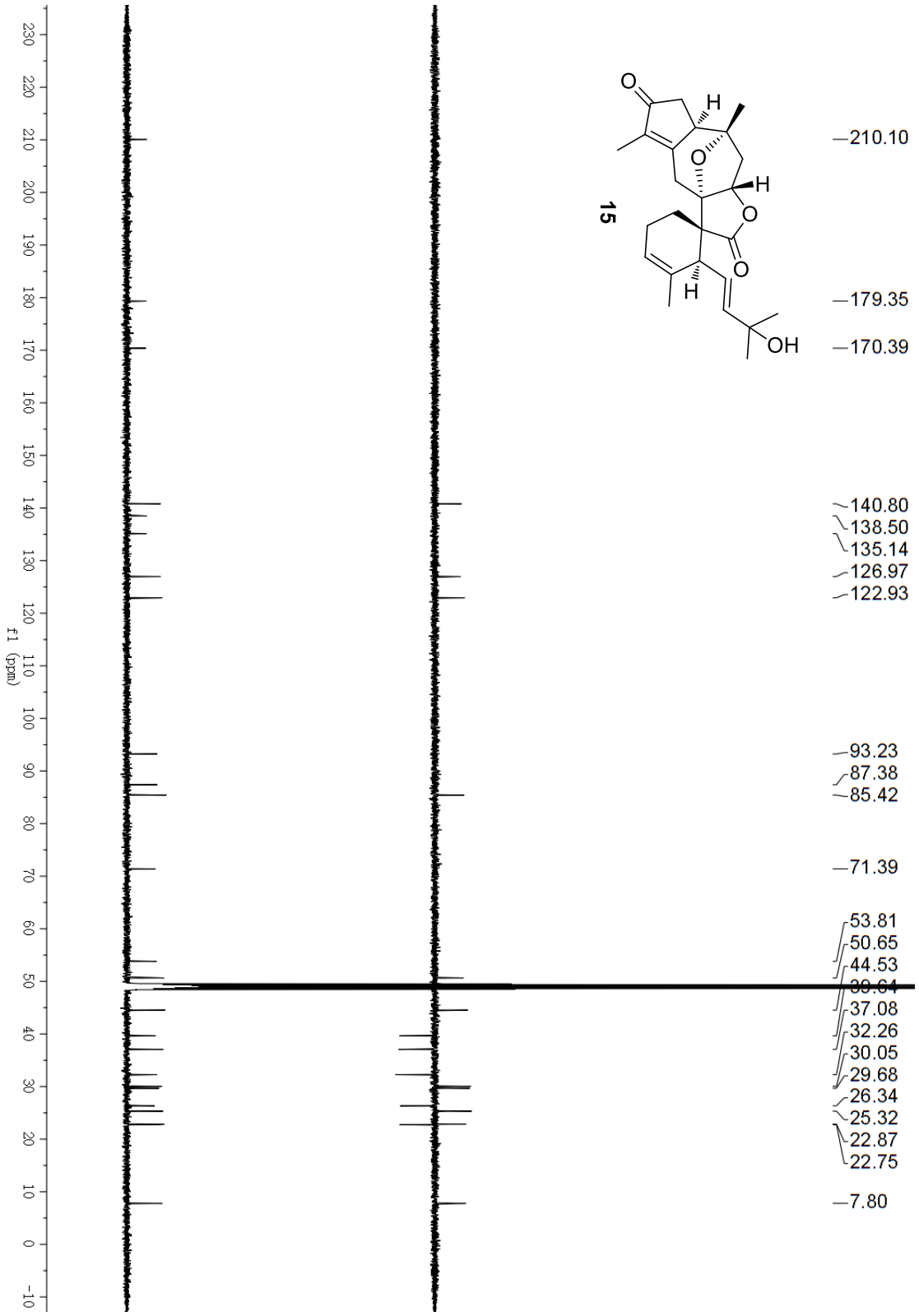

Fig. S47. ^{1}H–^{1}H COSY spectrum of compound **15** in Methanol-d_4.

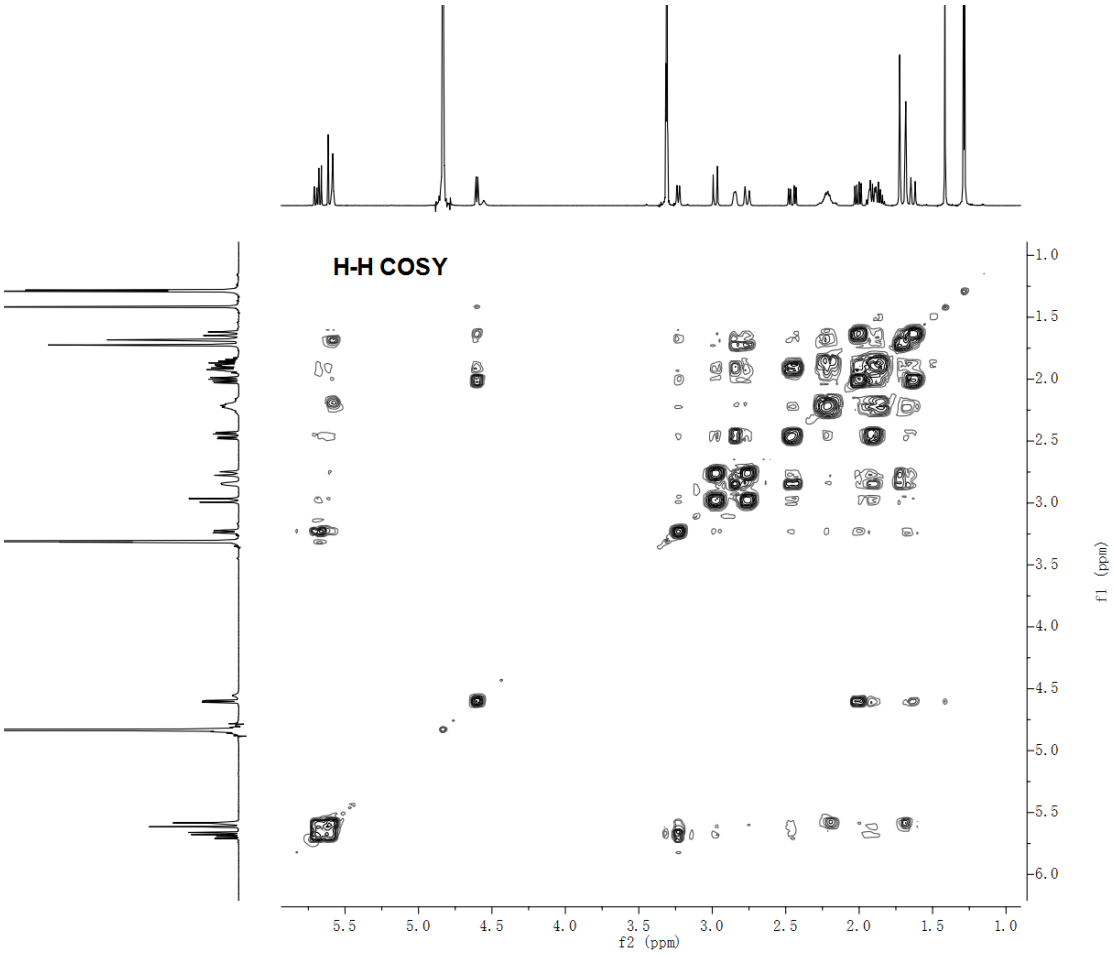

Fig. S48. HSQC spectrum of compound **15** in Methanol-d_4.

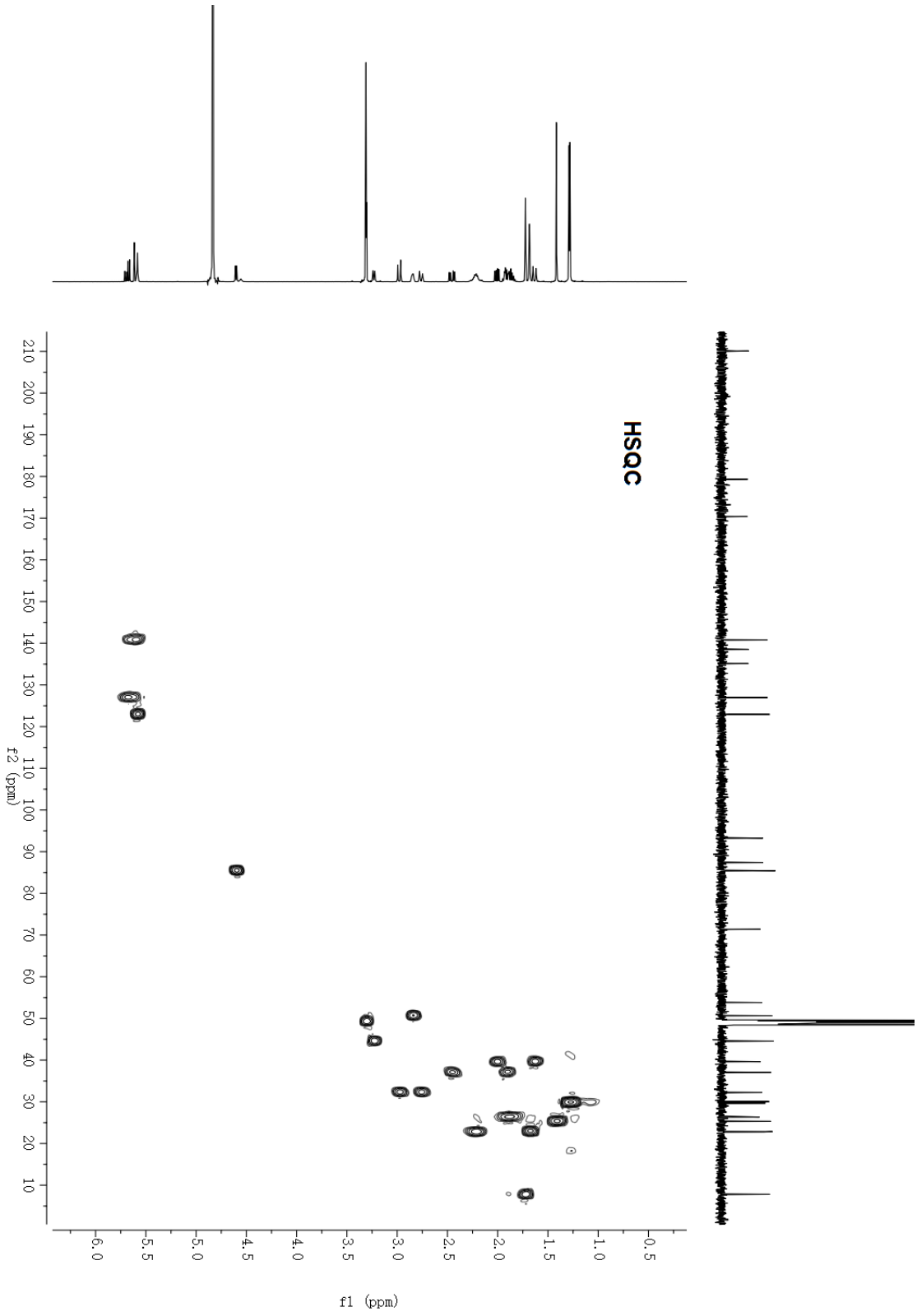

Fig. S49. HMBC spectrum of compound **15** in Methanol-d_4.

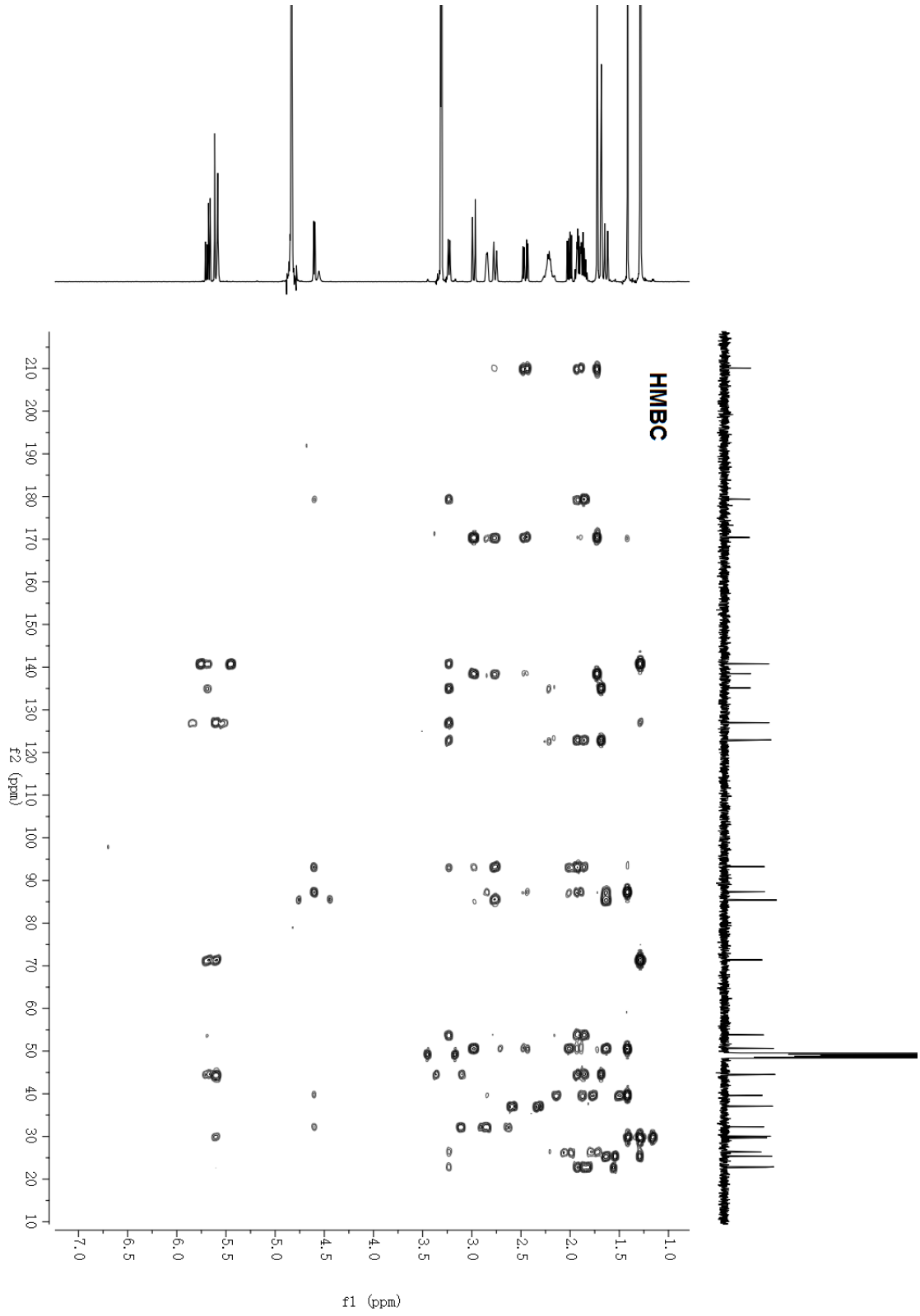

Fig. S50. NOESY spectrum of compound **15** in Methanol-d_4.

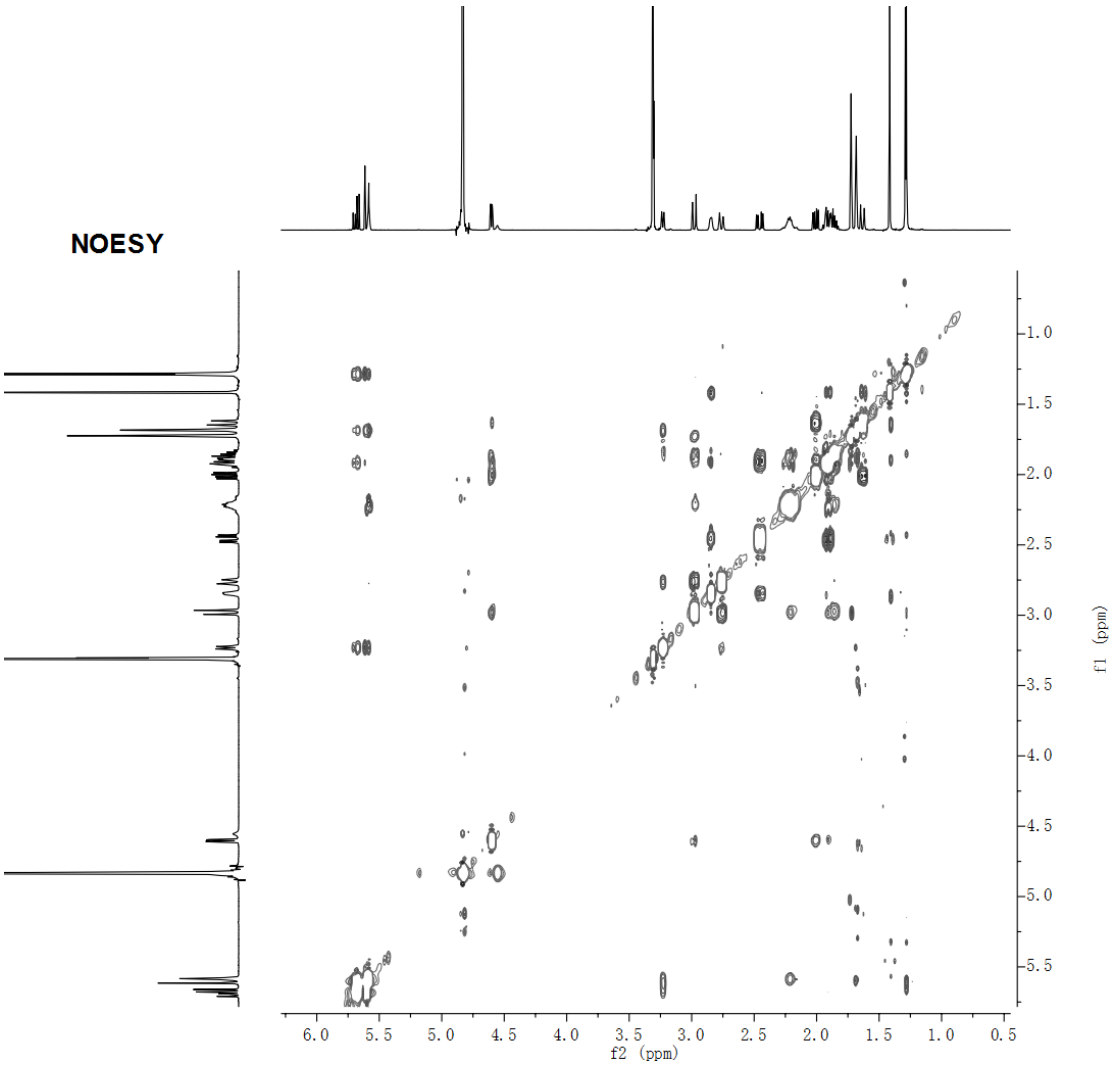

Fig. S51. Comparison of ^{1}H NMR spectra of natural and synthetic orientanoid A (**1**).

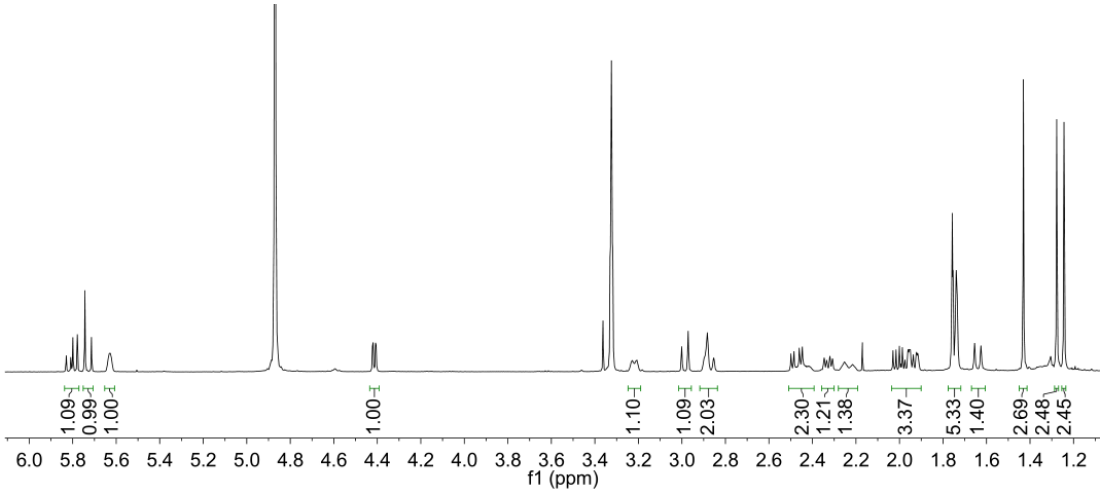

^{1}H NMR spectrum of natural orientanoid A (Methanol-d_4, 500 MHz)

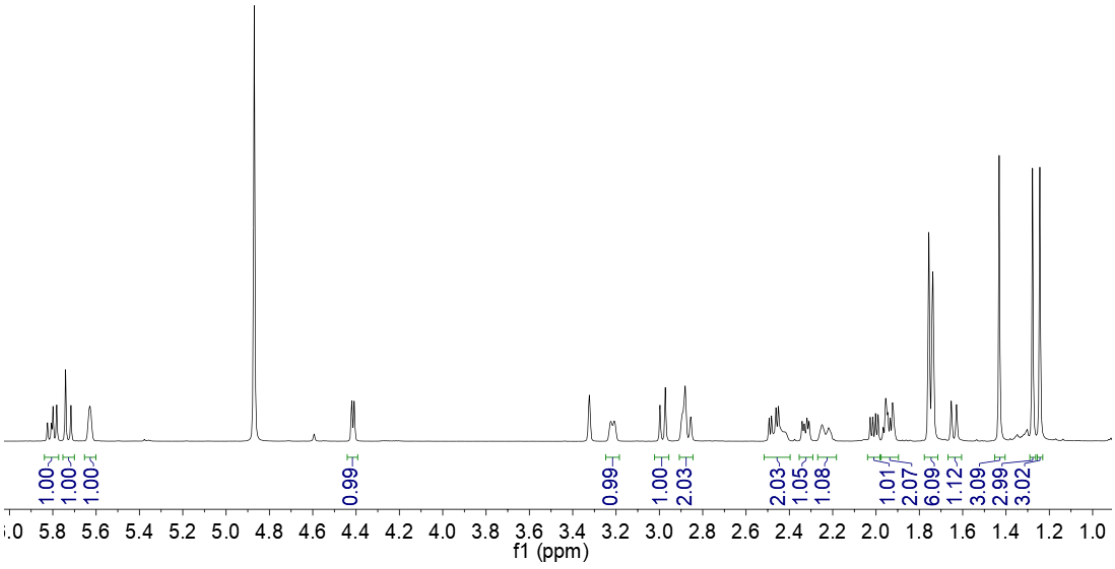

^{1}H NMR spectrum of synthetic orientanoid A (Methanol-d_4, 600 MHz)

Fig. S52. Comparison of ^{13}C NMR spectra of natural and synthetic orientanoid A (**1**).

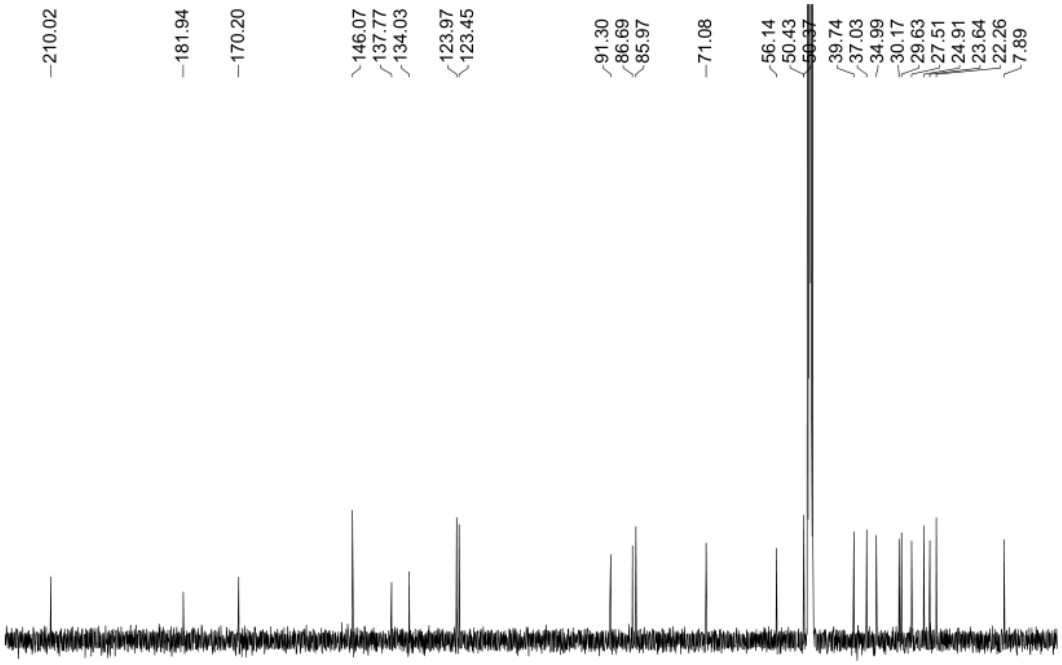

^{13}C NMR spectrum of natural orientanoid A (Methanol-d_4, 125 MHz)

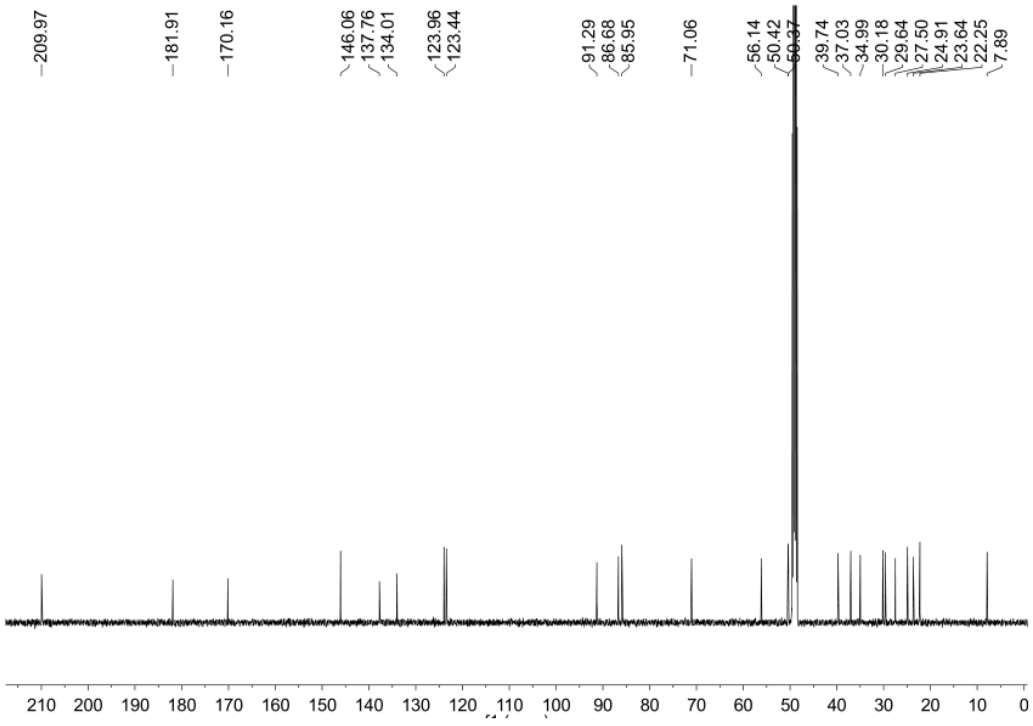

^{13}C NMR spectrum of synthetic orientanoid A (Methanol-d_4, 125 MHz)

Fig. S53. Comparison of ^{1}H NMR spectra of natural and synthetic orientanoid B (**2**).

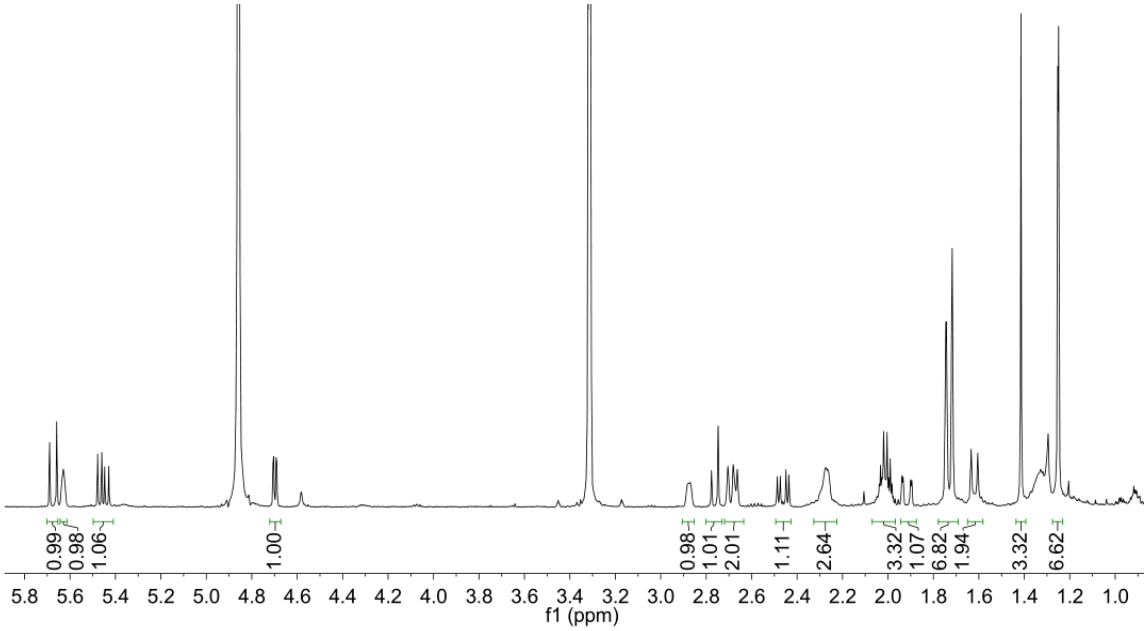

^{1}H NMR spectrum of natural orientanoid B (Methanol-d_4, 500 MHz)

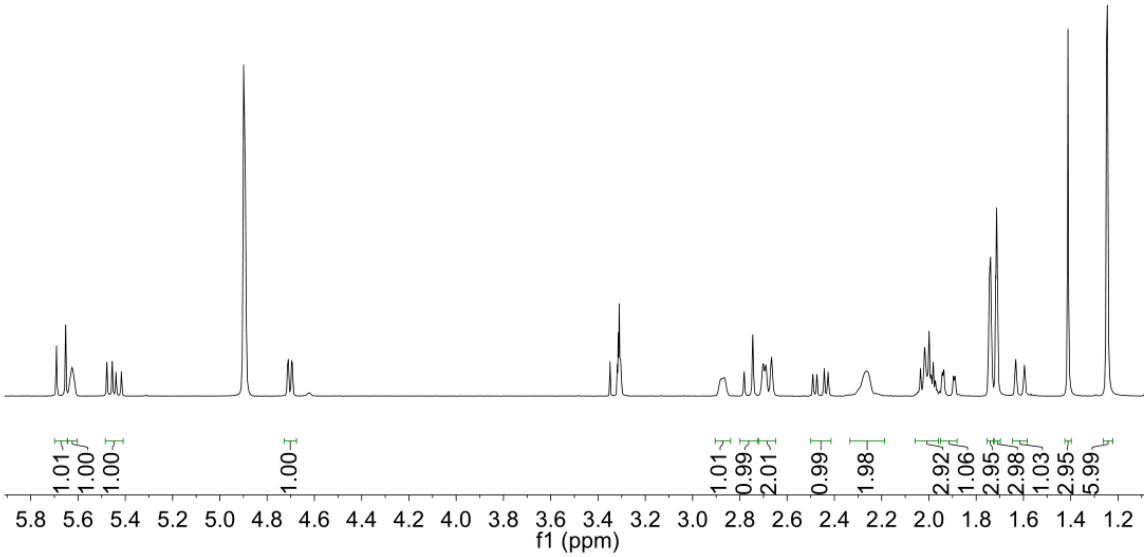

^{1}H NMR spectrum of synthetic orientanoid B (Methanol-d_4, 400 MHz)

Fig. S54. Comparison of ^{13}C NMR spectra of natural and synthetic orientanoid B (**2**).

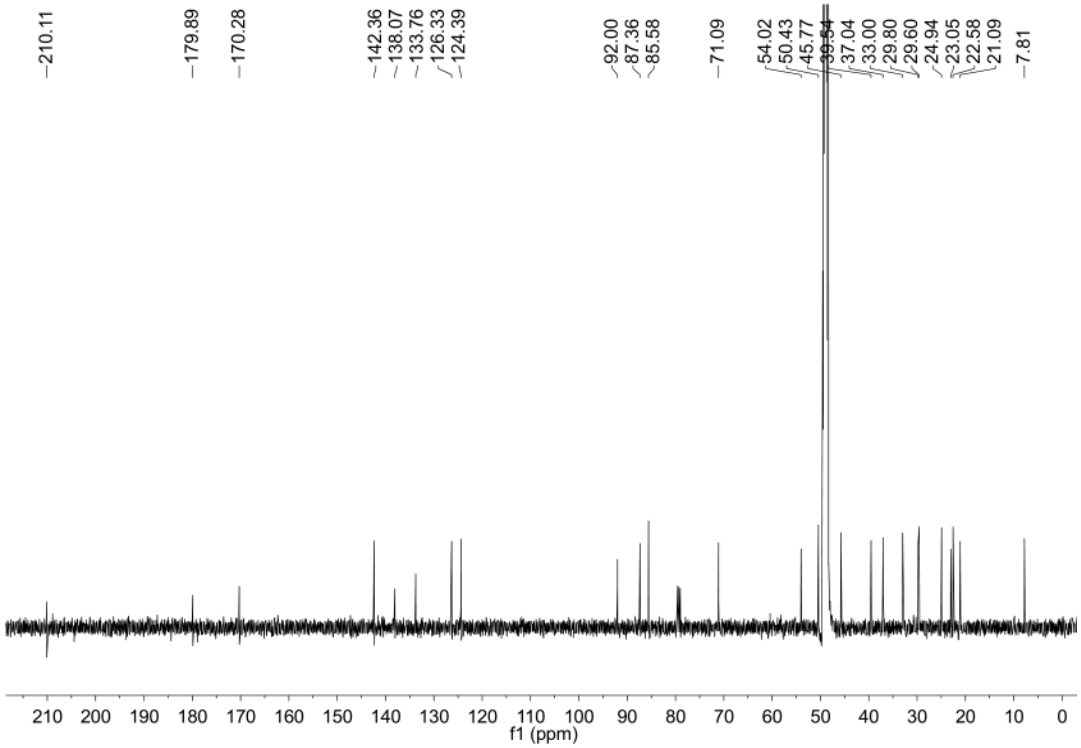

^{13}C NMR spectrum of natural orientanoid B (Methanol-d_4, 125 MHz)

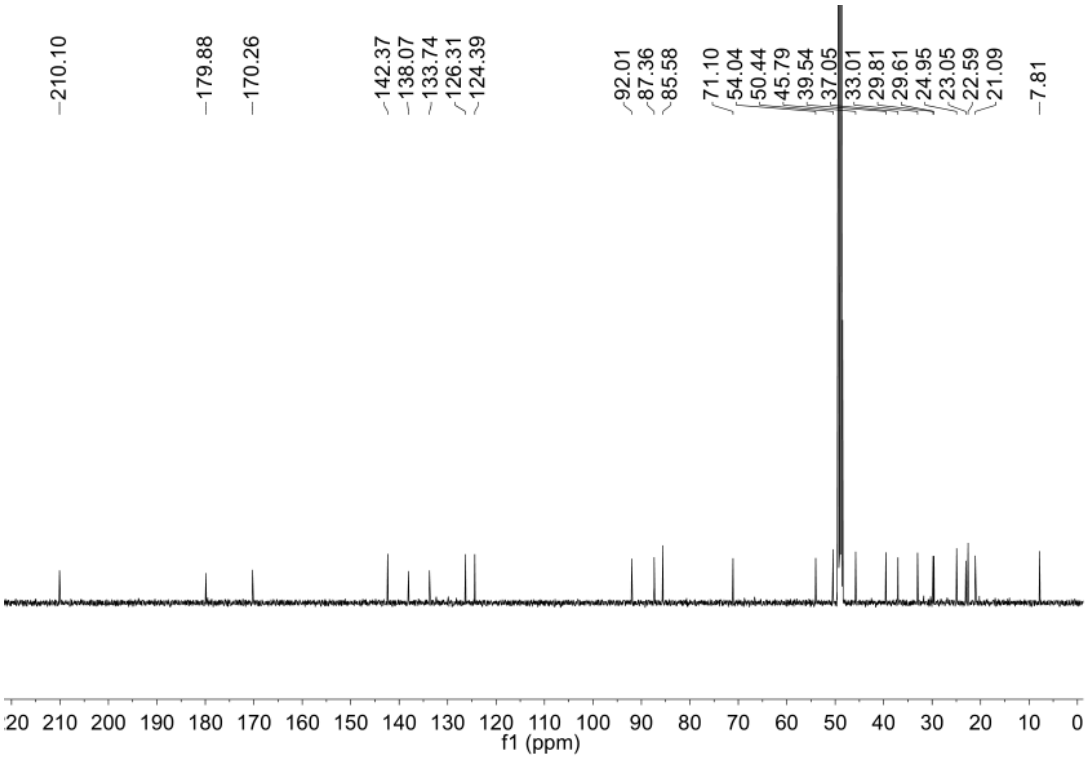

^{13}C NMR spectrum of synthetic orientanoid B (Methanol-d_4, 125 MHz)

Fig. S55. Comparison of ^{1}H NMR spectra of natural and synthetic orientanoid C (**3**).

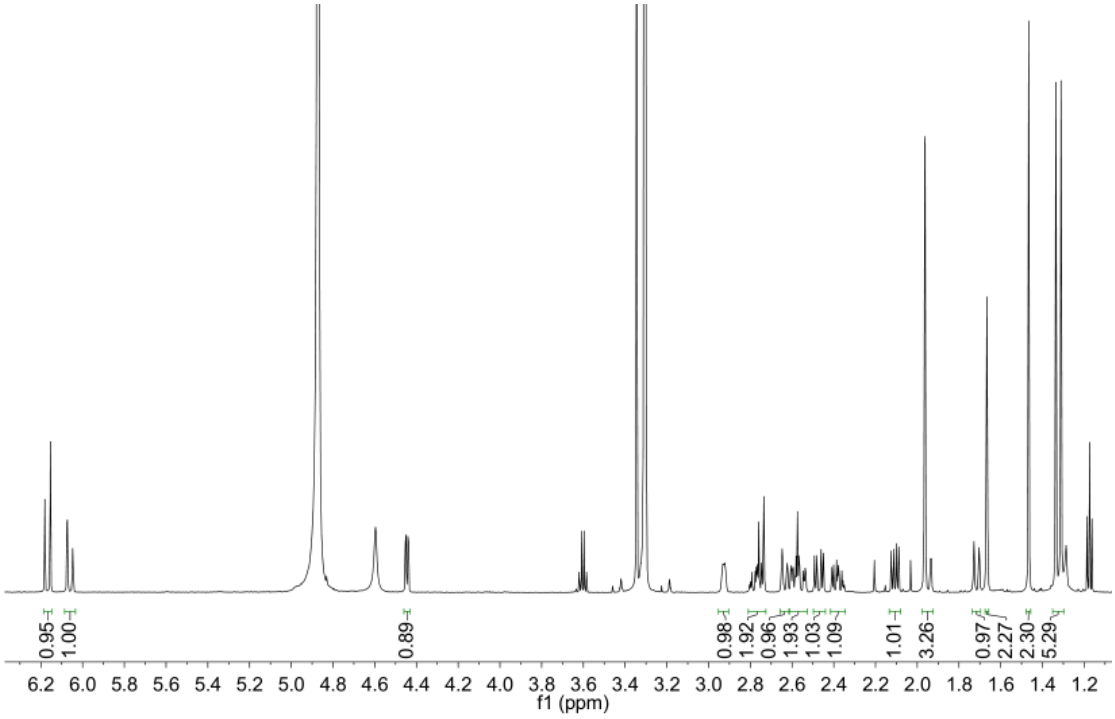

^{1}H NMR spectrum of natural orientanoid C (Methanol-d_4, 500 MHz)

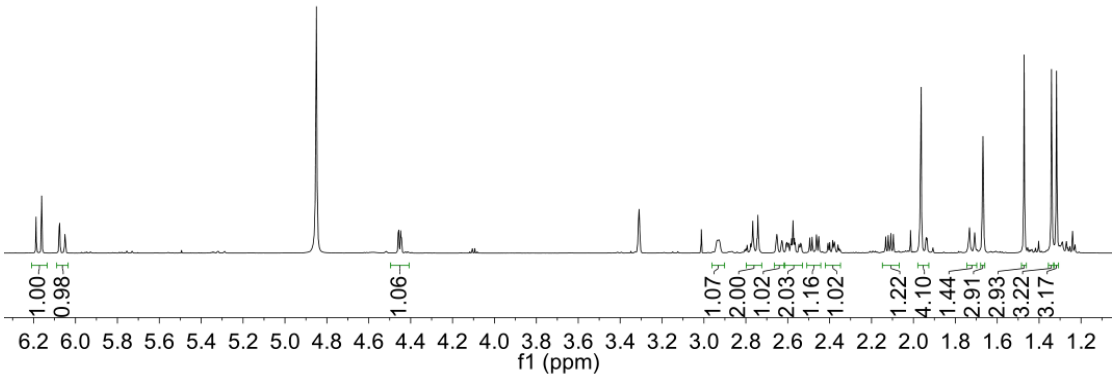

^{1}H NMR spectrum of synthetic orientanoid C (Methanol-d_4, 600 MHz)

Fig. S56. Comparison of ^{13}C NMR spectra of natural and synthetic orientanoid C (**3**).

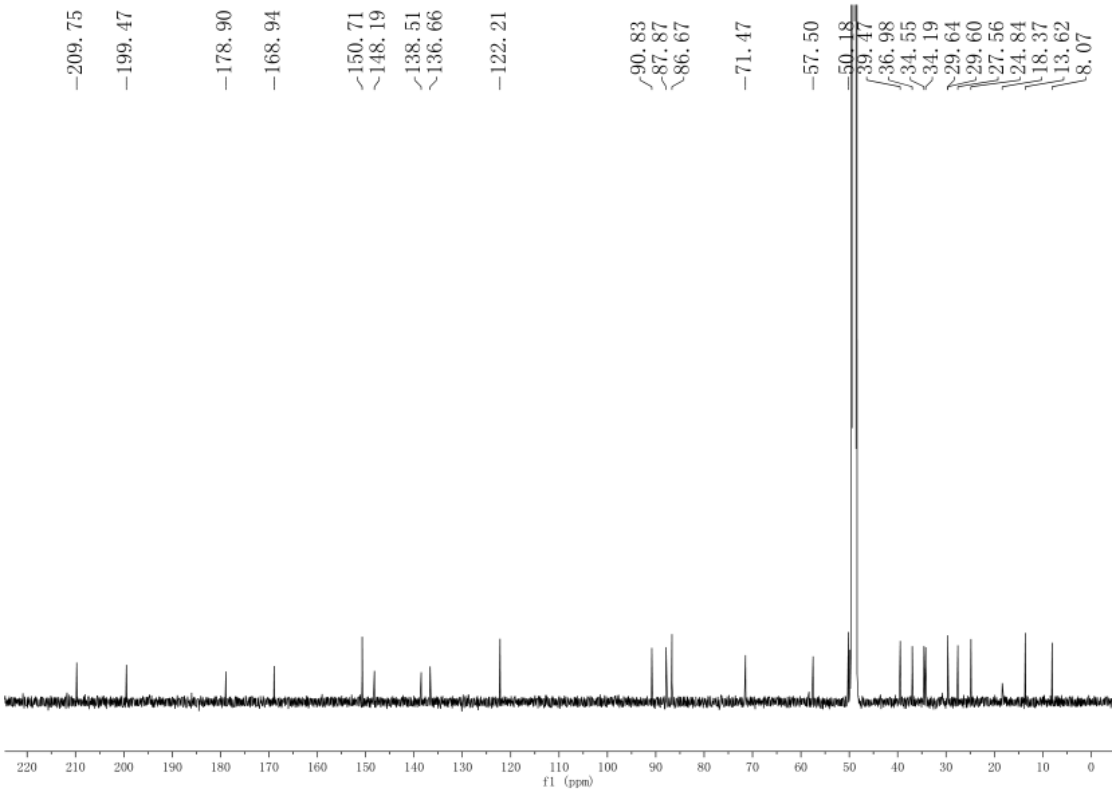

^{13}C NMR spectrum of natural orientanoid C (Methanol-d_4, 125 MHz)

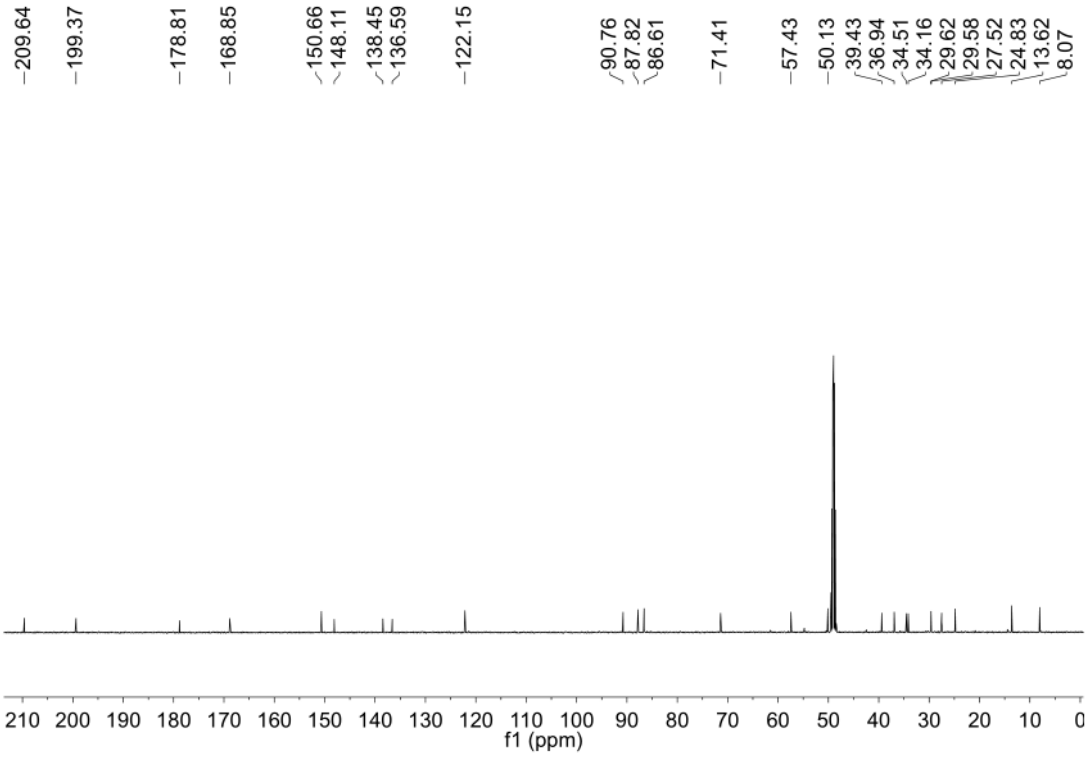

^{13}C NMR spectrum of synthetic orientanoid C (Methanol-d_4, 125 MHz)

^{1}H NMR spectrum of compound **9** (**400 MHz, $CDCl_3$**)

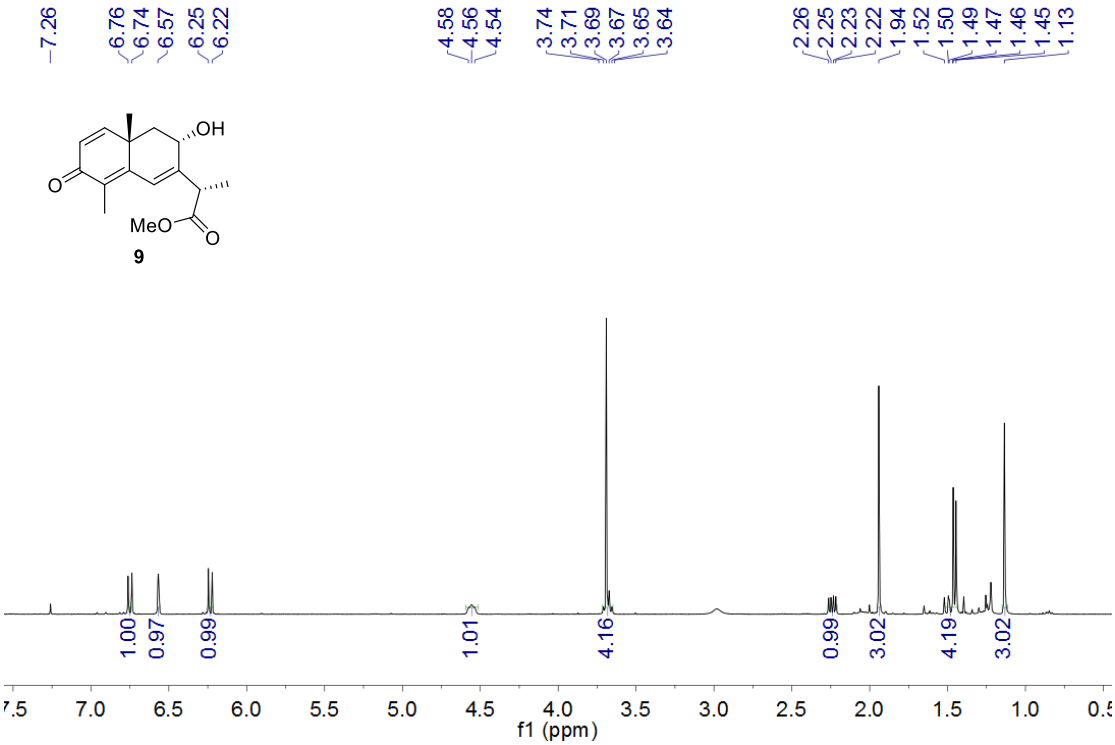

^{13}C NMR spectrum of compound **9** (**100 MHz, $CDCl_3$**)

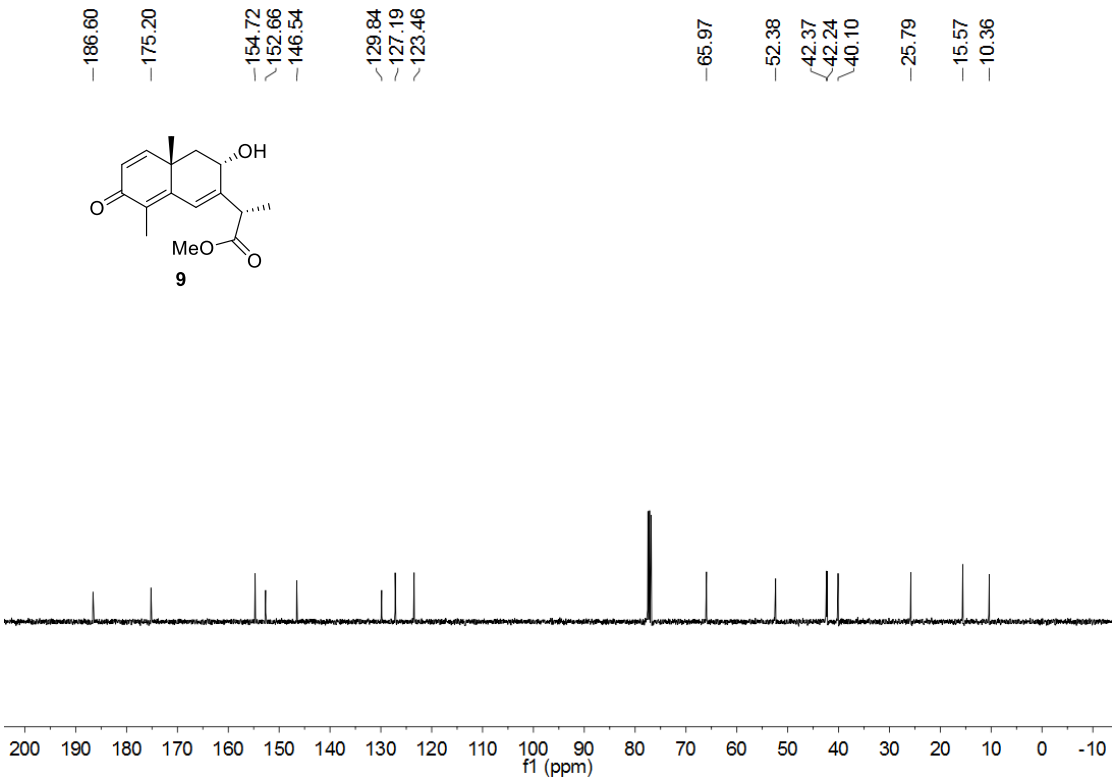

^{1}H NMR spectrum of compound **7** (**400 MHz, $CDCl_3$**)

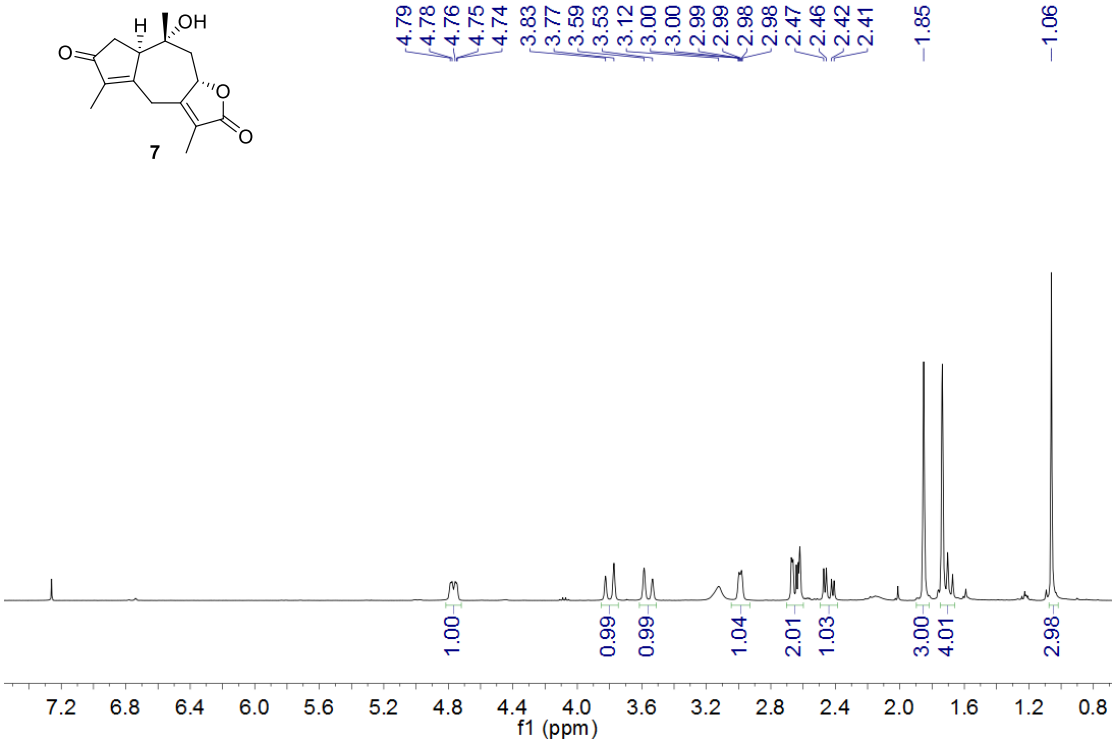

^{13}C NMR spectrum of compound **7** (**100 MHz, $CDCl_3$**)

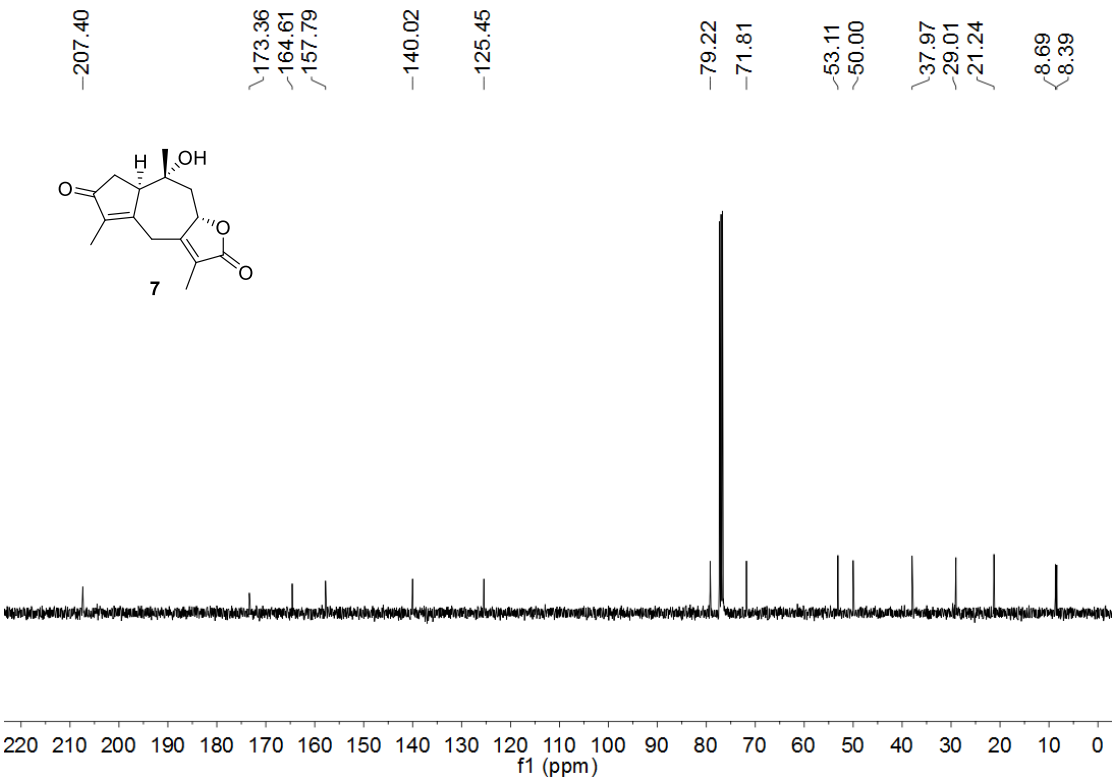

^{1}H NMR spectrum of compound **6** (**400 MHz, $CDCl_3$**)

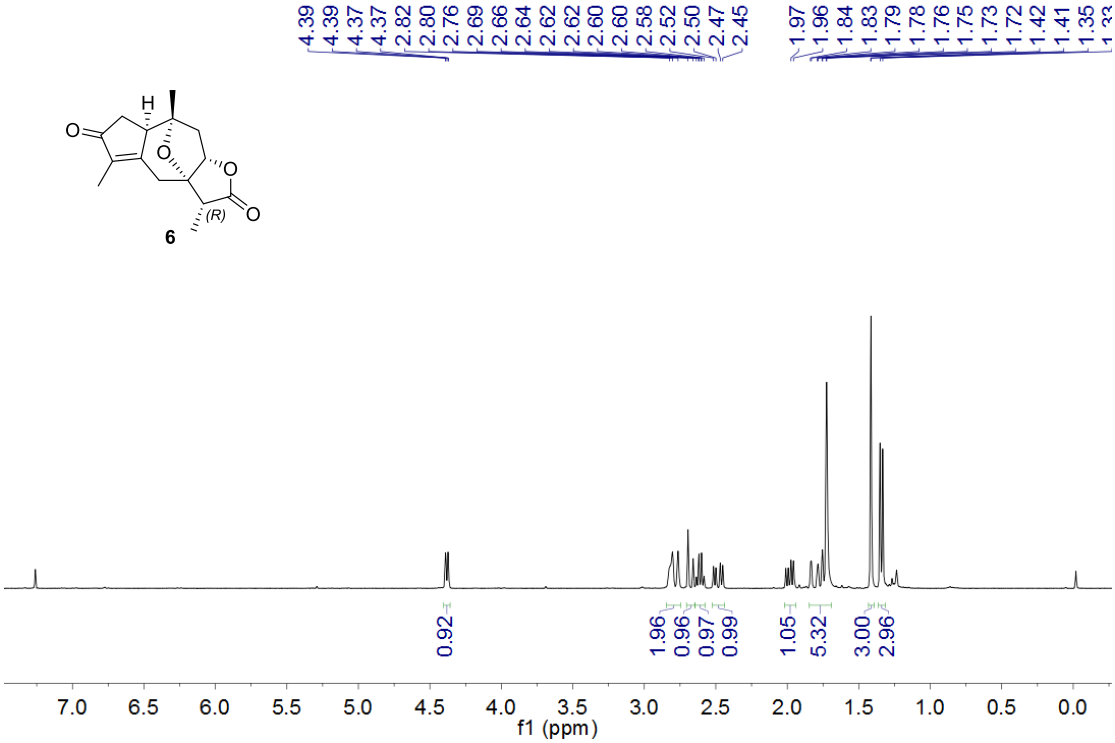

^{13}C NMR spectrum of compound **6** (**125 MHz, $CDCl_3$**)

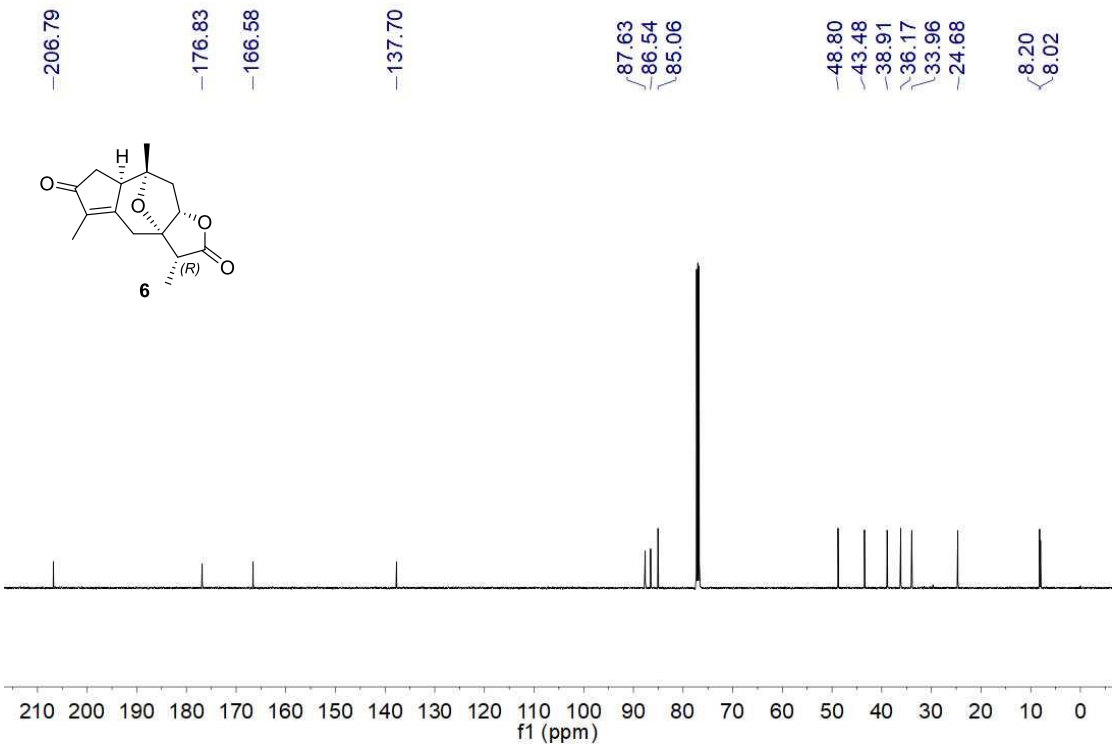

^{1}H NMR spectrum of compound **10** (**400 MHz, $CDCl_3$**)

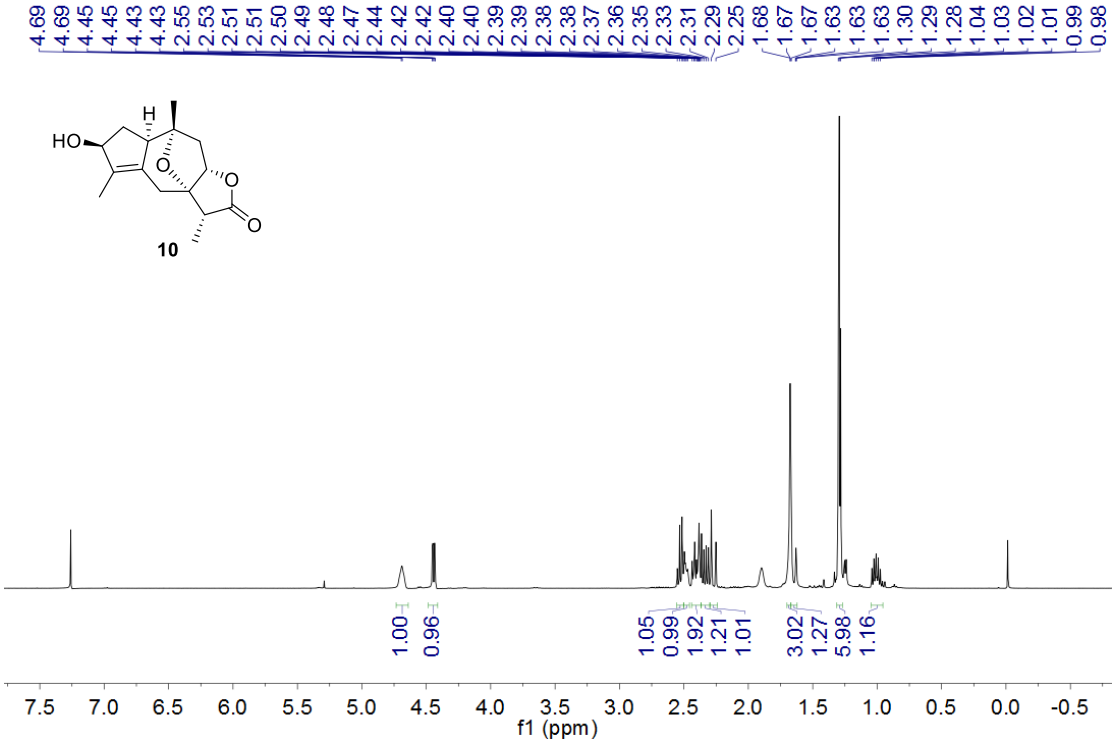

^{13}C NMR spectrum of compound **10** (**125 MHz, $CDCl_3$**)

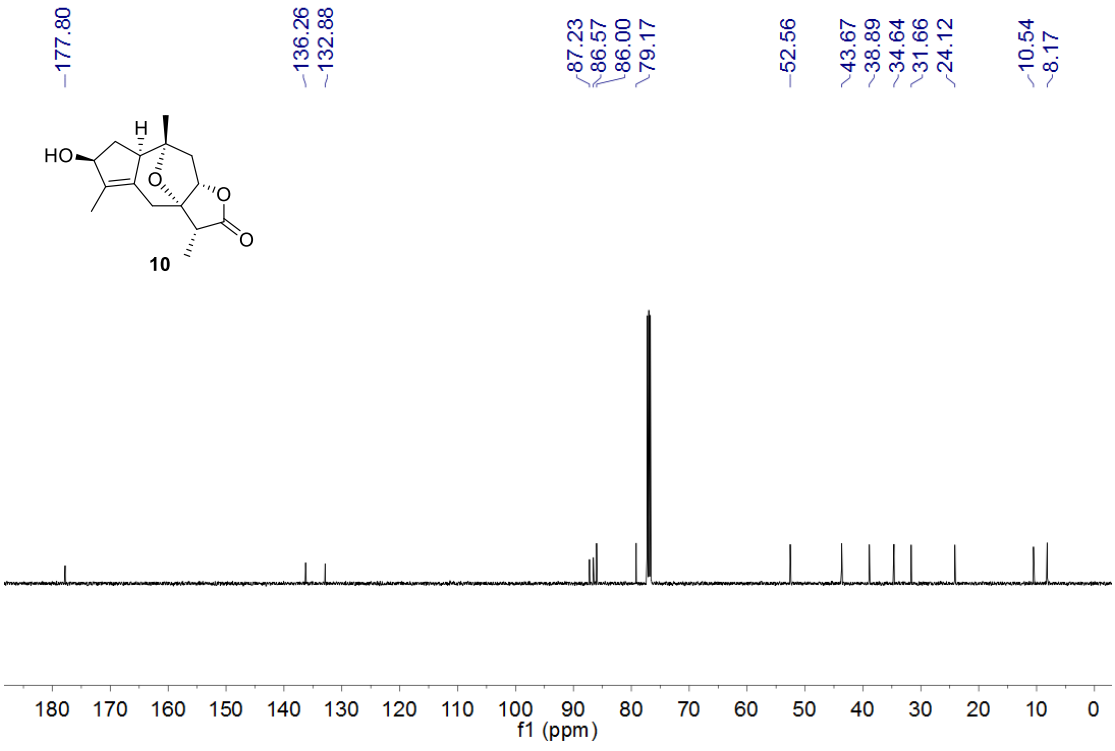

^{1}H NMR spectrum of compound **11** (**400 MHz, $CDCl_3$**)

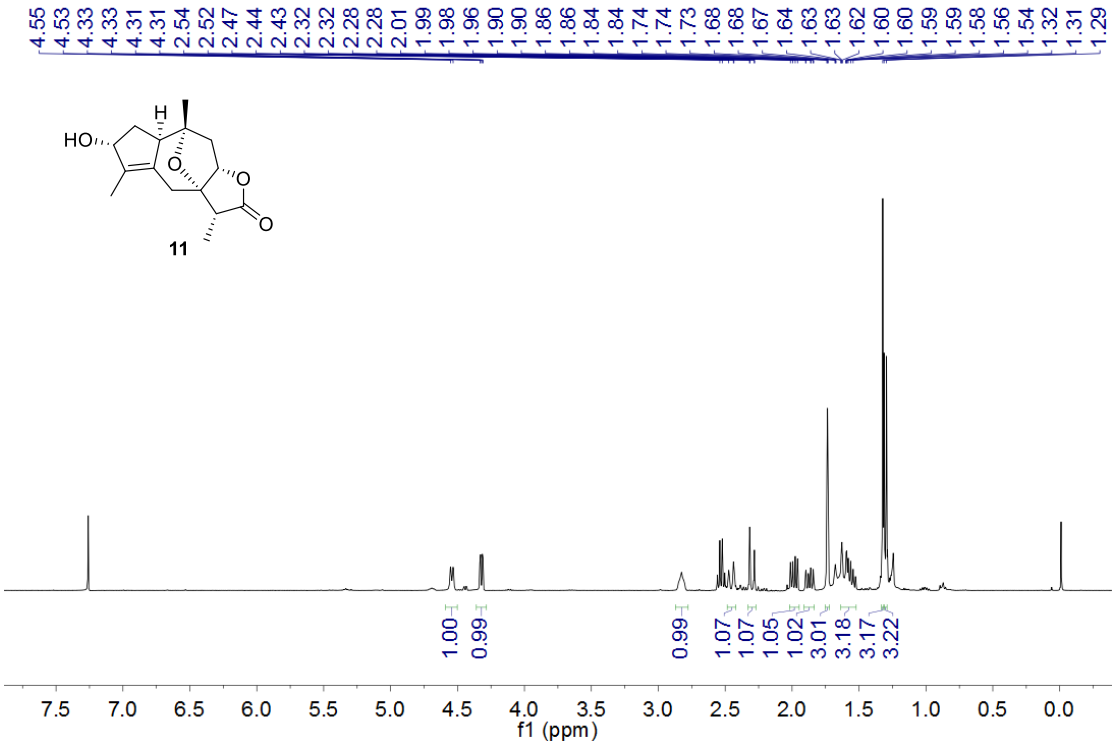

^{13}C NMR spectrum of compound **11** (**125 MHz, $CDCl_3$**)

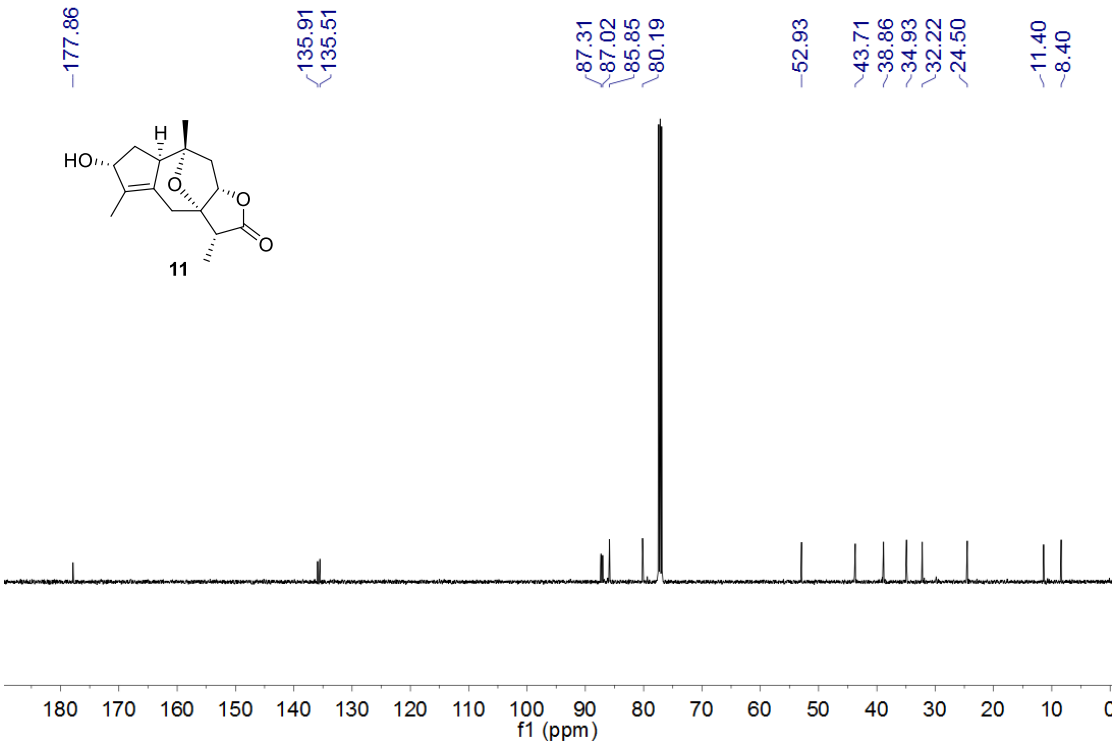

^{1}H NMR spectrum of compound **5** (**400 MHz, $CDCl_3$**)

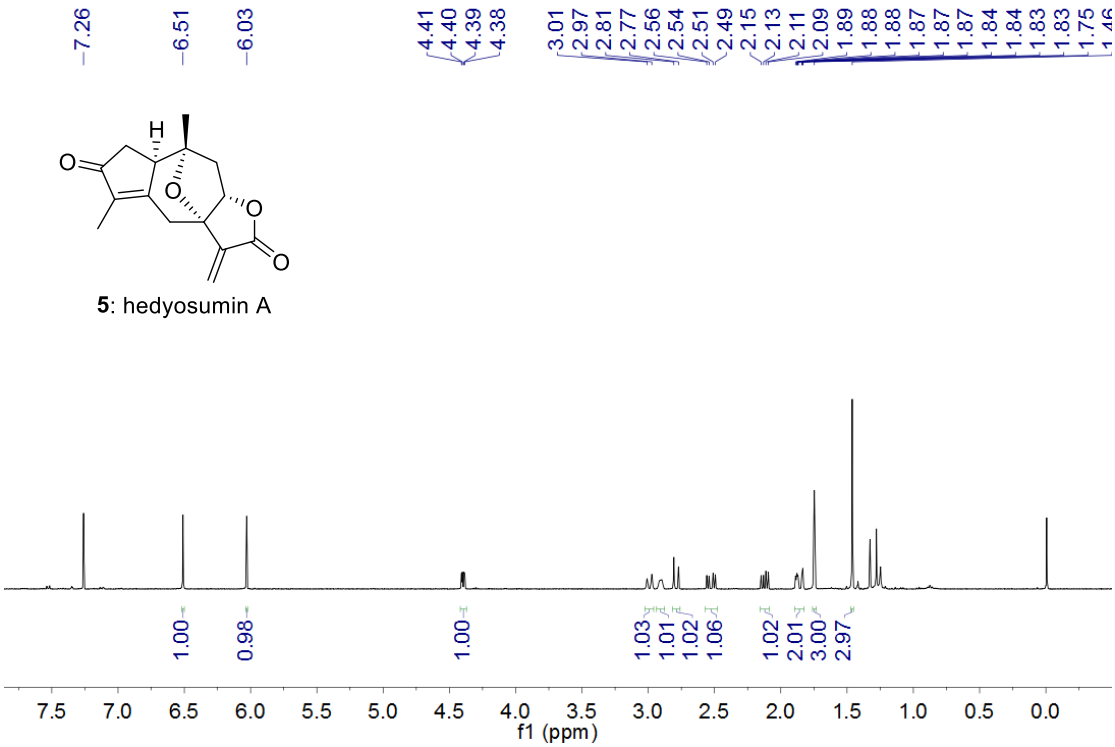

5: hedyosumin A

^{13}C NMR spectrum of compound **5** (**125 MHz, $CDCl_3$**)

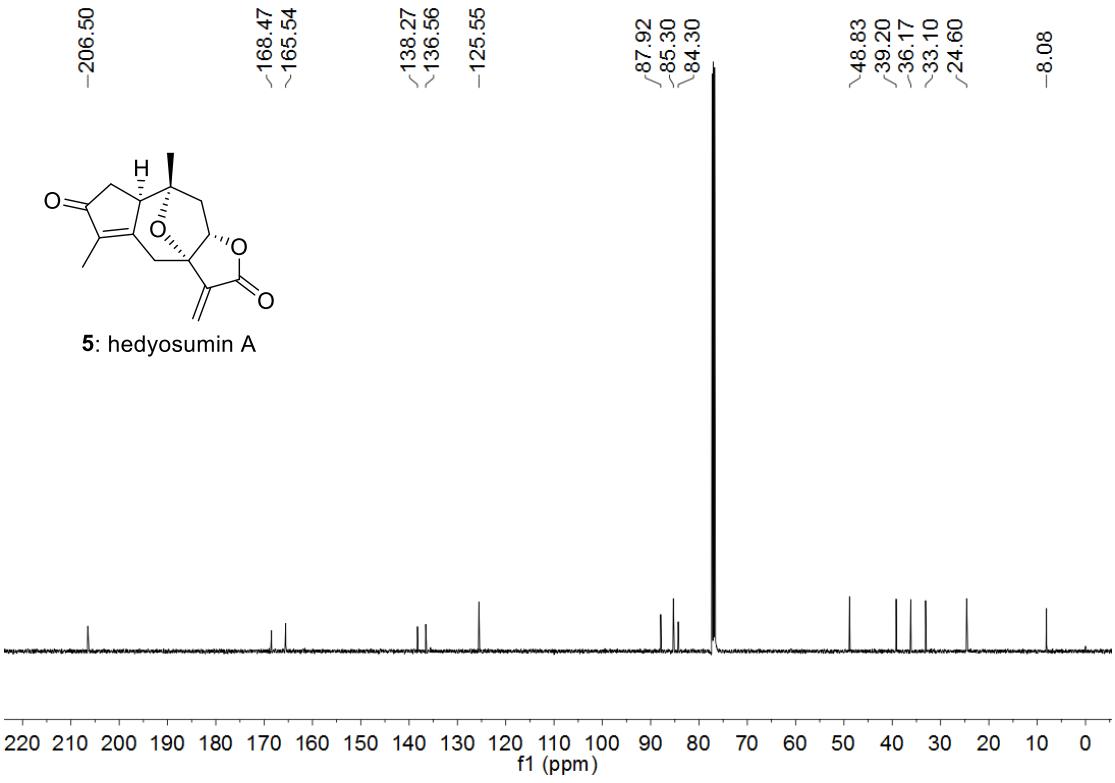

5: hedyosumin A

^{1}H NMR spectrum of compound **4** (**400 MHz, $CDCl_3$**)

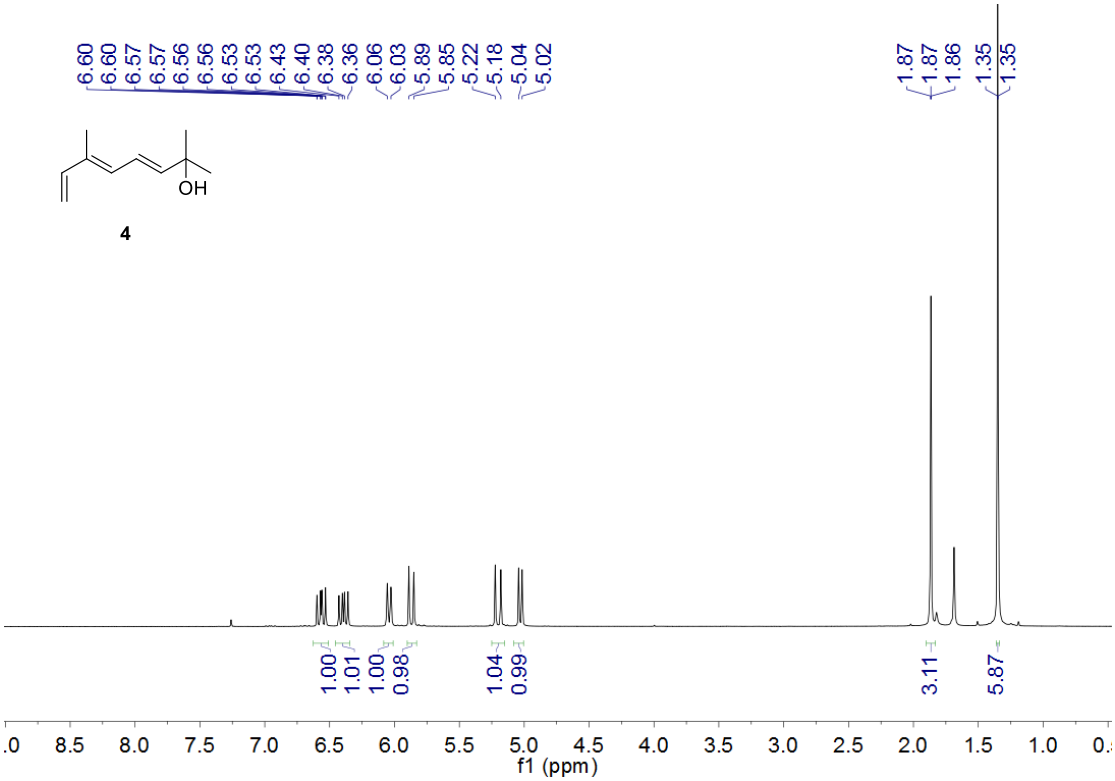

^{13}C NMR spectrum of compound **4** (**100 MHz, $CDCl_3$**)

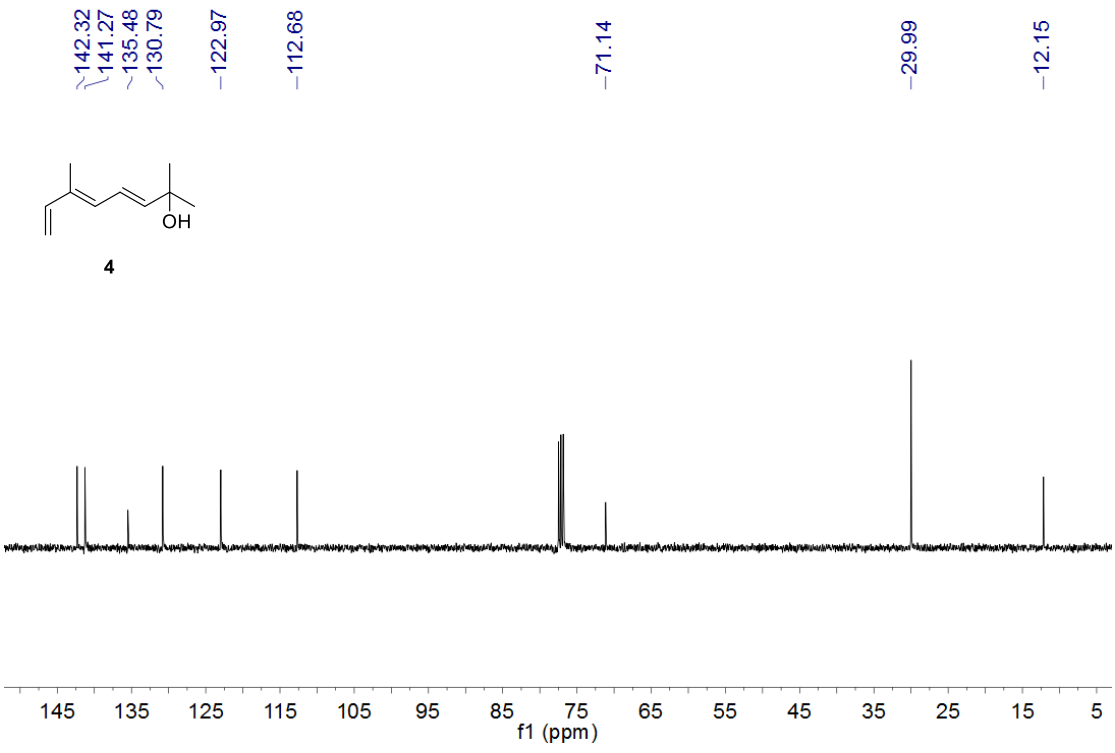

^{1}H NMR spectrum of synthetic orientanoid A **(1)** (**600 MHz, Methanol-*d*$_4$**)

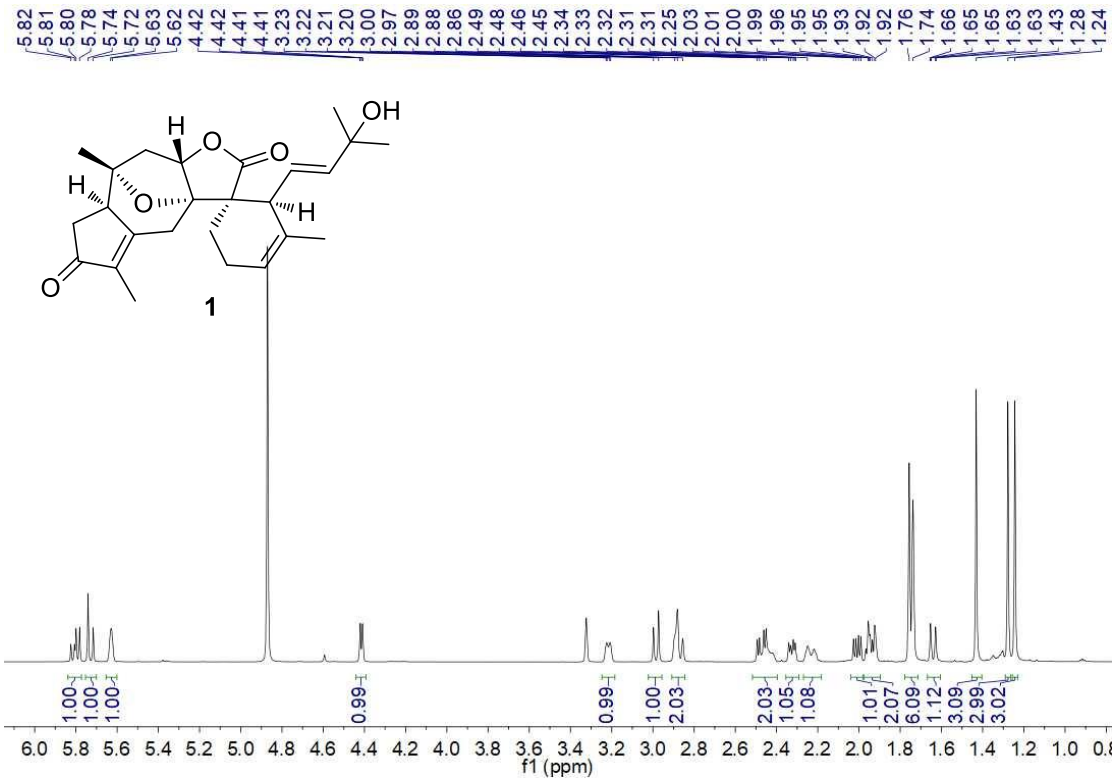

^{13}C NMR spectrum of synthetic orientanoid A **(1)** (**125 MHz, Methanol-*d*$_4$**)

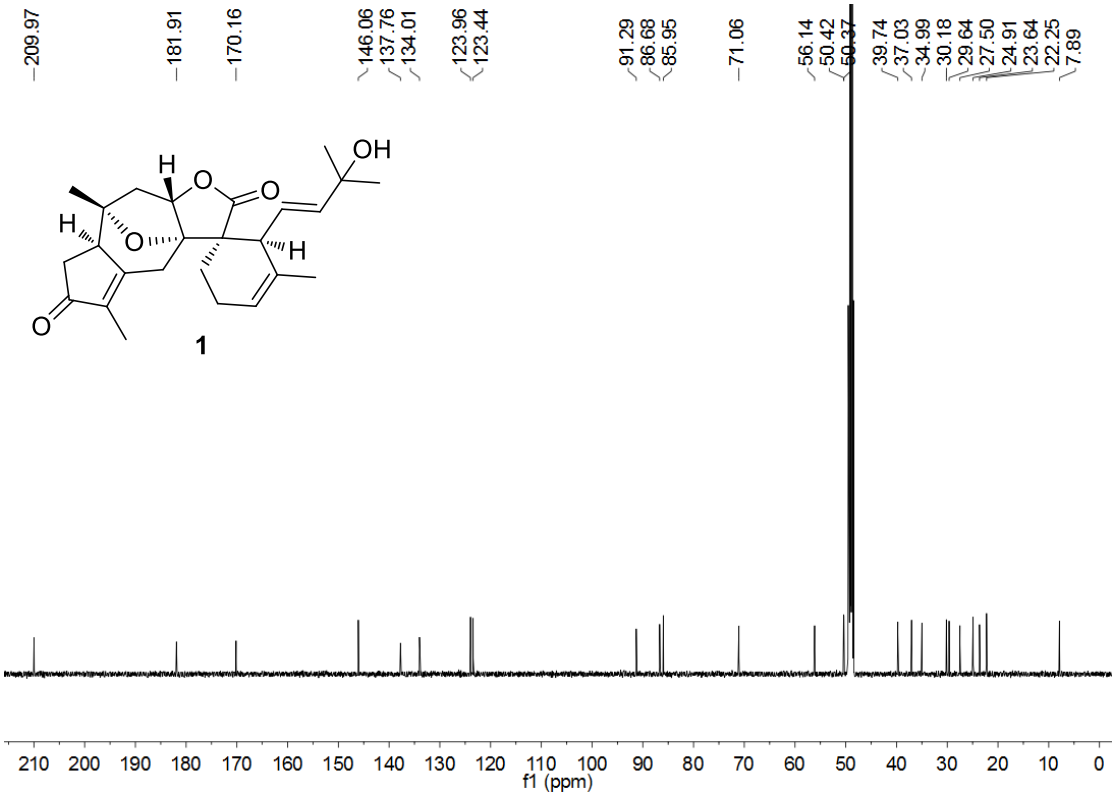

^{1}H NMR spectrum of synthetic orientanoid B **(2)** (**400 MHz, Methanol-*d*$_4$**)

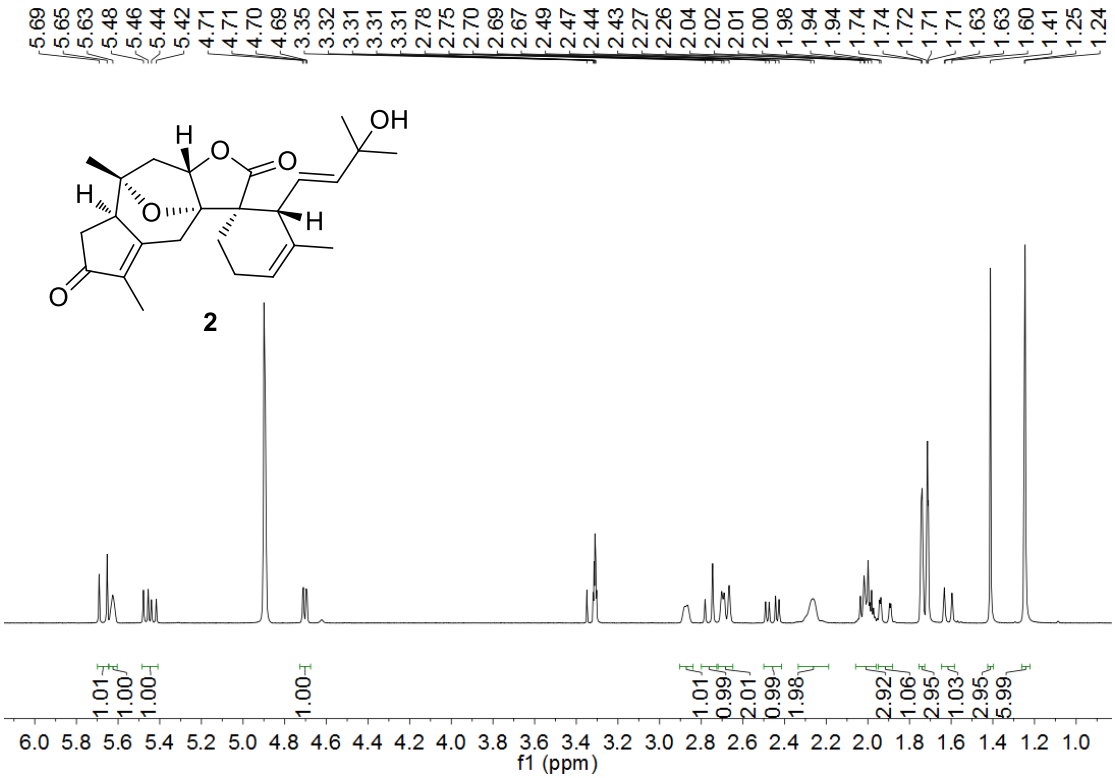

^{13}C NMR spectrum of synthetic orientanoid B **(2)** (**125 MHz, Methanol-*d*$_4$**)

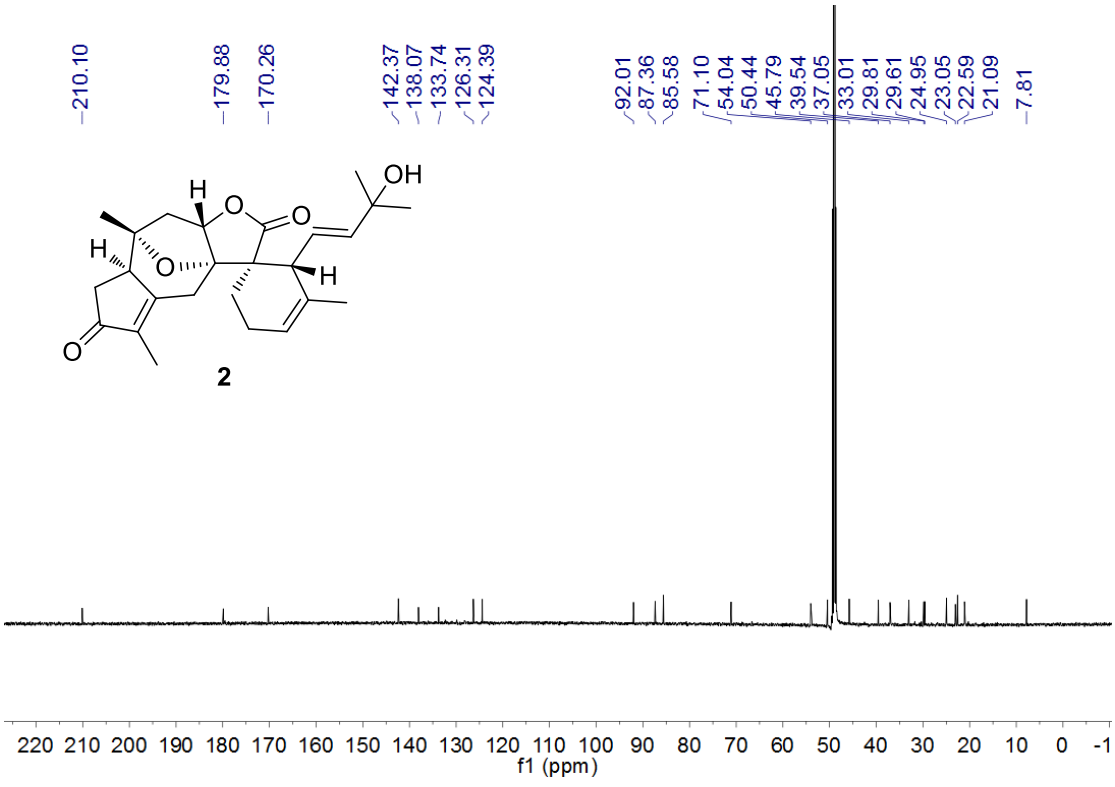

^{1}H NMR spectrum of compound **14** (**400 MHz, Methanol-*d*$_4$**)

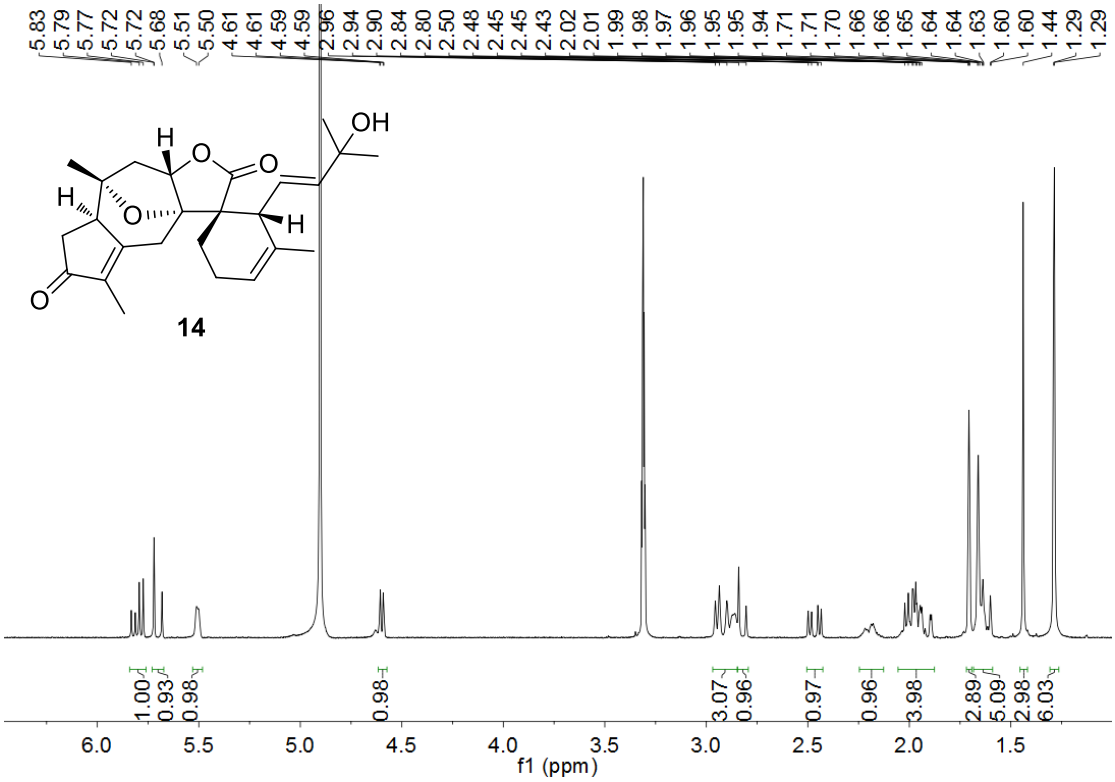

^{13}C NMR spectrum of compound **14** (**125 MHz, Methanol-*d*$_4$**)

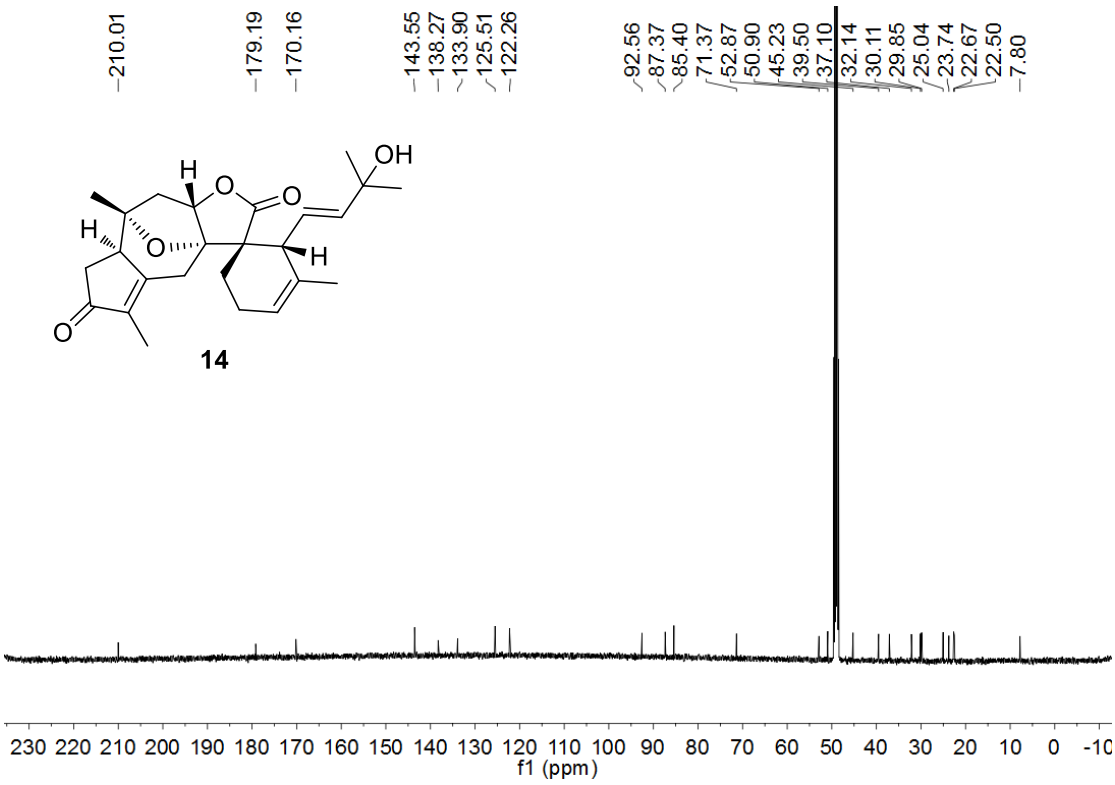

^{1}H NMR spectrum of compound **15** (**400 MHz, Methanol-*d*$_4$**)

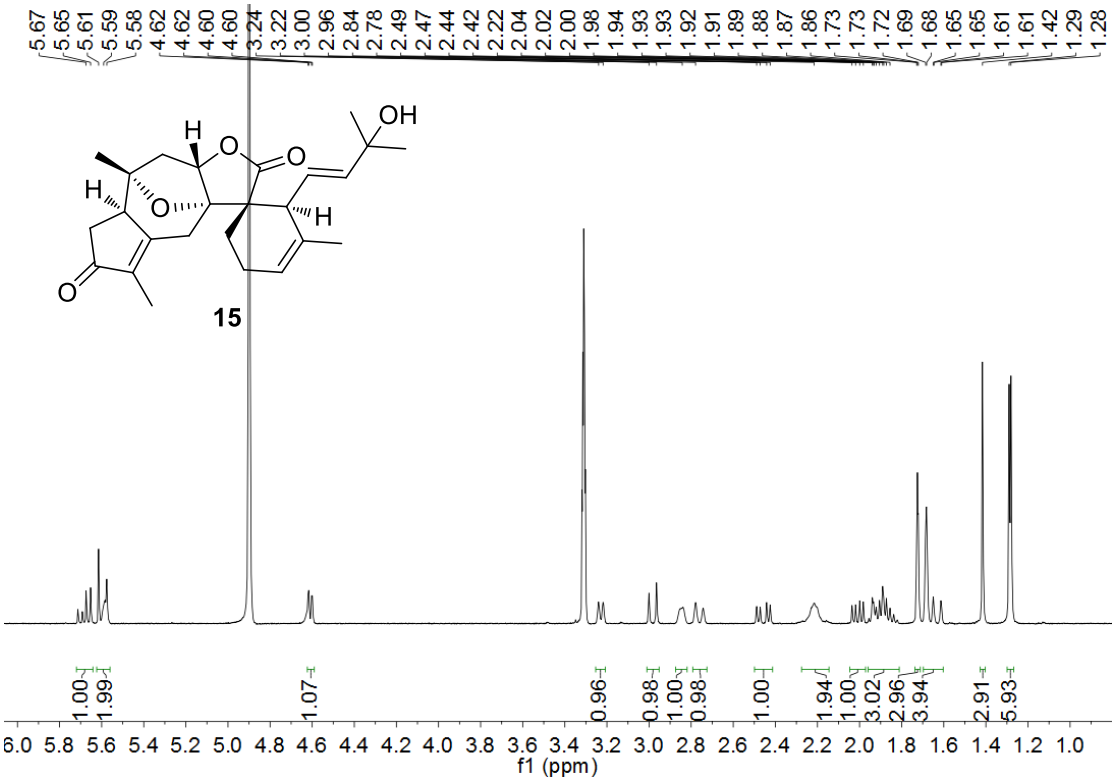

^{13}C NMR spectrum of compound **15** (**125 MHz, Methanol-*d*$_4$**)

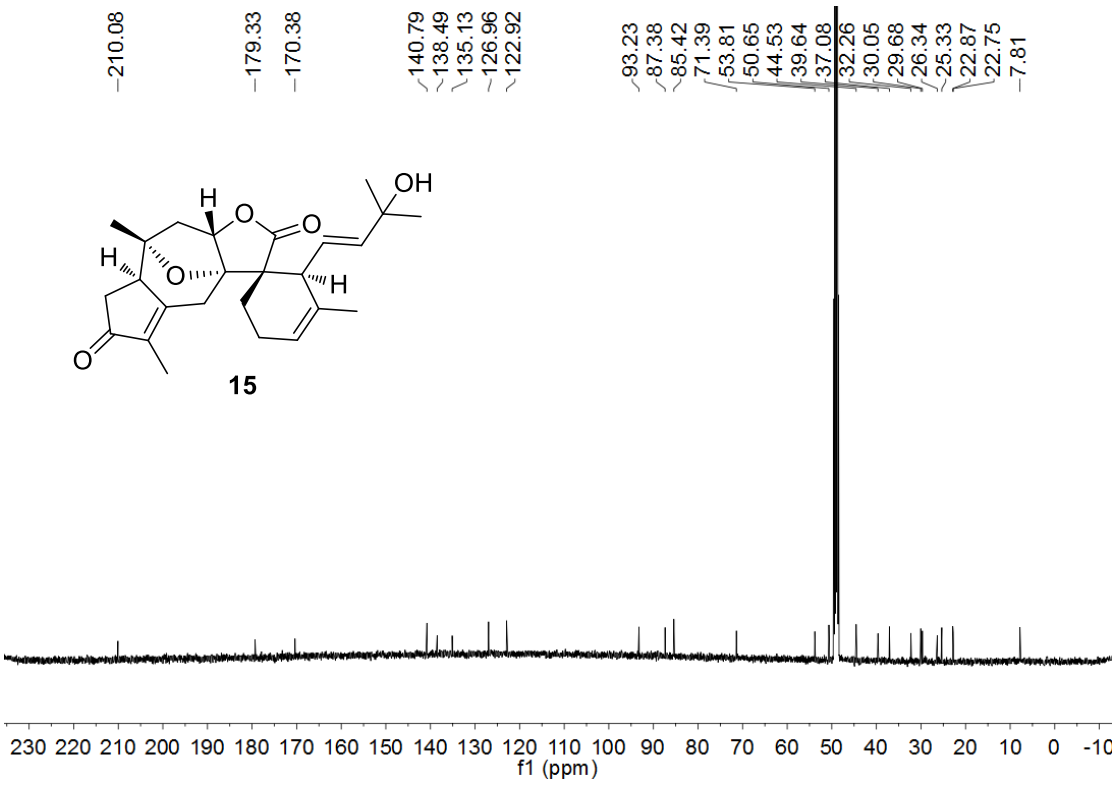

^{1}H NMR spectrum of synthetic orientanoid C (**3**) **(600 MHz, Methanol-*d*$_4$)**

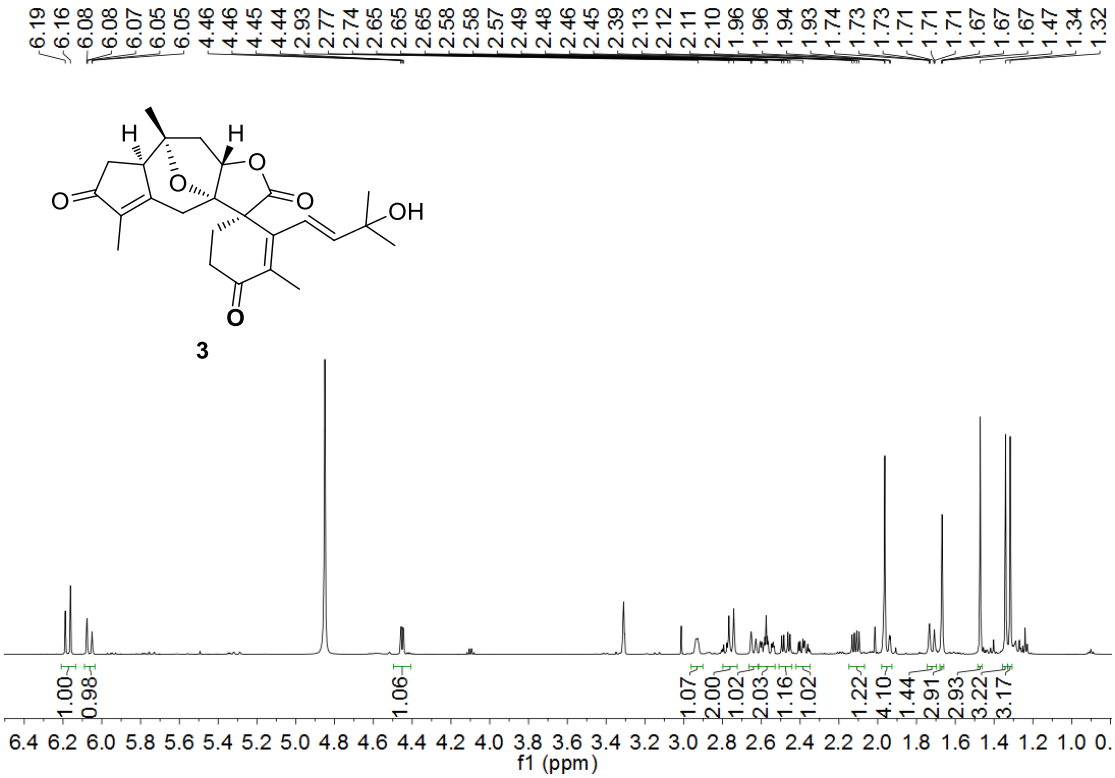

^{13}C NMR spectrum of synthetic orientanoid C (**3**) **(125 MHz, Methanol-*d*$_4$)**

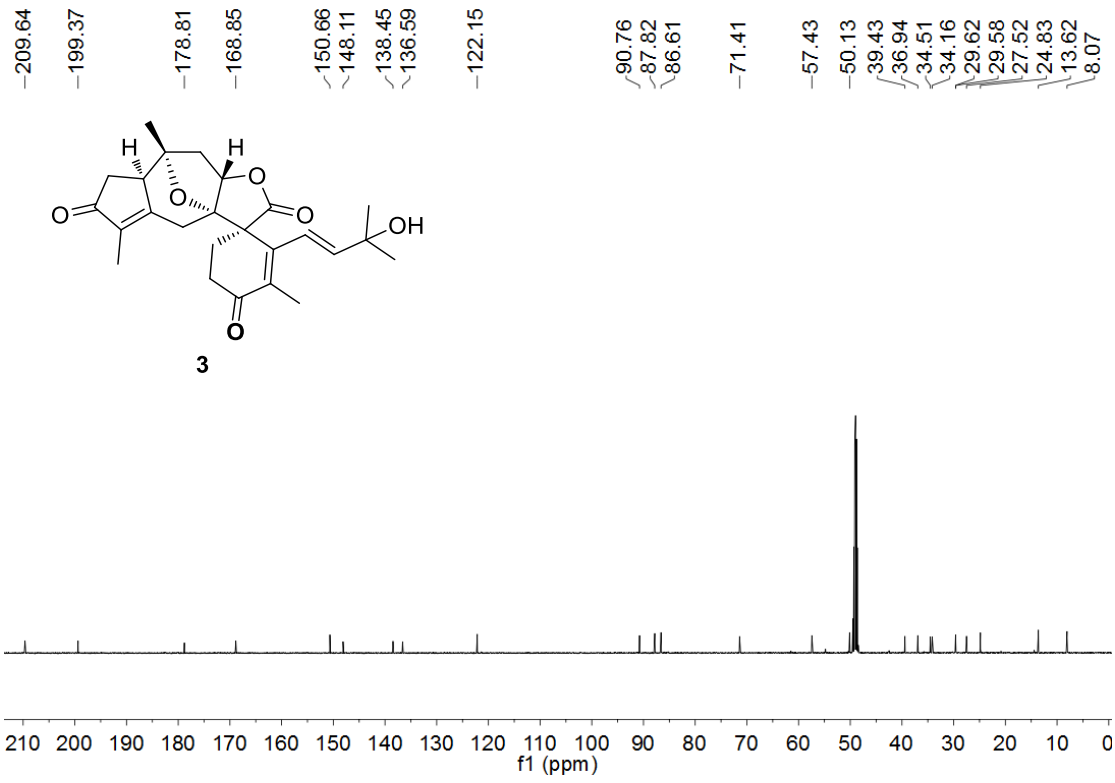

7. References

1 E. Harder, W. Damm, J. Maple, C. Wu, M. Reboul, J. Y. Xiang, L. Wang, D. Lupyan, M. K. Dahlgren, J. L. Knight, J. W. Kaus, D. S. Cerutti, G. Krilov, W. L. Jorgensen, R. Abel and R. A. Friesner, *J. Chem. Theory Comput.*, 2016, **12**, 281–296.

2 M. J. Frisch, G. W. Trucks, H. B. Schlegel, G. E. Scuseria, M. A. Robb, J. R. Cheeseman, G. Scalmani, V. Barone, B. Mennucci, G. A. Petersson, H. Nakatsuji, M. Caricato, X. Li, H. P. Hratchian, A. F. Izmaylov, J. Bloino, G. Zheng, J. L. Sonnenberg, M. Hada, M. Ehara, K. Toyota, R. Fukuda, J. Hasegawa, M. Ishida, T. Nakajima, Y. Honda, O. Kitao, H. Nakai, T. Vreven, J. A. Jr. Montgomery, J. E. Peralta, F. Ogliaro, M. Bearpark, J. J. Heyd, E. Brothers, K. N. Kudin, V. N. Staroverov, R. Kobayashi, J. Normand, K. Raghavachari, A. Rendell, J. C. Burant, S. S. Iyengar, J. Tomasi, M. Cossi, N. Rega, J. M. Millam, M. Klene, J. E. Knox, J. B. Cross, V. Bakken, C. Adamo, J. Jaramillo, R. Gomperts, R. E. Stratmann, O. Yazyev, A. J. Austin, R. Cammi, C. Pomelli, J. W. Ochterski, R. L. Martin, K. Morokuma, V. G. Zakrzewski, G. A. Voth, P. Salvador, J. J. Dannenberg, S. Dapprich, A. D. Daniels, O. Farkas, J. B. Foresman, J. V. Ortiz, J. Cioslowski and D. J. Fox, Gaussian 09 Rev. A.01, Gaussian Inc., Wallingford, CT, **2009**.

3 T. Bruhn, A. Schaumlöffel, Y. Hemberger and G. Bringmann, *Chirality*, 2013, **25**, 243–249.

4 T. Bruhn, A. Schaumlöffel, Y. Hemberger and G. Pescitelli, SpecDis version 1.71, Berlin, Germany, **2017**.

5 G. Pescitelli and T. Bruhn, *Chirality*, 2016, **28**, 466–474.

6 G. Blay, M. Luz Cardona, B. Garcia and J. R. Pedro, *J. Org. Chem*. 1991, **56**, 6172–6175.

LC-MS Analysis Report for Mixtures of Compounds 1, 2, 14, and 15

pages 106-108

Qualitative Analysis Report

Data Filename	LCMS202300141-2.d	**Sample Name**	D4-mix-1
Sample ID		**Position**	P1-F4
Instrument Name	Agilent 6545 Q-TOF LCMS	**Acq Method**	20210825_LCMS_POS.m
Acquired Time	4/7/2023 9:51:44 AM (UTC+08:00)	**IRM Calibration Status**	Success
DA Method	0.1323.m	**Comment**	
Chromatograms			

Fragmentor Voltage ## **Collision Energy** 0 **Ionization Mode** ESI

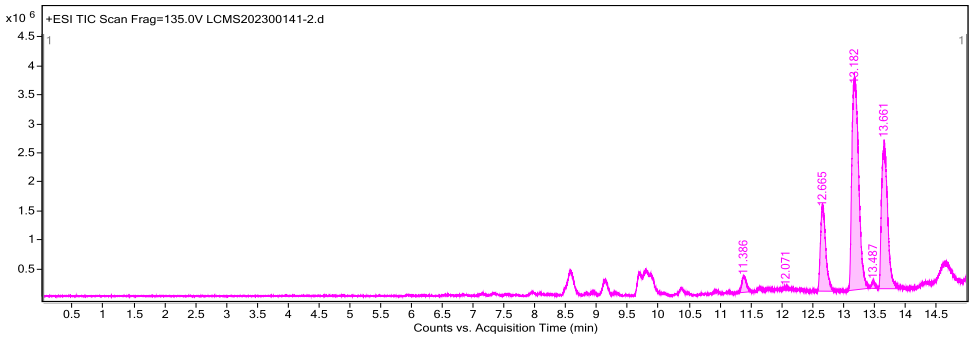

Integration Peak List

Peak	Start	RT	End	Height	Area	Area %	AreaSumPercent %
1	11.224	11.386	11.519	274490	1481229	5.3	2.62
2	11.932	12.071	12.349	48585	521626	1.87	0.92
3	12.568	12.665	12.916	1473281	8876704	31.76	15.73
4	13.051	13.182	13.425	3627426	27949736	100	49.53
5	13.425	13.487	13.561	116890	470754	1.68	0.83
6	13.561	13.661	14.003	2413213	17128008	61.28	30.35

Fragmentor Voltage ## **Collision Energy** 0 **Ionization Mode** ESI

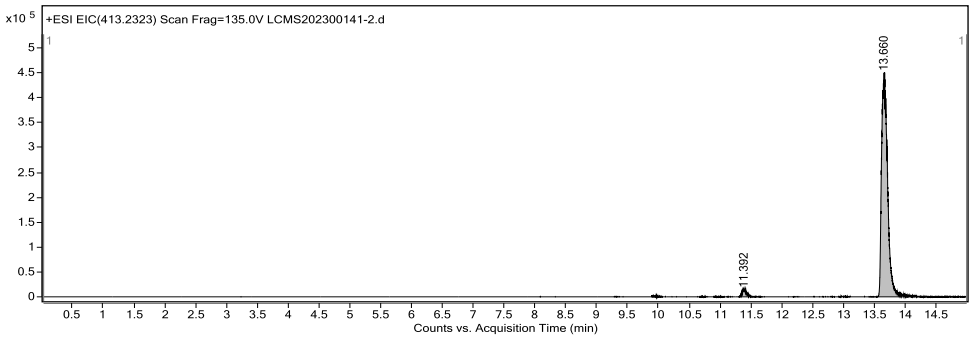

Integration Peak List

Peak	Start	RT	End	Height	Area	Area %	AreaSumPercent %
1	11.302	11.392	11.701	13456	75455	2.48	2.42
2	13.417	13.66	14.723	428841	3045602	100	97.58

Fragmentor Voltage ## **Collision Energy** 0 **Ionization Mode** ESI

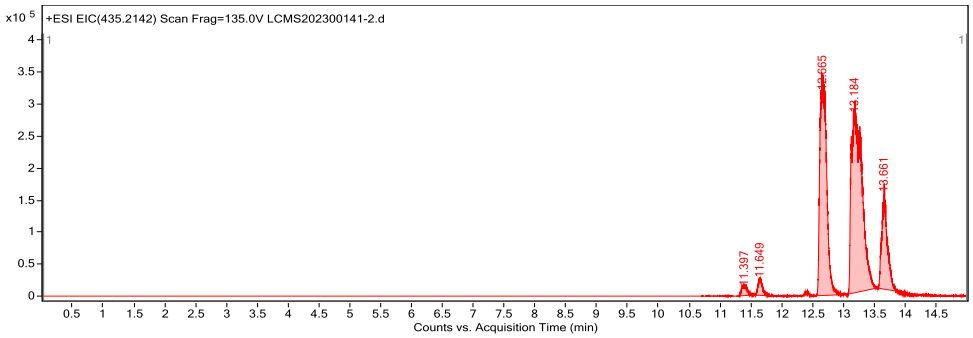

Integration Peak List

Peak	Start	RT	End	Height	Area	Area %	AreaSumPercent %
1	11.254	11.397	11.543	14599	98083	2.82	1.35
2	11.543	11.649	11.974	25032	130042	3.74	1.79
3	12.527	12.665	13.049	328285	2630405	75.7	36.31
4	13.049	13.184	13.547	284037	3474899	100	47.96
5	13.547	13.661	14.28	140292	911770	26.24	12.58

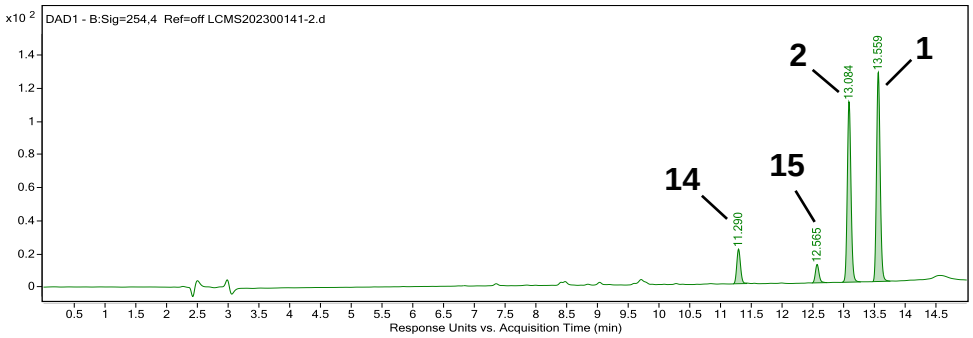

Integration Peak List

Peak	Start	RT	End	Height	Area	Area %	AreaSumPercent %
1	11.208	11.29	11.422	20.95	88.61	16.9	7.94
2	12.488	12.565	12.728	11.15	46.82	8.93	4.2
3	12.968	13.084	13.268	109.63	456.05	86.95	40.87
4	13.468	13.559	13.748	127.17	524.48	100	47

Spectra

Fragmentor Voltage	Collision Energy	Ionization Mode
135	0	ESI

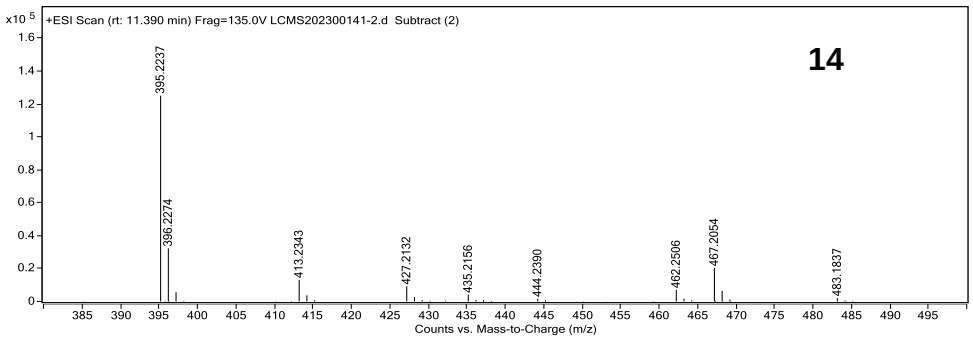

Fragmentor Voltage	Collision Energy	Ionization Mode
135	0	ESI

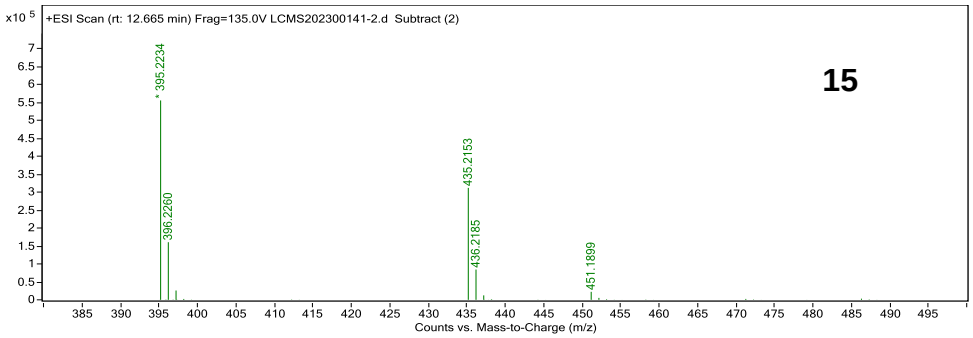

Fragmentor Voltage	Collision Energy	Ionization Mode
135	0	ESI

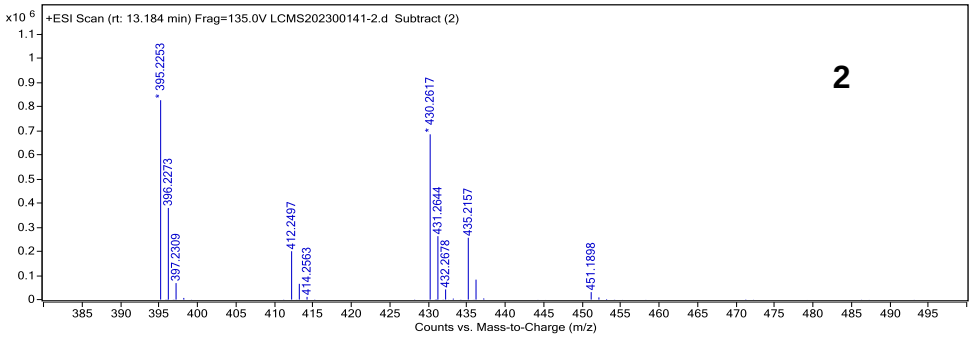

Fragmentor Voltage	Collision Energy	Ionization Mode
135	0	ESI

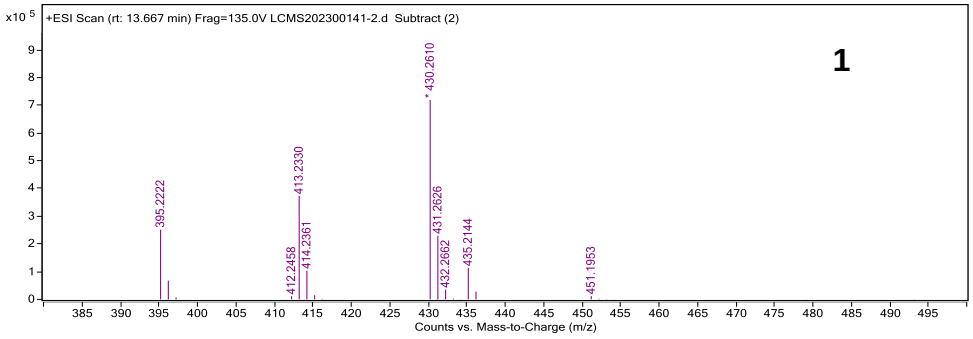

--- End Of Report ---

Qualitative Analysis Report

Data Filename	LCMS202300142-2.d	**Sample Name**	D4-np-1
Sample ID		**Position**	P1-F5
Instrument Name	Agilent 6545 Q-TOF LCMS	**Acq Method**	20210825_LCMS_POS.m
Acquired Time	4/7/2023 10:11:11 AM (UTC+08:00)	**IRM Calibration Status**	Success
DA Method	0.1323.m	**Comment**	

Chromatograms

Fragmentor Voltage ## **Collision Energy** 0 **Ionization Mode** ESI

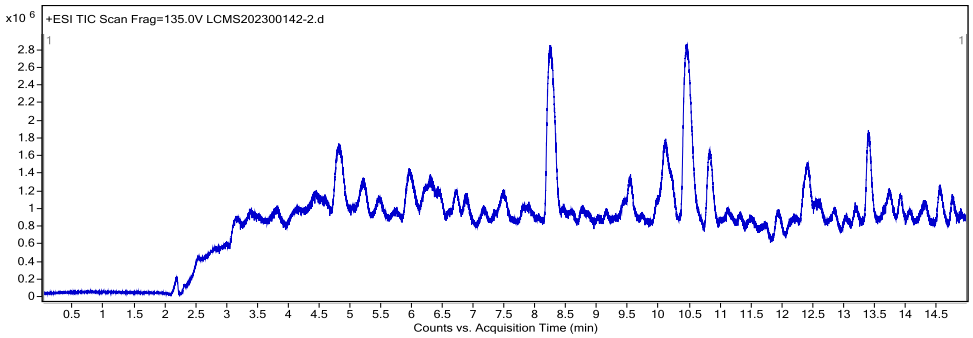

Fragmentor Voltage ## **Collision Energy** 0 **Ionization Mode** ESI

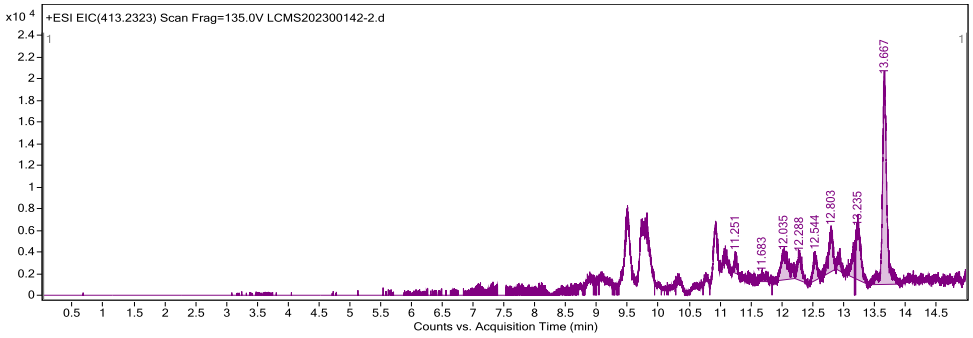

Integration Peak List

Peak	Start	RT	End	Height	Area	Area %	AreaSumPercent %
1	11.184	11.251	11.598	1386	3122	3.33	1.49
2	11.598	11.683	11.819	638	4132	4.4	1.97
3	11.819	12.035	12.214	2390	22419	23.89	10.7
4	12.214	12.288	12.437	2338	12841	13.68	6.13
5	12.437	12.544	12.648	2236	10320	11	4.93
6	12.648	12.803	12.88	3755	19576	20.86	9.35
7	12.88	12.927	13.025	1067	5066	5.4	2.42
8	13.025	13.235	13.409	4891	38129	40.63	18.2
9	13.409	13.667	13.922	18420	93842	100	44.8

Fragmentor Voltage ## **Collision Energy** 0 **Ionization Mode** ESI

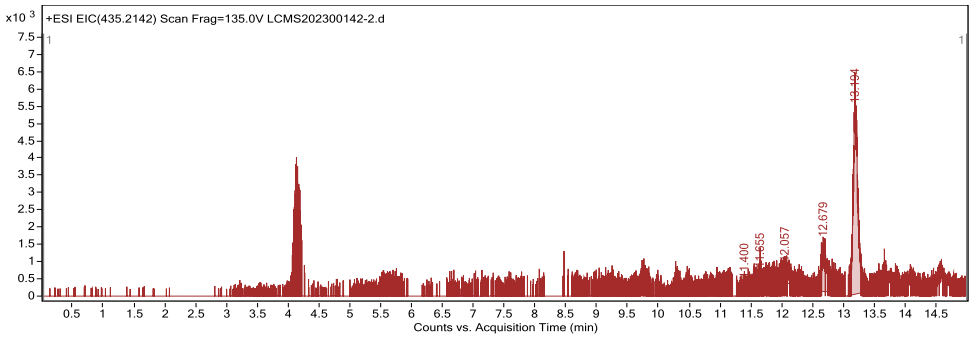

Integration Peak List

Peak	Start	RT	End	Height	Area	Area %	AreaSumPercent %
1	11.233	11.4	11.47	421	2255	7.21	4.68
2	11.47	11.655	11.696	464	2530	8.09	5.25
3	11.919	12.057	12.266	414	3836	12.27	7.96
4	12.576	12.679	12.87	1168	8303	26.57	17.23
5	13.053	13.194	13.406	5385	31254	100	64.87

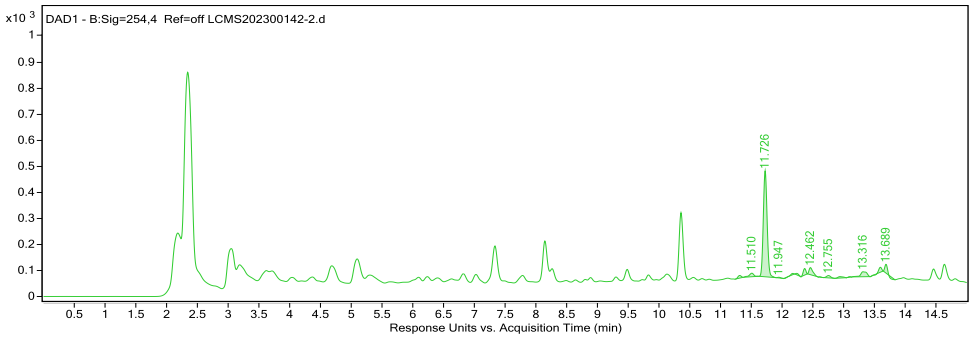

Integration Peak List

Peak	Start	RT	End	Height	Area	Area %	AreaSumPercent %
1	11.238	11.314	11.371	10	36.43	2.08	1.5
2	11.371	11.51	11.625	13.6	71.12	4.07	2.92
3	11.625	11.726	11.906	406.02	1747.26	100	71.85
4	11.906	11.947	12.032	2.58	8.05	0.46	0.33
5	12.032	12.173	12.204	4.91	12.25	0.7	0.5
6	12.204	12.239	12.308	5.54	19.44	1.11	0.8
7	12.308	12.368	12.413	25.07	74.43	4.26	3.06
8	12.413	12.462	12.591	27.23	115.57	6.61	4.75
9	12.591	12.612	12.672	0.88	1.93	0.11	0.08
10	12.672	12.755	12.859	9	41.19	2.36	1.69
11	12.859	12.942	13.045	5.51	31.58	1.81	1.3
12	13.045	13.098	13.128	1.95	4.88	0.28	0.2
13	13.128	13.316	13.433	19.09	137.16	7.85	5.64
14	13.433	13.598	13.644	18.9	59.67	3.42	2.45
15	13.644	13.689	13.832	33.64	70.92	4.06	2.92

Spectra

Fragmentor Voltage	Collision Energy	Ionization Mode
135	0	ESI

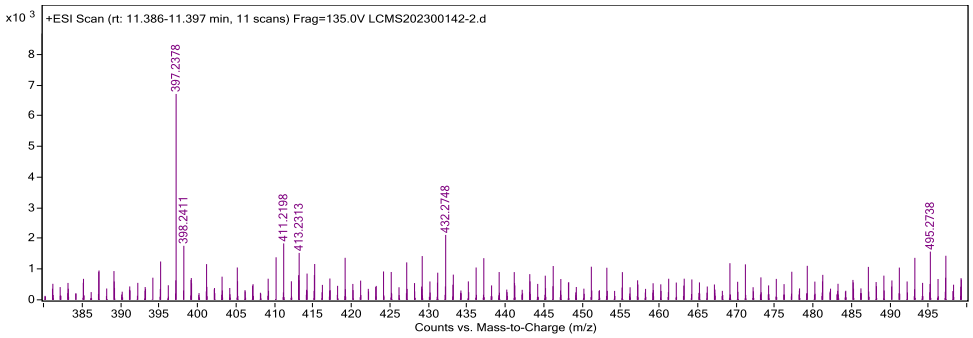

Fragmentor Voltage	Collision Energy	Ionization Mode
135	0	ESI

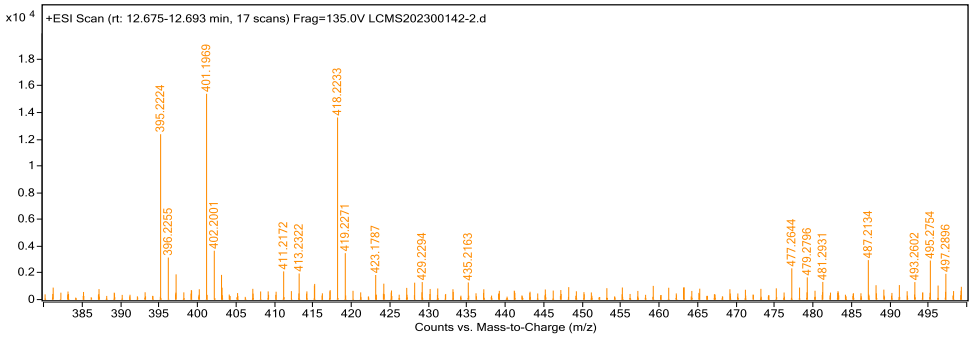

Fragmentor Voltage	Collision Energy	Ionization Mode
135	0	ESI

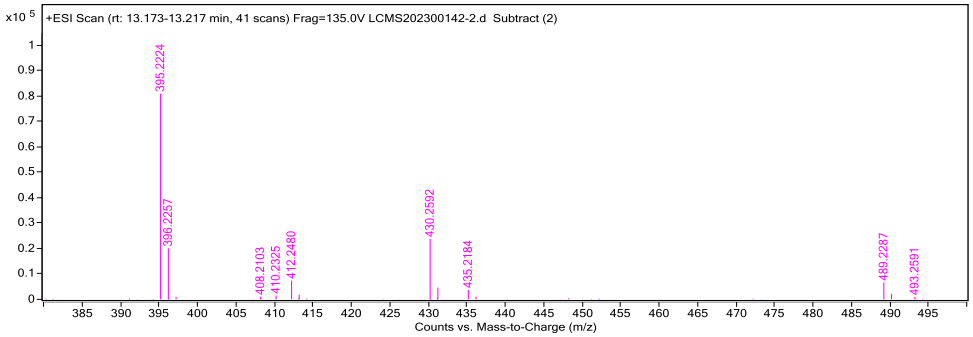

Fragmentor Voltage	Collision Energy	Ionization Mode
135	0	ESI

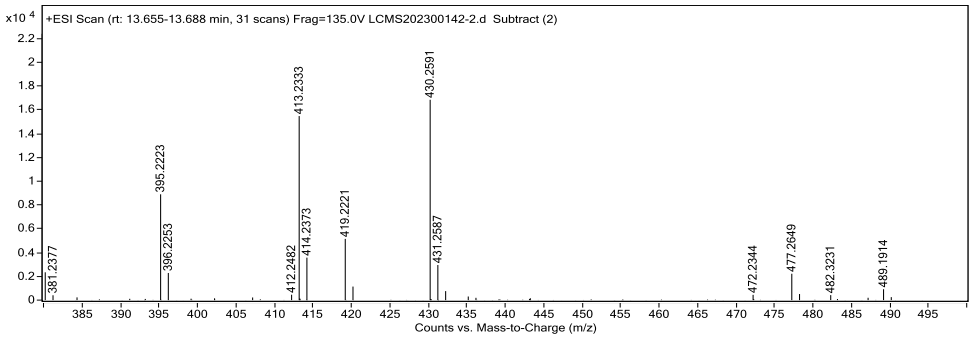

--- End Of Report ---